

Salt Tectonics and Basement  
Fractures: Key Controls of  
Recent Sediment Distribution  
on the Balearic Rise,  
Western Mediterranean

GILBERT KELLING, ANDRÉS MALDONADO,  
and DANIEL JEAN STANLEY

## SERIES PUBLICATIONS OF THE SMITHSONIAN INSTITUTION

Emphasis upon publication as a means of “diffusing knowledge” was expressed by the first Secretary of the Smithsonian. In his formal plan for the Institution, Joseph Henry outlined a program that included the following statement: “It is proposed to publish a series of reports, giving an account of the new discoveries in science, and of the changes made from year to year in all branches of knowledge.” This theme of basic research has been adhered to through the years by thousands of titles issued in series publications under the Smithsonian imprint, commencing with *Smithsonian Contributions to Knowledge* in 1848 and continuing with the following active series:

*Smithsonian Contributions to Anthropology*  
*Smithsonian Contributions to Astrophysics*  
*Smithsonian Contributions to Botany*  
*Smithsonian Contributions to the Earth Sciences*  
*Smithsonian Contributions to the Marine Sciences*  
*Smithsonian Contributions to Paleobiology*  
*Smithsonian Contributions to Zoology*  
*Smithsonian Studies in Air and Space*  
*Smithsonian Studies in History and Technology*

In these series, the Institution publishes small papers and full-scale monographs that report the research and collections of its various museums and bureaux or of professional colleagues in the world of science and scholarship. The publications are distributed by mailing lists to libraries, universities, and similar institutions throughout the world.

Papers or monographs submitted for series publication are received by the Smithsonian Institution Press, subject to its own review for format and style, only through departments of the various Smithsonian museums or bureaux, where the manuscripts are given substantive review. Press requirements for manuscript and art preparation are outlined on the inside back cover.

S. Dillon Ripley  
Secretary  
Smithsonian Institution

Salt Tectonics and Basement  
Fractures: Key Controls of  
Recent Sediment Distribution  
on the Balearic Rise,  
Western Mediterranean

*Gilbert Kelling, Andrés Maldonado,  
and Daniel Jean Stanley*



SMITHSONIAN INSTITUTION PRESS

City of Washington

1979

## ABSTRACT

Kelling, Gilbert, Andrés Maldonado, and Daniel Jean Stanley. Salt Tectonics and Basement Fractures: Key Controls of Recent Sediment Distribution on the Balearic Rise, Western Mediterranean. *Smithsonian Contributions to the Marine Sciences*, number 3, 52 pages, 19 figures, 9 tables, 1979.—The Balearic Rise is a morphologically and structurally complex feature on the southern margin of the Balearic Platform, in the western Mediterranean. Originating as a faulted block in Late Miocene time, the rise has acquired a sedimentologically diverse cover of Plio-Quaternary sediments. A study by means of high-resolution reflection profiling (3.5 kHz) and gravity/piston cores emphasizes the effects of a variety of sedimentary processes and of structural controls in the genesis of these Plio-Quaternary sequences. During this geologically recent time interval the Menorca Canyon-Valley-Fan system has exerted an important influence on the sedimentary development of this marginal feature.

On the basis of the 3.5kHz profiles, eight categories of acoustic response of the seafloor and shallow subbottom sediments have been defined and can be linked to distinctive sub-environments of the rise that are characterized by specific sedimentary and structural attributes. Abrupt variations in thickness of the Plio-Quaternary sequence attest to the continuing activity of faulting, which has generated a horst-and-graben morphology across most of the rise. More continuous subsidence is evident below the Menorca Fan but even here subrecent fracturing, accompanied by salt-diapirism, has produced a physiographic and sedimentologic complexity which differs significantly from most of the currently accepted submarine fan models.

The cored sediments fall into five main types: *bioclastic* (and *terrigenous*) *sand*, *silt*, *turbidite mud*, *hemipelagic mud*, and *calcareous ooze*. Combinations of these sediment types form three principal associations or sequences: *channel sands*, *turbiditic sequences*, and *hemipelagic sequences*. Four distinct core assemblages are also recognized, on the basis of predominant sediment type and sequence: *channel sand assemblage*, *proximal turbiditic/hemipelagic assemblage*, *hemipelagic/turbiditic mud assemblage*, and *basin plain assemblage*.

Radiocarbon dating of core samples yields average sedimentation rates of 6 to 7 cm per thousand years, the highest rates being encountered on the Balearic Basin plain and in the main Menorca Fan channel while the lowest rates occur in the hemipelagic muds of the elevated regions of the rise. Most of the thick channel sands were deposited between 23,000 and 16,000 years BP, during the last major lowering of sea level.

The Menorca Fan differs significantly in physiography and sediment distribution from most other modern submarine fans, mainly because of the reduced importance of overbank flow and channel migration, which results from the activity of shallow fractures and the blocking effects of salt-diapirs, together with the exceptionally coarse grade of material supplied to the fan.

OFFICIAL PUBLICATION DATE is handstamped in a limited number of initial copies and is recorded in the Institution's annual report, *Smithsonian Year*. SERIES COVER DESIGN: Seascape along the Atlantic coast of eastern North America.

---

### Library of Congress Cataloging in Publication Data

Kelling, Gilbert.

Salt tectonics and basement fractures.

(Smithsonian contributions to the marine sciences ; no. 3)

Bibliography: p

I. Marine sediments—Western Mediterranean. 2. Geology, Stratigraphic—Recent. 3. Geology—Western Mediterranean. I. Maldonado, Andrés, joint author. II. Stanley, Daniel J., joint author. III. Title. IV. Series: Smithsonian Institution. Smithsonian contributions to the marine sciences : no. 3

GC389.K44 551.4'62 78-24463

# Contents

	<i>Page</i>
Introduction .....	1
Acknowledgments .....	2
Morphology and Structure .....	4
General Setting .....	4
Menorca Fan .....	5
Pinnacles-Southeast Ridge Complex .....	5
Marginal Depressions Province .....	7
Gross Stratigraphy .....	7
Structural Framework .....	8
Echo Character and Plio-Quaternary Sediment Distribution .....	8
Echo Character Classification .....	9
Regional Distribution and Interpretation of Echo Character .....	9
Distribution of Reflector Density .....	20
Major Sediment Types on the Balearic Rise .....	21
Facies Distribution and Processes .....	28
Channel Sand Assemblage (A) .....	28
Proximal Turbiditic-Hemipelagic Assemblage (B) .....	30
Hemipelagic-Turbiditic Mud Assemblage (C) .....	30
Basin Plain Assemblage (D) .....	32
Sedimentation Rates .....	33
Structural and Physiographic Controls on Recent Sedimentation .....	35
Morphologic and Subbottom Considerations .....	35
Lithofacies Considerations .....	36
Subbottom and Lithofacies Correlations .....	37
Sediment Transport and Dispersal on the Balearic Rise .....	38
Evolution of the Menorca Fan .....	40
Summary and Conclusions .....	41
Appendix: Tables .....	44
Literature Cited .....	50



# Salt Tectonics and Basement Fractures: Key Controls of Recent Sediment Distribution on the Balearic Rise, Western Mediterranean

*Gilbert Kelling, Andrés Maldonado,  
and Daniel Jean Stanley*

## Introduction

The study of continental margins is at present one of the most rapidly growing and dynamic fields in geology. Great strides have been made in the elucidation of the gross structural and stratigraphic attributes of various margin types largely on the basis of geophysical evidence (Burk and Drake, 1974). Sedimentary models remain only partially formulated, however, primarily because of the lack of the appropriate data concerning depositional patterns on the various types of margin (Kelling and Stanley, 1976).

The importance of structural controls on continental margin sedimentation is apparent in most continental margin studies, and especially in those dealing with compressional settings. The present investigation of the Balearic Rise in the western Mediterranean was initiated to evaluate the relations between tectonics and deposition in a sector

that is not primarily compressional. This margin, which has remained mobile until recent geological time, lies south of the Balearic islands in the Algéro-Balearic Basin (Figure 1A).

An earlier seismic survey of this region indicated that the Balearic Rise is a large detached block that has subsided during the Oligo-Miocene and particularly from the Late Miocene to the Recent and has not yet completely merged with the Balearic Basin plain (Stanley et al., 1976). This large-scale vertical displacement of the Balearic margin, which is directly related to the overall development of the western Mediterranean, has resulted in physiographic and structural features that display some similarity with those of margins in rift zones. In addition to ample evidence of faulting, earlier investigations of the Balearic Basin plain contiguous with the rise have shown the importance of salt tectonism (Ryan et al., 1970; Auzende et al., 1971). Detailed studies of this region demonstrate that during the Late Quaternary the rates of deformation due to salt migration locally have exceeded rates of sediment accumulation (Stanley et al., 1974b).

In an attempt to identify and interpret the Quaternary depositional patterns of this struc-

---

*Gilbert Kelling, Geology Department, University of Keele, Staffordshire, England. Andrés Maldonado, Sección de Estratigrafía, Instituto "Jaime Almera," C.S.I.C., University of Barcelona, Spain. Daniel Jean Stanley, Division of Sedimentology, National Museum of Natural History, Smithsonian Institution, Washington, D.C. 20560.*

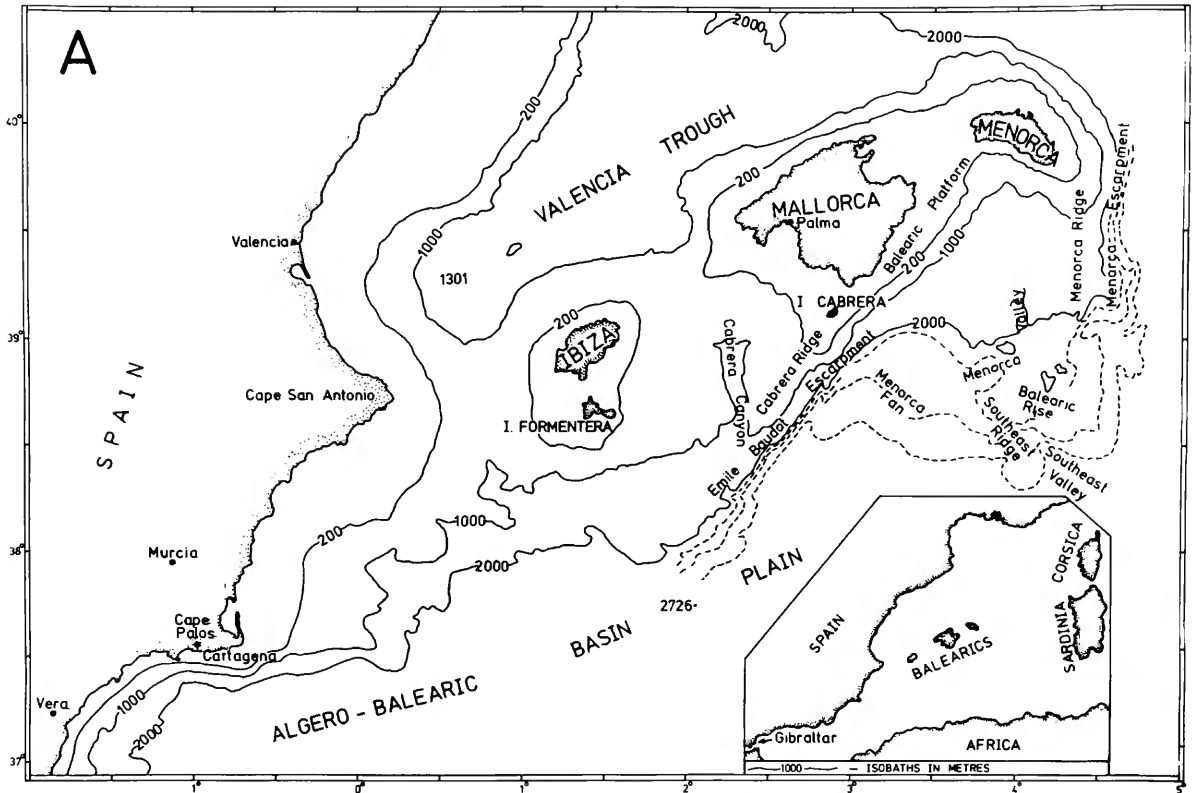


FIGURE 1.—A, Map of Balearic Islands, Balearic Rise, and adjacent physiographic features (bathymetry in meters; inset shows location of Balearics in western Mediterranean); B, ship's tracks in vicinity of Balearic Rise (tracks indicate coverage of 3.5kHz profiles utilized in this study; dashed lines with figures and letters = location of 3.5kHz profiles illustrated in Figures 4 and 5; dots labelled MC1-MC11 = location of core samples obtained on *Lynch I* cruise (Jan-Feb 1972); cores RC9-199 and RC9-200 derived from R/V *Conrad* Cruise 9 of Lamont-Doherty Geological Observatory; DSDP-124 = drill core obtained on Leg 13 of Deep Sea Drilling Program).

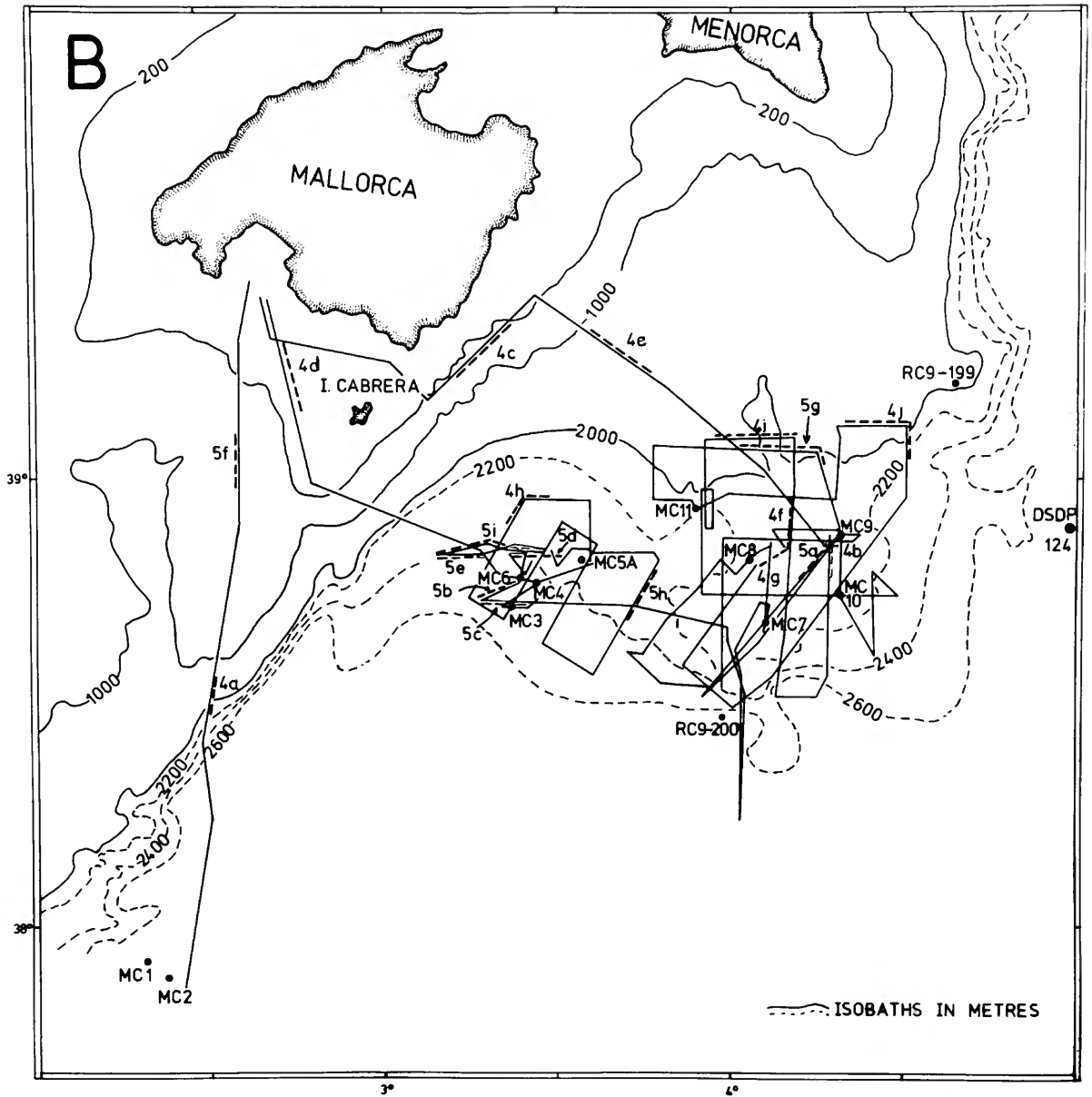
turally mobile margin and to more accurately evaluate the influence of tectonism on sedimentation, we have surveyed the Balearic Rise with a 3.5kHz high resolution subbottom system and collected cores in the same area (Figure 1B). Analyses of the resulting data and samples have enabled us to distinguish major sediment types and their distribution and have provided much information on the dominant transport processes operating on the Balearic Rise. Studies of a similar nature have been applied with success in other world oceans (cf. Hollister and Heezen, 1972; Damuth, 1975; Jacobi, 1976; Damuth and Hayes, 1977). Most of the data and samples described here were obtained on a cruise of the USNS *Lynch* in February 1972 with supplementary information from cruises of T/S

*Empire State IV* (June 1972) and RRS *Discovery* (August 1970).

As an outgrowth of this study, we call attention to the submarine fan deposition on the western part of the rise. The Menorca Fan, a rare example of a fan formed on an actively subsiding block, provides us with an unusual model, i.e., a fan largely controlled by tectonic imprint rather than by climatic and sediment input factors.

ACKNOWLEDGMENTS—We thank the US Naval Oceanographic Office for ship-time in February 1972 aboard the USNS *Lynch* and, in particular, Mr. R. S. Anderson of that office (Washington, D.C.) for assistance in the collection of the data at sea. Appreciation is also expressed to Dr. Y. Weiler, The Israel Institute of Petroleum, Tel-Aviv, for





help in the preliminary processing of seismic records and cores, and Mr. H. Sheng, Smithsonian Institution, for petrologic examination of core samples. Thanks are expressed to Dr. R. Stuckenrath, Smithsonian Carbon Dating Laboratory, for providing the eight radiocarbon dates used in this study.

The invaluable assistance of Mrs. J. Install, Mr. J. U. Edwards, and Mr. D. Kelsall during the com-

pilation of this paper is acknowledged, while financial support to one of us (GK) by the Royal Society of London and the Research Fund of the University of Keele facilitated the publication of the results of this study.

This project, part of the long-term Mediterranean Basin (MEDIBA) Project, is supported by Smithsonian Research Foundation grants 450137 and 460132 (DJS), the British Institute of Barcelona

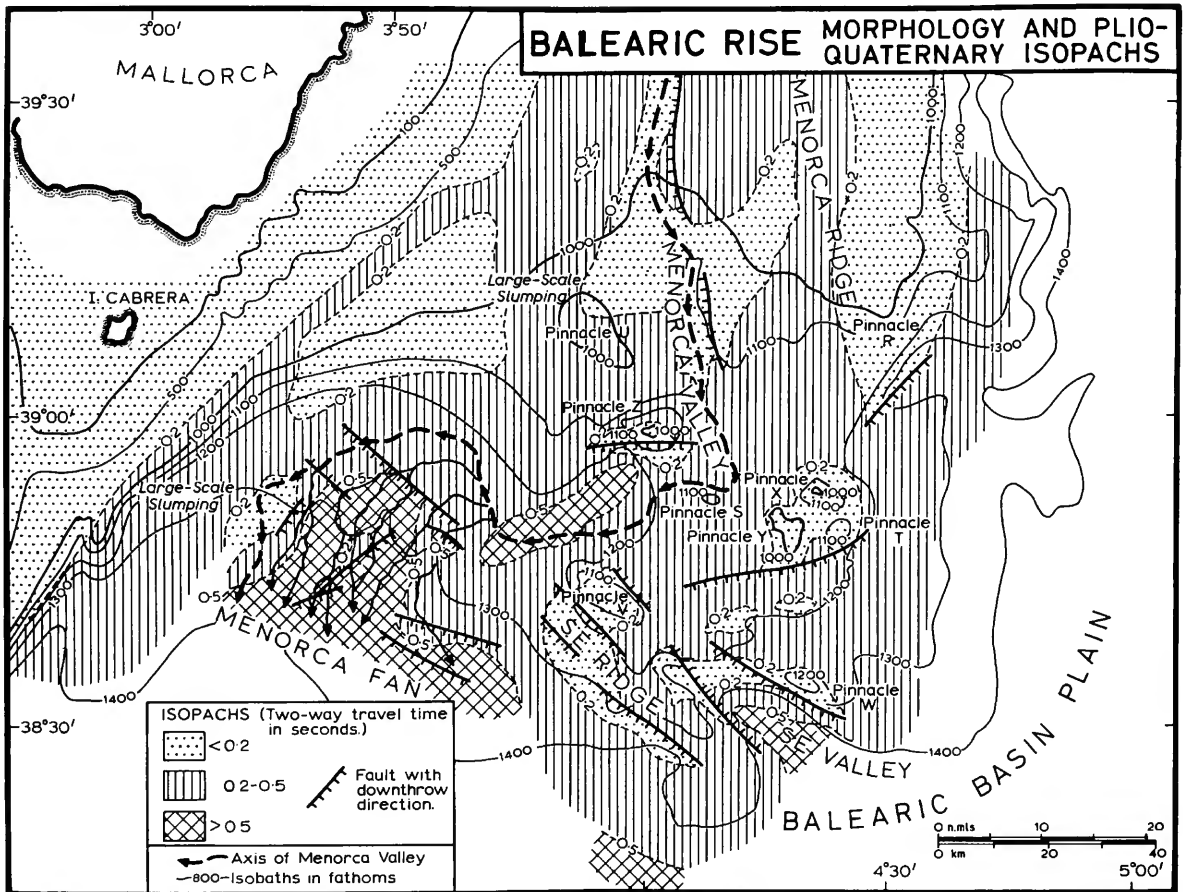


FIGURE 2.—Principal morphologic features of Balearic Rise, together with isopachs of Plio-Quaternary sequence derived from sparker profiles (main faults affecting this sequence are also depicted).

(AM) and the Consejo Superior de Investigaciones Científicas of Spain (AM)).

We are much indebted to Douglas Hamilton and Michael Brooks for their valuable comments and advice. The conclusions and opinions offered, however, are solely our responsibility.

## Morphology and Structure

### GENERAL SETTING

The Balearic Rise is a physiographically complex region located between the steep, fault-defined Emile Baudot Escarpment and the relatively flat Algéro-Balearic Basin plain (see Stanley et al., 1976). Within the restricted area of the rise (some 13,500

km<sup>2</sup>) five main morphologic elements may be recognised (Figure 2 and Table 1): the Menorca Ridge, the Menorca Canyon/Valley, the Menorca Fan, the pinnacles complex/Southeast Ridge, and the basin margin depressions.

The Menorca Ridge is a broad, south-trending swell that effectively defines the northeastern margin of the rise and thus delimits the entire Balearic Block. Truncating the northeastern extension of the Emile Baudot Escarpment south of the Island of Menorca, the ridge slopes gently southwards from the Mallorca-Menorca shelf, with a general gradient of approximately 2°. The crest and flanks of this feature display a fairly rugged topography, especially on the more steeply sloping (6°) eastern flank; transverse profiles reveal that while the ridge crest

TABLE 1.—Classification of physiographic features on the Balearic Rise

I	MAJOR CHANNELS	A.	Acute profile, rough floored (Menorca Canyon)		
		B.	Broad, flat-based, with minor channels (Menorca Valley)		
II	MINOR CHANNELS	A.	Rough floored		
		B.	Smooth floored		
III	BROAD, SMOOTH ELEVATIONS	A.	Interchannel levees		
		B.	Gently sloping platforms		
IV	PINNACLES	A.	Penetrative		
		B.	Layered		
V	STEEP, ROUGH ROCKY SLOPES (Fault-scarps etc.)			VI	FAN LOBES
VII	DIAPIRIC PROTRUSIONS			VIII	SLUMP-ZONES

has a mean elevation of about 550 m (300 fm) above the Menorca Canyon to the west, it lies between 1100 and 1600 m (600 and 874 fm) above the Balearic Basin plain to the east. At its southern termination the Menorca Ridge merges abruptly into the smooth, plateau-like northern portion of the pinnacles complex.

The Menorca Canyon and Valley is a major linear depression that commences on the southern margin of the Balearic Shelf, south of the Island of Menorca. In its upper course, traversing the Emile Baudot Escarpment, this depression is narrow (5 km), steep-sided ( $5^{\circ}$  to  $15^{\circ}$ ) and compound, with tributary ravines and a high axial gradient ( $2^{\circ}$ , average), and is properly termed a submarine canyon. Beyond an axial depth of approximately 1300 m (710 fm) this feature, while maintaining its southward trend, changes character appreciably and may be termed a submarine valley. Here the depression is relatively wide (more than 6 km and increasing downslope) and flat-floored, with relatively steep flanks and an effective wall-relief varying between 55 m and 90 m. At an axial depth of approximately 2140 m (1170 fm) the course of the Menorca Valley alters abruptly to a southwestward trend (Figure 2). Near this bend the valley becomes deeper and constricted and is marked by nearly vertical, erosive eastern walls and a more gently inclined western flank. This transverse asymmetry is comparable with the profiles produced by fluvial flow through a right-handed meander-loop. Beyond this bend the valley becomes much wider (up to 25 km across) and the small-scale relief of the floor becomes more pronounced. This morphologic change marks the transition of the valley into the

apical region of the Menorca Fan, which is arbitrarily deemed to commence at the profile in which more than two minor channels can be discerned in the valley floor.

#### MENORCA FAN

The Menorca Fan resembles most modern deep sea fans in its location at the mouth of a major submarine canyon or valley, in its arcuate plan form and in its broadly convex-upward transverse profiles. This feature also displays (especially in the eastern portion) broad, low swells (1 to 5 km across and 20 m high) that are interpreted as fan-lobes (see Figure 3, letter S). The Menorca Fan, however, displays the following morphological aspects that are not generally regarded as typical of such features (cf. Normark, 1970).

1. The Menorca Valley splits to give rise to a number of small distributary channels in the "inner fan" region, but the main channel of this system forms a discrete major depression around the inner (northern) periphery of the fan, skirting the base of the Emile Baudot fault escarpment and ultimately merging with the flat basin plain province (Figures 2 and 3).

2. Channel, levee, and inter-channel sectors may be distinguished, both morphologically and by their seismic response, throughout the fan. The fan surface, however, exhibits substantially more relief in the middle and lower sectors than in the inner fan region (Figure 3), contrasting with the more normal situation. Consequently, few distributary channels can be traced with confidence for distances of more than a few kilometers across the fan surface. Sub-bottom evidence indicates that the principal cause of the enhanced relief of the middle and outer Fan regions is the presence of numerous salt-diapirs, uplifting or penetrating the fan surface.

3. The boundary between the distal edge of the fan and the adjacent basin plain is marked by a fairly abrupt change in average surface slope (from 15 to 5 m or less per 300 m).

#### PINNACLES-SOUTHEAST RIDGE COMPLEX

The Pinnacles-Southeast Ridge Complex is a relatively elevated region located east of the Menorca Fan, southeast of the Emile Baudot Escarpment and

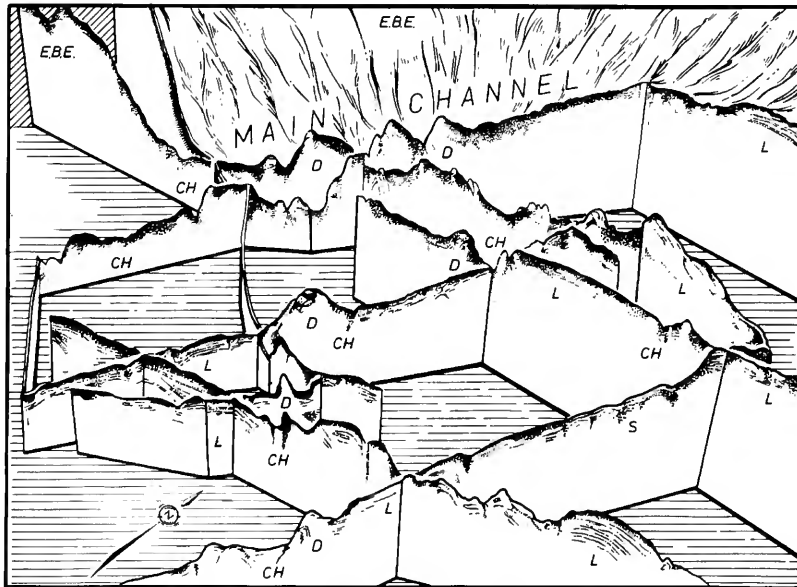
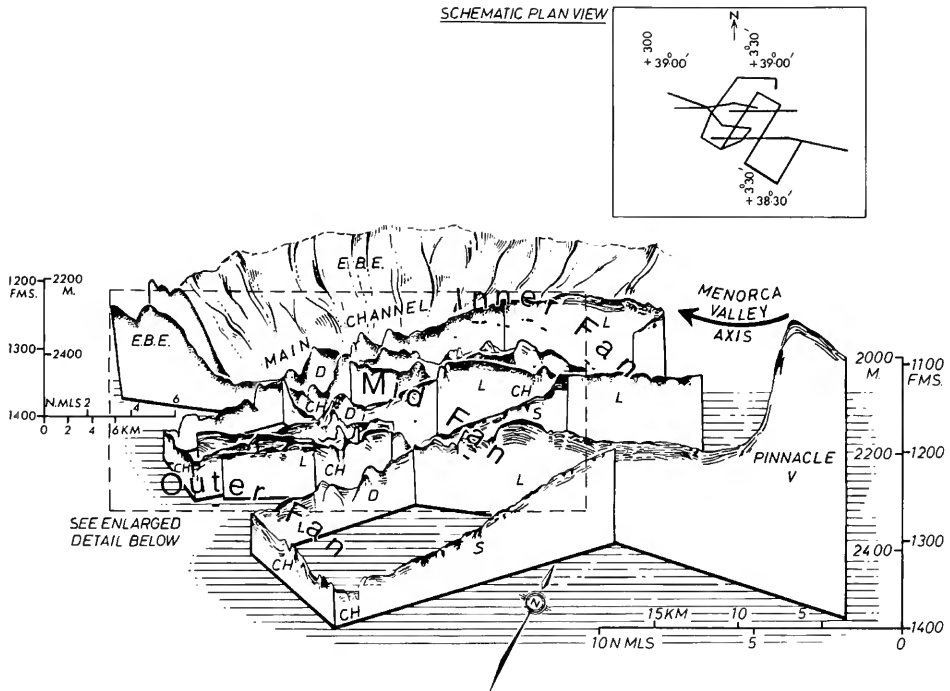


FIGURE 3.—Upper: fence-diagrams illustrating detailed morphology and shallow subbottom structure of Menorca Fan and adjacent parts of Balearic Rise; constructed from 3.5kHz profiles (location indicated in schematic plan at top right); lower: enlargement of central part of fan (dashed outline in upper diagram); CH = channel; D = surficial diapir; E.B.E. = Emile Baudot Escarpment; L = levee; S = slumps).

southwest of the Menorca Ridge. This region merges south into the Balearic Basin plain, through the Marginal Depressions province and is traversed by the Menorca Valley (Figure 2). Individual Pinnacles are subconical to elongate, sub-elliptical ridges ranging in diameter from 3 to 12 km and from 150 to 510 meters in relative height above the adjacent seafloor (Figure 2, 4, and 5). Type 1 (Penetrative) pinnacles (R, S, E, W, Y, and X) rise abruptly to a considerable height above the adjacent flatter seafloor (average gradient is approximately  $10^\circ$ ), whereas type 2 (layered) pinnacles (U, V, and Z) are less steeply inclined, wider at the base and exhibit more complex surficial micromorphology. In addition to these physiographic differences the two pinnacle types display contrasts in seismic structure which are detailed in a later section (pp. 8-9). Several Penetrative (and one of the Layered) Pinnacles display depressions or "moats" running, at least partially, around their bases. These range from 15 m to 45 m in maximum depth and from 950 m to 3100 m in width. The Southeast Ridge is a larger, compound example of the Layered Pinnacle style of morphology and structure.

#### MARGINAL DEPRESSIONS PROVINCE

The Marginal Depressions Province is confined to the southeastern and eastern flanks of the rise, intervening between the pinnacles region and the Balearic Basin plain. The largest of these depressions is here termed the Southeast Valley. This feature effectively separates the seaward extension of the Southeast Ridge from Pinnacle W and the more northerly part of the Pinnacles Province (Figure 2). Profiles across the more distal portion of the Southeast Valley reveal a flat-floored configuration with an abrupt wall-to-floor junction at a depth of approximately 2560 m (1400 fm: see Figure 2), and suggest encroachment by an accreting fill of relatively recent sediments. Profiles across inner sectors of the Southeast Valley display a more typical submarine valley morphology, with probable small slumps contributing to the fill.

#### GROSS STRATIGRAPHY

The stratigraphic framework and structural configuration of the Balearic Rise, the Menorca Valley, and adjacent regions are detailed elsewhere (Stanley

et al., 1974a, 1976). The following account summarizes the gross aspects of sequence and structure in the rise region, interpreted primarily from sparker and air-gun continuous reflection profiles, as a preliminary to the more detailed description of the distribution, shallow structure and stratigraphy of the young sediments mantling this area.

The gross succession observed in the Balearic margin commences with an acoustic "basement", best displayed on the Emile Baudot Escarpment and in the pinnacles complex. Locally this highly reflective rock-group underlies the more stratified succession at considerable depths (e.g., below the Menorca Fan) while elsewhere, as in the pinnacles area, the top of the "basement" occurs at shallow depths below the seafloor and, in certain pinnacles, appears to be penetrative through the overlying sediments (Figure 4). It is considered that this acoustic zone represents an older series of rocks (pre-Miocene cf. Mauffret, 1976), block-faulted in the rise region and possibly associated with younger volcanics (Gonnard et al., 1975) forming the Penetrative Pinnacles.

An acoustically transparent zone that occurs above the basement, particularly in the central and western part of the Rise, includes, in some areas, a thin group of indistinct to moderately developed reflectors near the base (Figure 6; see also Stanley et al., 1976, figs. 25E, 25H). The normal thickness of this transparent "couche fluante" zone (Montadert et al., 1970) is between 100 and 400 m but this varies greatly and the upper boundary is commonly modified by diapiric protrusions, many of which penetrate overlying sediments to attain the seafloor. This feature, together with direct evidence obtained during legs 13 and 42A of the Deep Sea Drilling Project, supports the interpretation of this acoustic layer as a salt sequence of probable Late Miocene age (Ryan et al., 1973a, 1973b; Hsü et al., 1975). The moderately defined reflectors near the base of the acoustically transparent zone may equate with the N reflector of Ryan et al. (1973b) and may represent earlier Tertiary (but probably post-Oligocene) sediments (Hsü et al., 1975).

Capping the transparent zone is a prominent group of laterally extensive reflectors, the M reflector sequence (Ryan et al., 1970; Ryan et al., 1973b, etc.), which varies in thickness between 100 and 300 m. Below much of the Menorca Rise the M zone is disrupted by halokinetic features originating from

the subjacent layer, and it has also been substantially displaced by near-vertical faulting not directly related to the salt movements. Evidence from JOIDES Site 124 indicates that this unit comprises a group of carbonates, gypsum, and anhydrite of Messinian to lowermost Pliocene age (Ryan et al., 1973a; Biscaye et al., 1972).

The uppermost layer above the M reflectors is an acoustically near-transparent zone that passes gradually upward into a unit displaying numerous well-defined, parallel reflectors. The thickness of this layer ranges from about 200 to 700 m and in many sectors is related to the existing morphology, i.e. attaining a maximum in topographic depressions and minimal over the intervening highs (Stanley et al., 1976, figs. 28–33). Isopachytes for this layer confirm that it achieves greatest development in the lower reaches of the Menorca Valley, below the Menorca Fan, and on the Balearic Basin plain (Figure 2). The unconsolidated sediment section of the fan above the M reflectors of Messinian age is about 400 to 500 (and may be as much as 700) meters thick; air-gun and sparker profiles show that these series are extensively dislocated and form an irregular surface resulting from vertical fault displacement that has offset even the uppermost sequences. Evidence from short cores and from Site 124 of JOIDES Leg 13 and Site 372 of Leg 42A demonstrates the Pliocene and Quaternary age of this layer is composed of lutites with subordinate sandy and silty turbidites (Ryan et al., 1973a; Hsü et al., 1975). The existence of a significantly higher proportion of coarse-grained layers in the Pleistocene than in the underlying Pliocene section has not been confirmed (Stanley et al., 1976). The uppermost few meters of this sequence are described in more detail in later sections.

#### STRUCTURAL FRAMEWORK

The sum of the seismic evidence suggests that the Balearic Rise is essentially a vertically displaced block of Balearic Platform material that has foundered as a result of movements on two roughly rectilinear fracture-systems: the earlier NNW-SSE Menorca Ridge system and the younger NE-SW trending Emile Baudot fault-plexus (cf. Mauffret, 1976; Stanley et al., 1976).

Most of the smaller (throws of less than 30m), and presumably younger, faults that affect the Plio-

Quaternary sediments fall into two groups of differing trend (Figure 2): (1) a few fractures of N-S orientation, which appear to define the middle portion of the Menorca Canyon; (b) a larger group of faults trending E-W or WNW-ESE (this may represent an antithetic system related to the Emile Baudot fracture pattern).

The irregular "horst-and-graben" topography of much of the rise, the existence of many faults affecting the Plio-Quaternary sequence (Figure 2) and even the course of the Menorca Canyon-Fan Valley, with its abrupt alteration in trend, all demonstrate that faulting of this foundered block has continued until geologically recent times.

#### Echo Character and Plio-Quaternary Sediment Distribution

Numerous studies (Ryan and Heezen, 1965; Hollister and Heezen, 1972; Damuth, 1975; Jacobi, 1976; Damuth and Hayes, 1977, and others) have demonstrated the value of high-resolution acoustic depth recorders in delineating the microtopography and gross sediment character of portions of the deep-sea floor. Short-ping (< 5msec), high frequency (3.5 to 12kHz) systems provide echograms of optimum quality for this purpose, often incorporating data on the shallow subbottom (to depths of around 100 m) in addition to response from the sediment/water interface.

In the present study the 3.5kHz transducer system achieved average penetration of about 35 m and a maximum of nearly 90 m. Resolution is probably about 1 meter in the water depths encountered. Positioning was achieved by satellite, Loran-C, and radar-ranging and the ship's average speed was 10 knots. Deeper seismic evidence derives from spark-array systems (30,000J Teledyne system with Raytheon Precision Electrographic Recorder, supplemented by an E.G. and G. 8000J Sparker). Further details of the systems used are provided in Stanley et al., 1974b and Stanley et al., 1976. The average spacing of parallel 3.5kHz lines on the Menorca Rise is approximately 10 km but is nearly 5 km over much of the Menorca Fan surface, enabling determination of the detailed morphology of this part of the rise, as depicted in Figure 3.

Examination of the 1427 km (780 n mi) of almost continuous profiles obtained in the Balearic Rise region by means of the 3.5kHz source has revealed

the existence of a variety of acoustic responses that have been allocated to 8 categories of echo character, utilizing both bottom echo (sediment/water interface) and subbottom response. These are listed in Table 2. It should be noted that, so far as possible, the validity of the echo type classes erected here was verified by examination of track intersections, in order to eliminate the influence of acoustic artefacts induced by azimuthal effects. Several of the categories recognized here compare closely with classes recognized elsewhere (for example, types 1, 2, 3, 4, and 8 of this study are very similar respectively to types IIIA, IIB, IIA, IB, and IIIB of Damuth and Hayes, 1977), but there are also several distinctive and previously uncategorized forms present on the Menorca Rise.

#### ECHO CHARACTER CLASSIFICATION

*Type 1:* Diffuse, large, irregular, and overlapping hyperbolae (amplitude 20 to 200 m plus) with no coherent sub-bottom reflectors (Figure 4A, B, C). *Type 2:* Continuous, sharp to slightly prolonged bottom echo, with minor irregularities at the sediment/water interface. No coherent subbottom reflectors are present but there are numerous small hyperbolae of irregular size in the subbottom (Figure 4D, E, F, H). *Type 3:* Continuous or rather diffuse, prolonged bottom echo, lacking surficial irregularities. Coherent sub-bottom reflectors are rare to absent but there are occasional isolated small (amplitude 10 to 40 m; wavelength, 100 to 250 m), poorly defined hyperbolae (Figure 4G, H). *Type 4:* Continuous, sharp bottom echo with conspicuous parallel

and multiple subbottom reflectors (Figure 4I, J, K; Figure 5A). *Type 5:* Continuous, sharp to slightly prolonged bottom echo with some minor surficial irregularities and rather diffuse, discontinuous multiple subbottom reflectors that are broadly lensoid and convergent (Figure 5B, C). *Type 6:* Continuous, sharp bottom echo with multiple parallel subbottom reflectors, interrupted by isolated, medium scale, acoustically transparent hyperbolae, some of which penetrate the sediment/water interface (Figure 5D, E, I). *Type 7:* Continuous, sharp to slightly prolonged bottom echo with multiple subbottom reflectors that converge or are abruptly truncated at, or below, the seafloor (Figure 5F). *Type 8:* Continuous, sharp bottom echo derived from an undulatory seafloor topography, underlain by multiple subbottom reflectors forming hyperbolae concordant with the undulatory seafloor. The hyperbolae are separated by subvertical planes (Figures 5G, H).

#### REGIONAL DISTRIBUTION AND INTERPRETATION OF ECHO CHARACTER

This section is concerned with the distribution of echo types throughout the Balearic Rise region and adjacent provinces. Evidence from the piston and gravity cores and from deeper seismic investigations (Figure 6) has been utilized to amplify the interpretation of the type of deposit that has generated the acoustic response recorded in the different categories of echo type (Figures 7 and 8). It should be noted that, in preparing the echo character distribution chart (Figure 7) some of the boundaries (notably for types 1 and 8) have been drawn to conform to the limits of the physiographic provinces from which they are recorded. Such provinces have been established from all available bathymetric data and not solely from the information obtained on the cruise described herein.

Type 1 echos characterize the steeper, south-westerly portion of the Emile Baudot Escarpment (Figure 7), together with Penetrative Pinnacles and the summit portions of the Layered Pinnacles. This type of echo-response is attributed to the rugged topography of these regions. Sparker records also indicate that in several of these zones the basement rocks either crop out at the seafloor or are mantled by only a thin veneer of Plio-Quaternary sediments (cf. Figure 2).

TABLE 2.—Correlation of acoustic character and physiographic features on the Balearic Rise

<u>Echo Character Type</u> (see Figure 7 and text)	<u>Physiographic Features</u> (Code as in Table 1)
1	IVA, V
2	IA, IIA, IVB
3	IB
4	IIIB, IVB
5	IB, IIIA, VI
6	VII
7	IIB
8	VIII

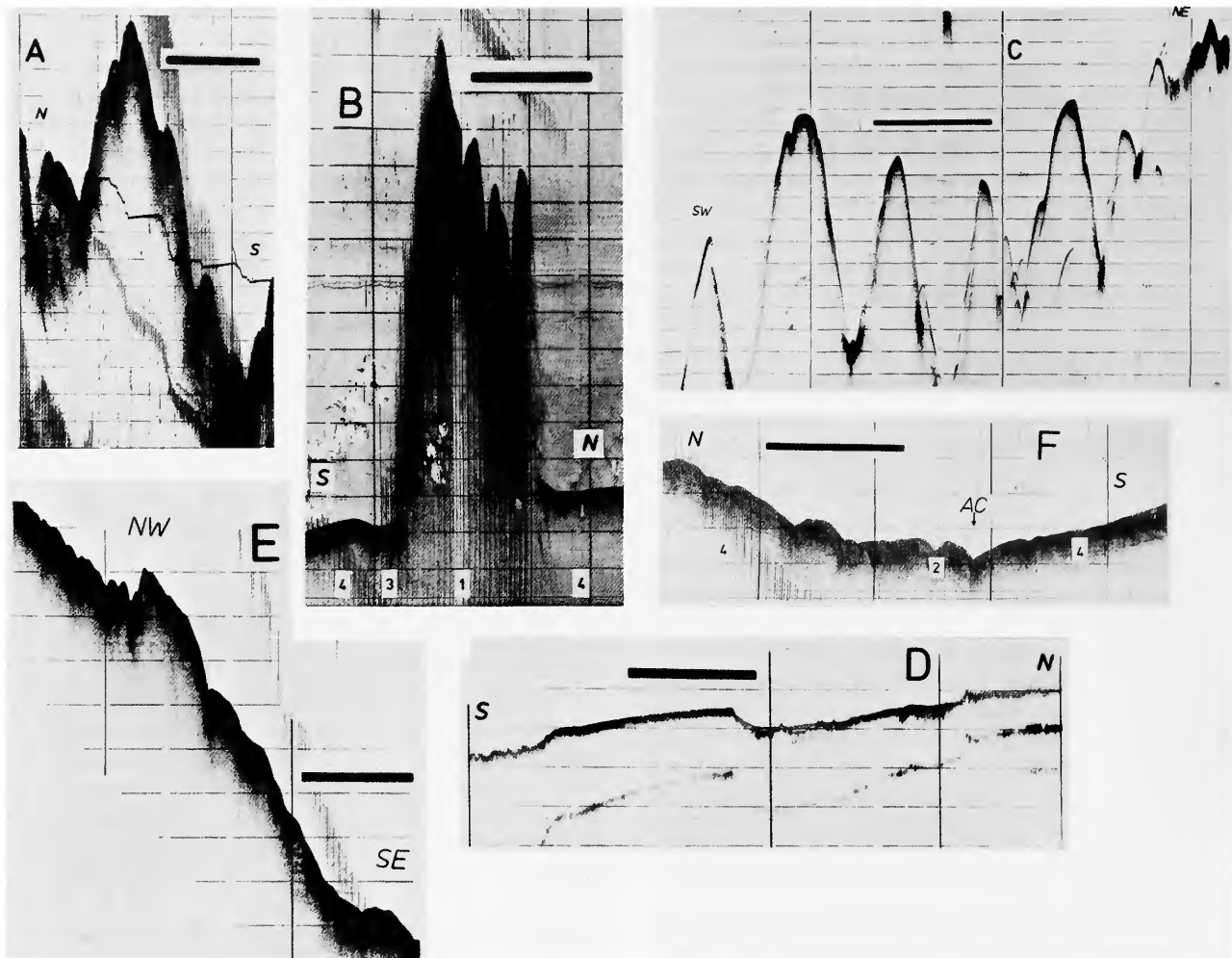


FIGURE 4.—Montage of 3.0 kHz profiles illustrating characteristics of echo character types 1-4 (for location of profiles, see FIGURE 1B: Thick horizontal bar = distance of 4km; thin horizontal lines are spaced 20 fms (36.6 m) apart in seawater): A, type 1 echo character, from Emile Baudot Escarpment; B, type 1 echo character (center) from Penetrative Pinnacle Y (note adjacent zones of type 4 character and narrow "moat" or depression on southern flank of Pinnacle displaying type 3 echo character); C, type 1 echo character: an along-slope profile of Emile Baudot Escarpment; D, type 2 echo character from outer shelf, south of Palma de Mallorca (note shallow shelf-channel in central part of profile, location X on Figure 7); E, type 2 echo character (upper left of profile) from slope northwest of Layered Pinnacle U (larger scale irregularities on lower two-thirds of profile are attributed to slumping of type 4 sediments); F, type 2 echo character developed in axial region of lower Menorca Canyon (note flanking type 4 regions, probably with minor slumping; A.C. = active channel of Menorca Canyon; cf. Figure 6F, right end); G, type 2 echo character (center of profile) from axial zone of lower Menorca Canyon, passing laterally into type 3 and (slumped) type 4 regions (A.C. = active channel of Menorca Canyon); H, type 3 echo character (on right of profile) from axial zone of Menorca Fan Valley, passing downslope into type 2 and type 6 regions (cf. Figure 6E, left end); I, typical type 4 echo character sediments flanking incized section of lower Menorca Canyon, floor of which displays type 3 echo character; J, profile Penetrative Pinnacle A (figure 8) demonstrating transition from Type 1 echo character in



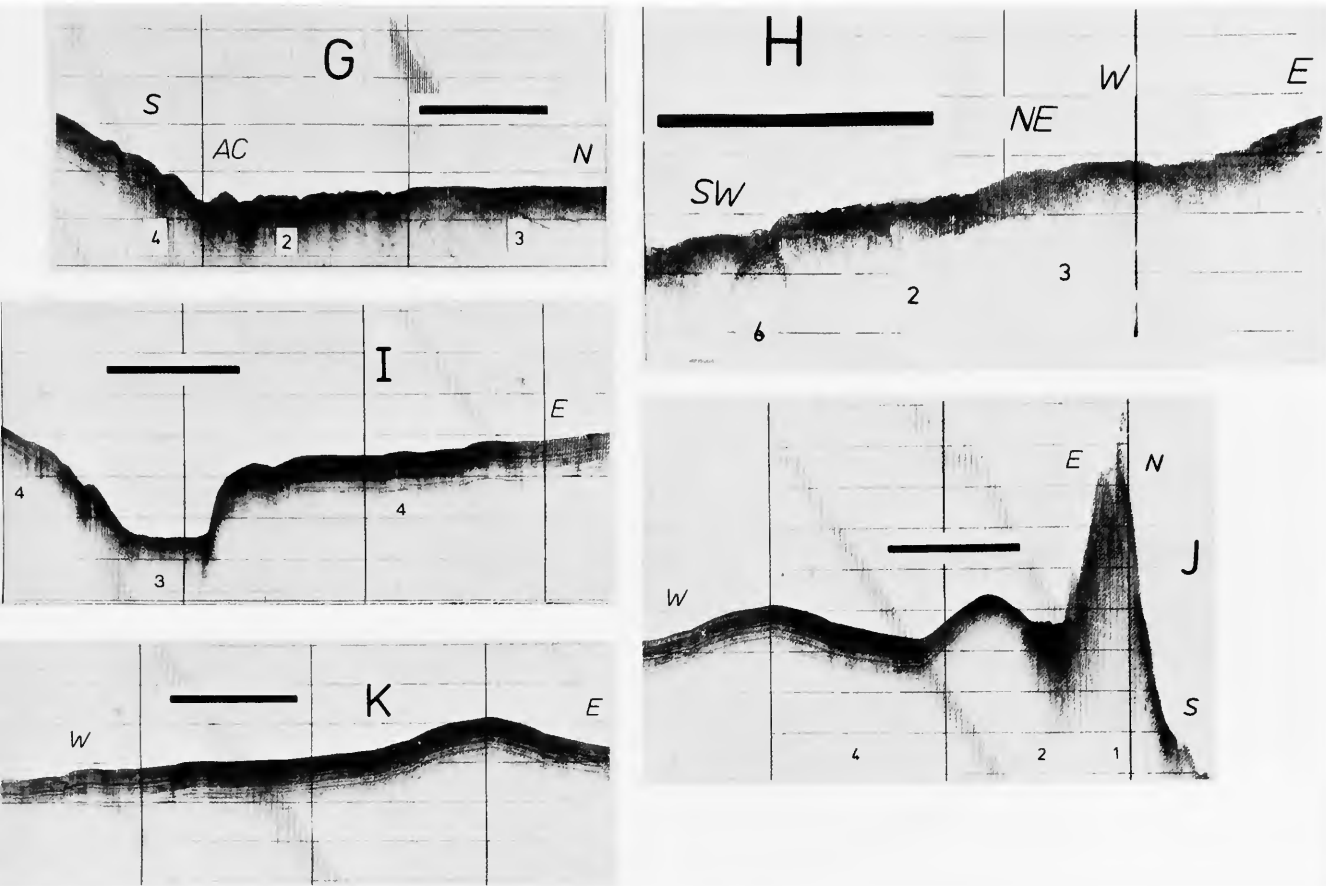


FIGURE 4.—Continued

pinnacle trough type 2 response, in narrow flanking depression or moat), to gently undulating type 4 seafloor (cf. Figure 6B, left end); K, type 4 echo character, typical of much of elevated pinnacles/Southeast Ridge Complex province.

Type 2 echos have been recorded from less steeply inclined portions of the Emile Baudot Escarpment, at the junction of the Escarpment with the Menorca Fan and in several more restricted valley floor regions (e.g., the head of the Southeast Valley). The "moated" areas at the base of some pinnacles (Figure 7) yield a similar acoustic response. Restricted areas displaying this echo character also occur in the axial zone of Menorca Canyon and Valley but these are too small to be portrayed on Figure 7. This type of echo response is attributed to a highly efficient reflection of sound from a seafloor of relatively muted morphology, presumably composed of indurated sediment or gravel. The minor surficial irregularities and small, irregular hyperbolae

may derive from rock ledges or from larger blocks or boulders on the seafloor. Little acoustic energy penetrates to underlying layers and thus subbottom reflectors are virtually absent from the sonic profiles.

Gradation into the type 3 echo character is marked by a more diffuse and prolonged return, with fewer, more isolated internal hyperbolae. Echo-grams of this type characterize the Mallorca Shelf region and the narrow axial zone of the Menorca Canyon and Valley, to an axial depth of about 2270 m (1240 fm). A few small patches exhibiting this echo character also occur in the re-entrants of the Balearic Basin plain that constitute the Marginal Depressions morphologic province on the eastern and

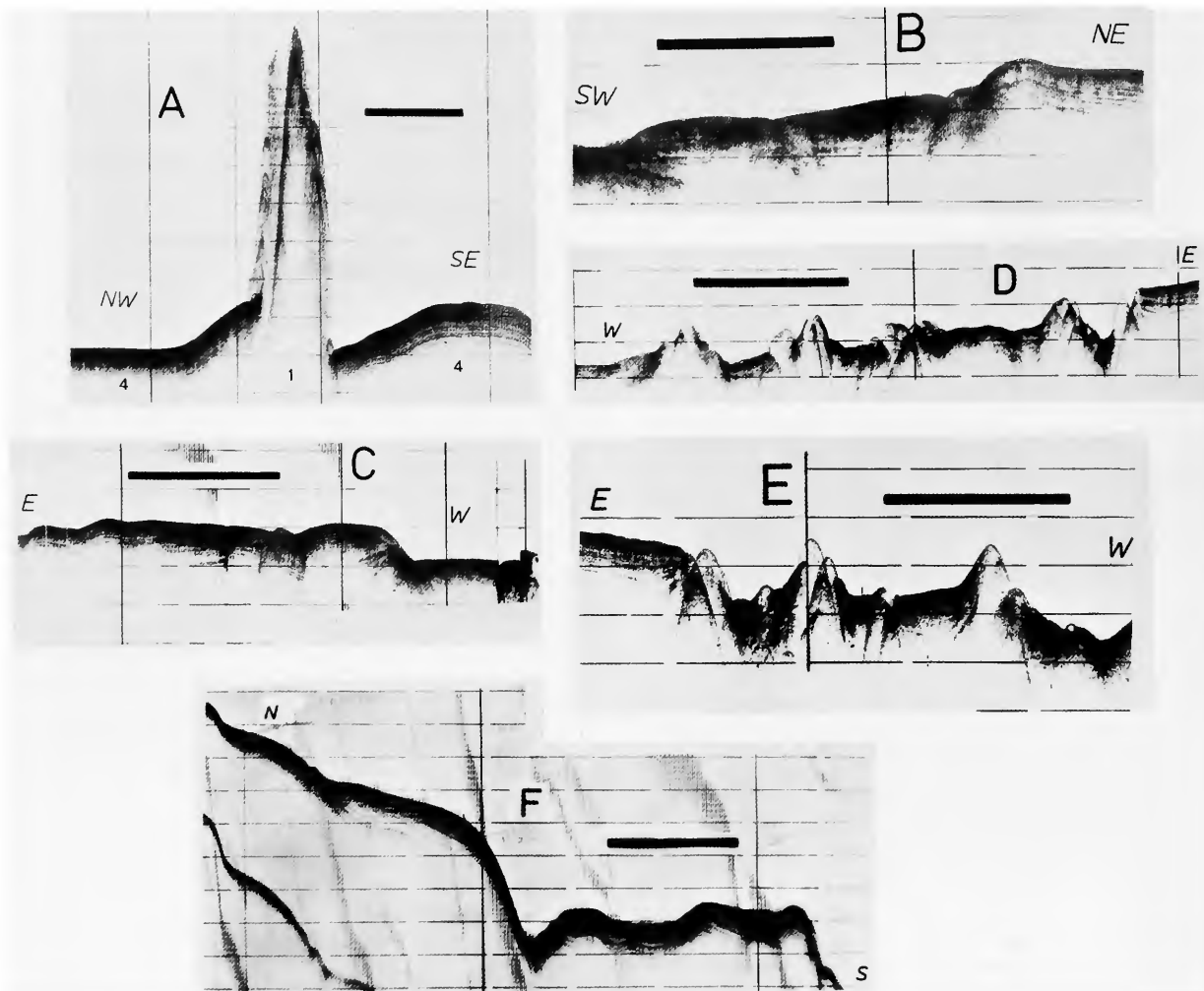


FIGURE 5.—Montage of 3.5kHz profiles illustrating characteristics of echo character type 4-8 (location of profiles shown in Figure 1B; thick horizontal bar = distance of 4km; thin horizontal lines are spaced 20 fms (36.6 m) apart in seawater): A, profile traversing Penetrative Pinnacle Y, with type 1 acoustic response, and flanking areas of type 4 echo character (note relatively greater accumulation of type 4 sequence on NW flank of pinnacle; cf. Figure 4B); B, type 5 echo character, displaying characteristic divergence of subbottom reflectors (from middle Menorca Fan channeled and leveed); C, type 5 echo character, as developed in fan-lobe zone of outer Menorca Fan; D, type 6 echo character with surface-penetrating diapirs (Middle Menorca Fan region); E, type 6 echo character as developed in western sector of middle Menorca Fan (note levee sequence at eastern, left, end of profile and draping of reflectors adjacent to the 35m high diapir near the western, right, end); F, type 7 echo character, displaying characteristic surficial truncation of subparallel reflectors (from tributary slope-gully system on eastern flank of Cabrera Canyon); G, type 8 echo character developed on eastern flank of Menorca Canyon (note irregular surface morphology and subvertical "shadow traces" in type 8 record; note also development of type 3 acoustic response in flat floor of canyon; cf. Figure 6D, center); H, type 8 echo character as displayed in leveed fan-lobe region of Menorca Fan (eastern margin); I, generalized profile across outer Menorca Valley and western part of Menorca Fan (Ab = abandoned channel; AC = active channel; D = diapir; E.B.E. = Emile Baudot Escarpment; L.F. =

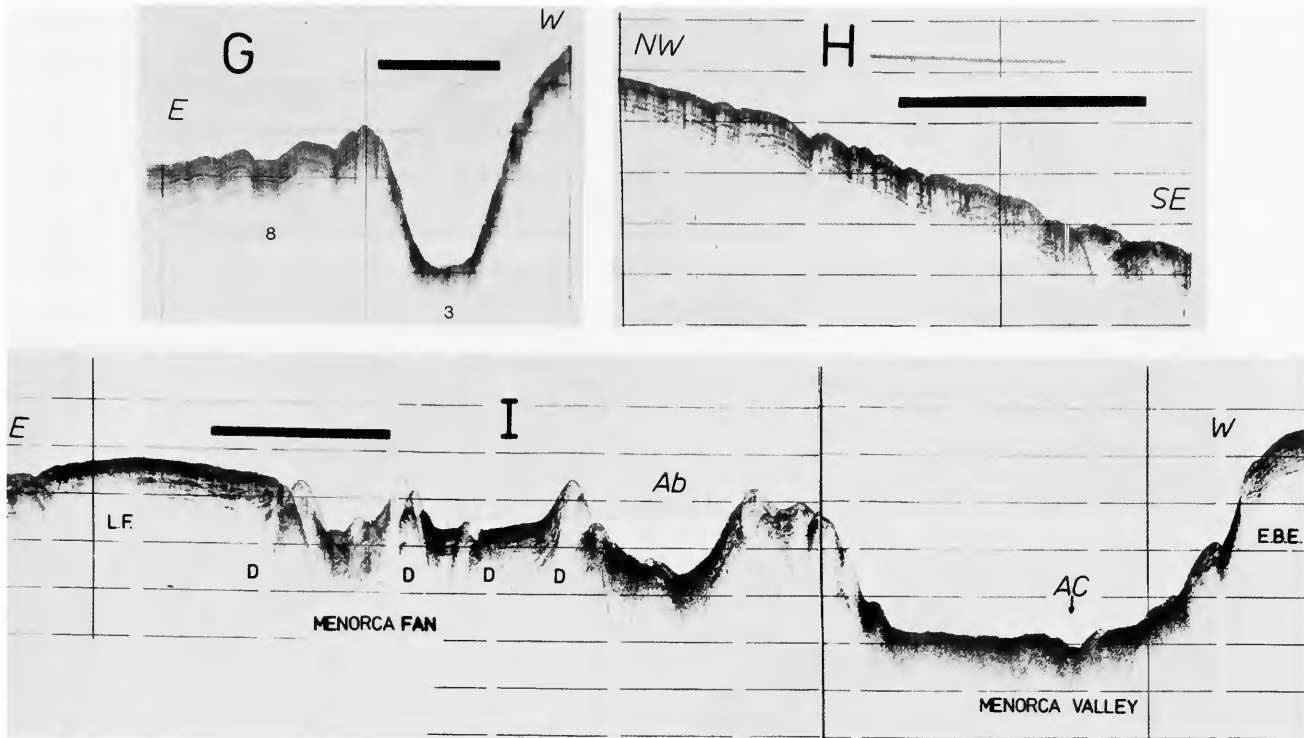


FIGURE 5.—Continued

leveled fan sediments; note slumped type 4 echo character of lower Emile Baudot Escarpment, type 2 character of Menorca Valley floor, type 6 character of diapir-dominated western sector of Menorca Fan and type 4/5 nature of elevated levee region at eastern, left, end of profile.

southeastern margins of the Balearic Rise (Figure 7). Although most commonly transitional into type 2, this form of echo character is frequently found in association with type 4 and type 5 zones (Figure 7). Analogy with comparable acoustic records elsewhere (e.g., Damuth, 1975; Damuth and Hayes, 1977) suggests that the type 3 acoustic signature is derived from a seafloor composed of, and probably underlain by, thick sand layers (accounting for the rare, poorly defined sub-bottom reflectors). This interpretation is supported by the fact that the core (MC8) that contains almost the highest proportion of sand layers (51% of total section) and the thickest sand units on the Balearic Rise was obtained from an area of type 3 echo character (see Figure 1B and Tables 3 and 4).

Echos assigned to the type 4 category have the most widespread distribution in the deeper Balearic margin (Figure 7) and occur on the lower

slopes of the Emile Baudot Escarpment, the Menorca Ridge, the Pinnacles Province, and on the Balearic Basin plain. This category, however, is conspicuously absent from the Menorca Canyon, Valley, and Fan regions. Moreover, areas yielding this type of acoustic response abut randomly against every other echo-type. The cores (1, 2, 7, and 10) from type 4 regions are mud-dominated (Table 4) with only a few thin, fine sand or silt units (Figure 1B). This observation, together with a comparison with analogous records elsewhere (Heezen and Johnson, 1969; Damuth, 1975; Maldonado and Stanley, 1976b) suggests that this category of echo is derived from relatively thick sequences of hemipelagic lutite. The precise mechanical reason for generation of the multiple subbottom reflectors in these mud-sequences is obscure (but see p. 00, and cf. Damuth, 1975:39-40).

Type 5 echo character has been recorded from

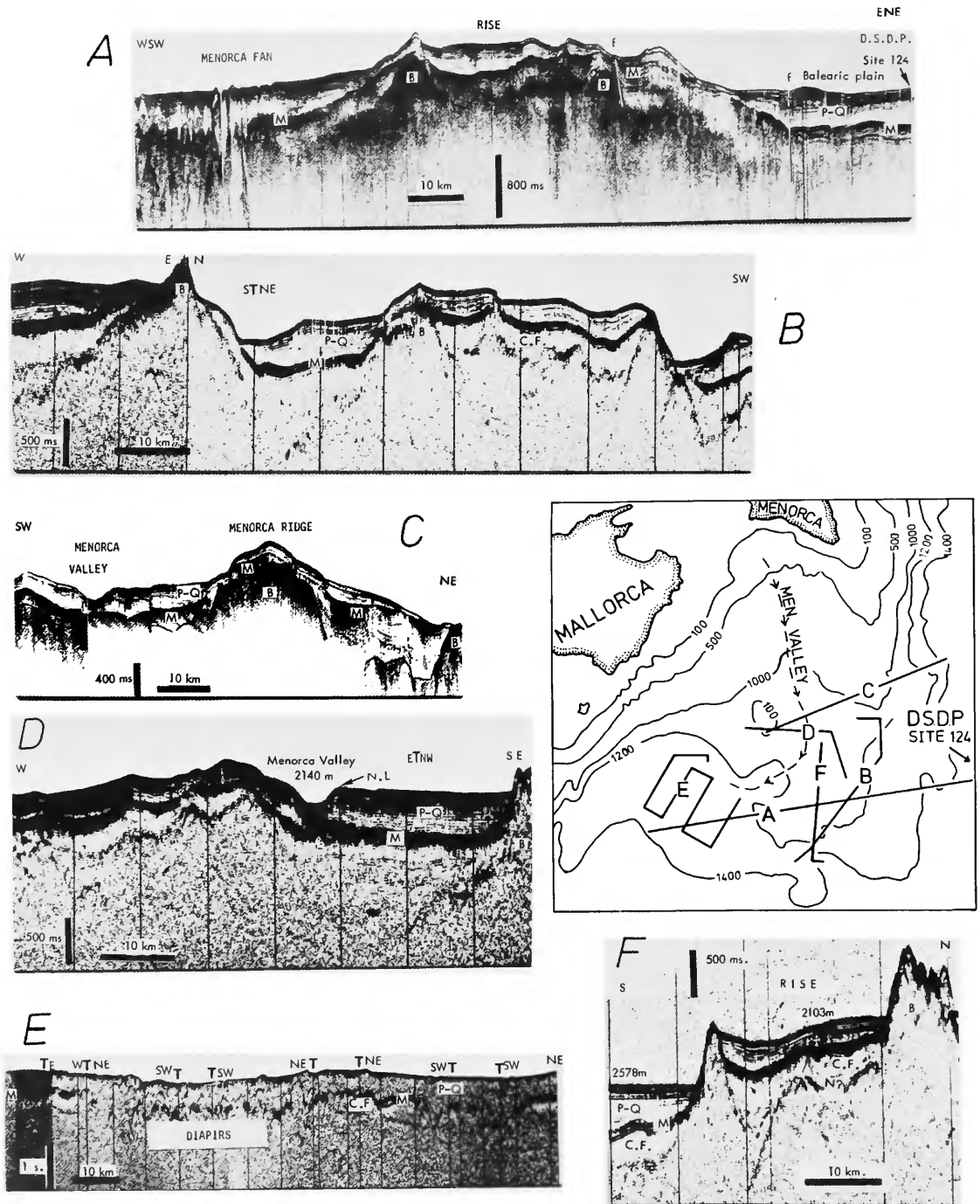


FIGURE 6.—Seismic profiles across Balearic Rise, illustrating typical horst and graben structure, variable thickness of Plio-Quaternary sequence, and importance of halokinetic features (inset shows location of profiles; all profiles from 30,000 J sparker records, except for A and C, which are from air-gun records, B = acoustic basement; C.F. = "couche fluante"; M = horizon M reflectors; N.L. = natural levee; P-Q = Plio-Quaternary sequence; T = turn and change of

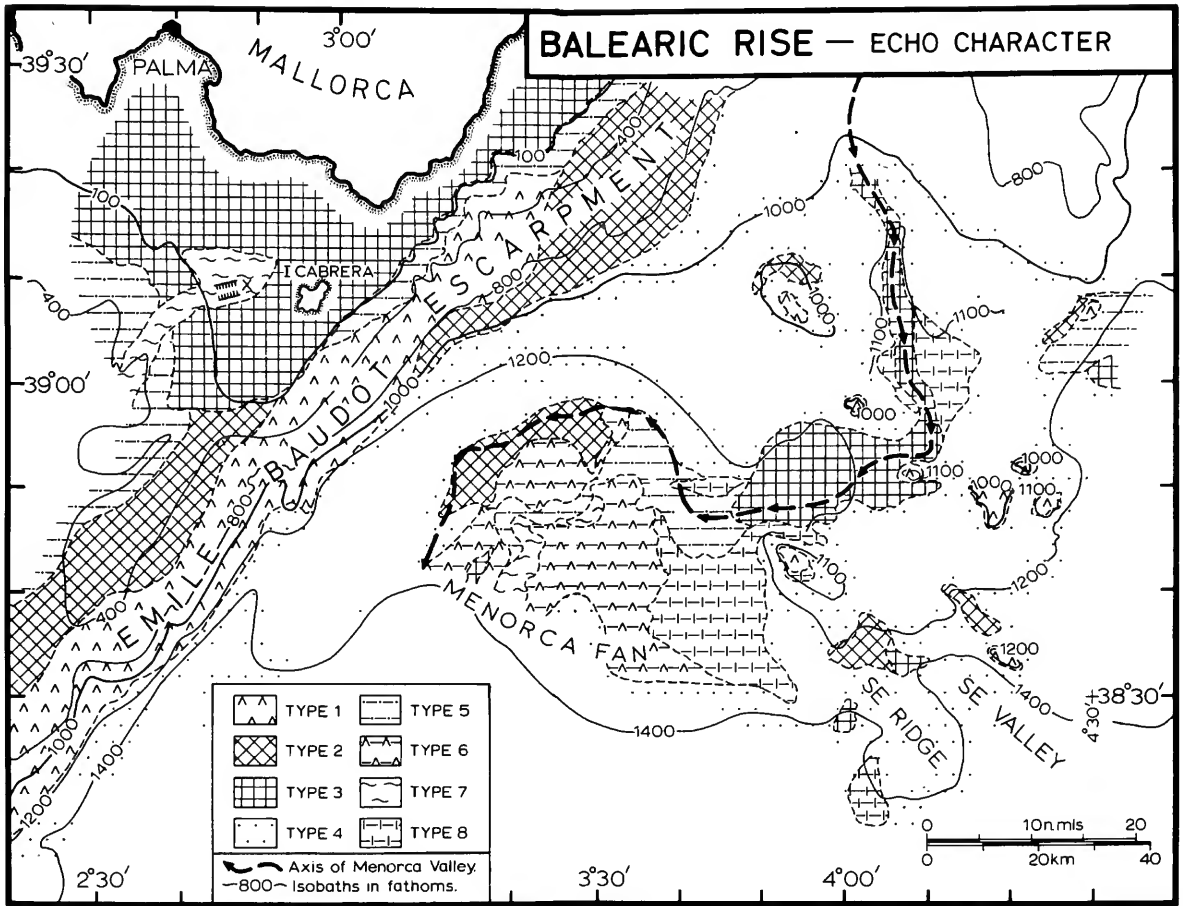


FIGURE 7.—Map showing generalized distribution of echo character based on 3.5kHz profiles, supplemented by 12kHz records in few places (feature X, near Cabrera Island, is an outer shelf channel; see text for explanation).

FIGURE 6.—Continued

heading; modified from Stanley et al., 1976): A, profile across southern sector of rise from Balearic Basin plain near DSDP Site 124 (note mantled basement high left of center in profile, which is Layered Pinnacle V (Figure 8), and salt domes penetrating surface of Menorca Fan); B, profile across eastern flank of rise in pinnacles/Southeast Ridge province; basement elevation at left is Penetrative Pinnacle R (Figures 4J,8); C, profile illustrating fault-bounded nature of Menorca Ridge, with marked offset of M (and P-Q) reflectors; D, profile across inner Menorca Valley and adjacent Balearic Rise; basement elevation at right end of profile is Penetrative Pinnacle Y, possibly volcanic, while Layered Pinnacle Z, thickly mantled by sediments, is located just west of Menorca Valley (Figure 8; note thick levee sequence to east of the valley; cf. Figure 5G). E, profile across Menorca Fan, illustrating relatively muted surface morphology and prevalence of salt diapirs, originating from "Couche Fluyente" horizon; F, profile across southeast sector of Pinnacles Complex and into Southeast Valley marginal depression (at left), showing faulted southern boundary of the Rise; basement elevation at right end of profile is Penetrative Pinnacle Y (Figures 4F,8).

TABLE 3.—Sand content and composition of the sand-size fraction of selected samples from Balearic Rise cores (symbols as in Figure 12)

Sediment Type %	● Total Sand (n = 34)				Sediment Type %	● Channel Sand (n = 16)					
	Sand	A	B	C		Sand	A	B	C		
	max.	95	24	91		25	max.	95	20	86	25
	mean	69	12	78		9	mean	87	10	80	9
	modes	90-100 80-90	10-15 5-10	80-85 75-80		5-10 0-5	modes	90-100	5-10 10-15	80-85	5-10 0-5
	min.	14	2	61		0	min.	70	3	74	3
Sediment Type %	● Turbiditic Sand (n = 18)				Sediment Type %	● (n = 7)					
	Sand	A	B	C		Sand	A	B	C		
	max.	90	24	91		25	max.	15	76	83	8
	mean	53	13	77		8	mean	7	37	59	3
	modes	(60-70)	10-15	70-80 80-90		5-10 (0-5)	modes	none	(20-30)	none	0-3
	min.	14	5	61		0	min.	0.1	13	22	0.9
Sediment Type %	⊙ (n = 11)				Sediment Type %	⊙ (n = 44)					
	Sand	A	B	C		Sand	A	B	C		
	max.	3	45	86		12	max.	9	76	68	6
	mean	1.5	29	64		6	mean	6	53	45	1
	modes	0-1 (2-3)	(40-45)	(50-60) (80-90)		(3-6) (6-9)	modes	3-5 (5-7)	50-60 (40-50)	40-50	0-2
	min.	0.1	11	45		0.8	min.	3	35	22	0
Sediment Type %	⊙ (n = 13)				A = pteropods (1) + planktonic forams (4) B = shells (molluscs) (2) + shell fragments (3) + benthonic forams (5) + ostracods (6) + bryozoa (7) + others (echinoderms, spongy spicules, ... ) (8) C = heavy minerals (10) + mica (11) + pyrite (12) + light minerals (13) + volcanic ash (14)						
	Sand	A	B	C							
	max.	21	72	67						2	
	mean	14	50	48						0.8	
	modes	10-12 (14-16)	(30-40)	(50-60)						0-1	
	min.	10	33	26						0	

Total number of samples, N = 131 (of these, 22 were not well defined or ascribed to a specific sediment type)

TABLE 4.—Percent of sediment types and relative abundance of sequence type in Balearic Rise cores

CORE	LENGTH (cm)	PERCENT OF SEDIMENT TYPE IN CORE					FREQUENCY OF SEQUENCE TYPE (*)		
		●	◐	◑	◒	◓	CHANNEL	TURBIDITE	HEMIPELAGIC
MC1	545	-	1.4	21.6	67.4	9.6	--	$T_e^t, (T_{de})$	++
MC2 (P)	250	2.0	6.8	28.0	60.4	2.8	--	$T_e^t, (T_{a-e})$	++
MC3	577	3.8	-	7.2	85.6	3.9	--	$T_{c,e}; T_e$	++
MC4 (G) (+)	78	-	-	-	89.2	10.2	--	--	++
MC5A	249	53.0	-	-	37.8	9.2	++	$(T_c)$	+
MC6	413	39.0	1.9	14.3	41.9	2.9	+	$T_c, T_{c-e}, T_e^t$	+
MC7	488	-	-	9.4	78.7	11.9	--	$(T_e^t)$	++
MC8	441	51.1	0.4	5.9	42.6	-	++	$(T_e^t)$	+
MC9	336	19.6	3.8	5.6	60.9	10.1	--	$T_{a-c}, T_{a-e}, (T_{d-e})$	++
MC10	360	-	4.7	7.8	82.3	5.2	--	$T_{d-e} T_e^t$	++
MC11	107	10.3	4.7	36.4	38.3	10.3	--	$T_e^t - T_{a-e}$	+

(\*) predominant, >50%: ++; abundant, 30-50%: +; absent: --

turbidite sequence types shown in their order of abundance;  
symbols shown in parentheses indicate low frequency

(+) core MC4 (P) collected next to MC4 (G) shows bioclastic sand.

two main regions of the Balearic Rise: the outer portion of the Menorca Valley (including a narrow zone traversing the fan), and a smaller development near Pinnacle R and associated with the Menorca Ridge-Balearic Basin plain boundary (Figure 7). Elsewhere, this acoustic category characterizes the strongly gullied slope west of Cabrera Island and south of Palma de Mallorca (Figure 7).

Areas exhibiting Type 5 echo character generally adjoin type 3 or type 4 regions, but some profiles demonstrate gradation of the type 5 echos into type 6, 8, or 7 (in declining order of importance).

The distinctive aspect of type 5 acoustic profiles is the presence of a number (between 2 and 8) of diffuse subbottom reflectors that appear gently flexed or lensoid and thus give the impression of being portions of very broad hyperbolae, somewhat overlapping. The minor surficial irregularities and the prolonged echo from the sediment/water interface are reminiscent of the type 3 response and suggest the presence of a sandy seafloor. The two piston cores obtained from type 5 areas (MC5A

and 6) contain high proportions of sand and include several thick arenite units (see Figure 1B and Tables 4 and 5), confirming the existence of a coarse sediment cover. The geometry and lensoid nature of the grouped subbottom reflectors suggests the presence of large-scale depositional features, perhaps major, low-amplitude dunes or, more probably, sandy fan lobes (cf. Damuth, 1975: 36, 40). It is important, however, to note that these subbottom reflectors are normally mantled by the surficial sand-layer, indicating that active deposition (not erosion) is responsible for the contemporary seabed physiography.

Acoustic responses assigned to type 6 are confined to the Menorca Fan region. Areas yielding type 6 echos are contiguous with regions exhibiting every other echo character, excepting type 1 (Figure 7). The unique feature of type 6 echograms is the occurrence of isolated, internally "transparent" hyperbolae that abruptly truncate adjacent subbottom reflectors and, in many instances, penetrate the sediment/water interface to form positive topo-

TABLE 5.—Association of sediment sequences in cores collected in the different Balearic Rise environments

TYPE A: Channel sequences predominate or are very abundant (channel areas)	
MC5A	No turbidite mud, only Tc
MC6	Tc, Tc-e, Te <sup>t</sup>
MC8	No turbidite sand, only Te <sup>t</sup>
TYPE B: Abundant sand turbidite sequences; hemipelagic sequences abundant to predominant (banks)	
MC9; MC11	Thick, complete sand turbidite sequences
MC4 (G)	(Too short to provide reliable data); characteristic parallel or irregular thin lamination in the mud; may be attributed to some sort of bottom currents or distal mud turbidite sequences. Core MC4 (P) shows sand turbidite at its base.
TYPE C: Rare turbidite sequences; hemipelagic sequences largely predominate (levees, gently sloping platform)	
MC3	Some thin sand turbidite sequences; flaser; thin irregular lamination (natural levee deposits)
MC7	Only mud turbidite sequences
MC10	One thick characteristic silt turbidite sequence; the others are mud turbidite sequences
TYPE D: Abundant to rare mud turbidite sequences; hemipelagic sequences predominate (basin plain)	
MC1	Some thin silt turbidite sequences
MC2	Some sand to silt turbidite sequences

graphic features on the seafloor (up to 45 m high and 1.5 km across; see Figure 5D, E, I). In some profiles the hyperbolae do not actually breach the seafloor but are discernible as acoustically transparent zones in the subbottom.

These features closely resemble the salt-domes and diapirs recorded from 3.5 kHz profiles across the Balearic Basin plain (Stanley et al., 1974b) and are attributed to the same cause. Sparker and air-gun records from the Menorca Fan region clearly display these diapirs, emanating from the "couche fluante" horizon below the 'M' reflectors (Stanley et al., 1976). The diapirs appear to penetrate randomly all the Plio-Quaternary sediment facies that have been distinguished here. The locations of salt-domes penetrating the seafloor and encountered on our profiles are indicated on Figure 8. It may be significant that this diapir field is associated with the zone of maximum thickness for the Plio-Quaternary sequence (Figure 2) on the Balearic Rise.

On the Balearic Rise proper, type 7 echo character has been encountered in only one sinuously elongate portion of the Menorca Fan, although a

slightly larger linear area occurs on the Mallorca Shelf and upper slope to the east of Cabrera island (Figure 7). This acoustic type most commonly occurs in proximity to areas of type 5 echo character and these two categories appear to be mutually gradational. The principal difference between type 5 and type 7 echograms is that in the latter there is evidence of the truncation of subbottom reflectors at the seafloor, and similar truncation is discernible within the subbottom sequence. Persisting and active erosional activity is thus indicated for these regions, a conclusion supported by the existence of an E-W oriented channel-like depression encountered on the Mallorca Shelf east of Cabrera (Figure 7) and within the area characterized by type 7 echo character. The sole piston core obtained from a type 7 area (MC3) is mud-dominated, with only a small proportion of bioclastic sand, forming a few thin turbidites (Table 4 and Figure 1B). Nevertheless, this echo type is interpreted as a channeled sequence and associated levee deposits now undergoing active erosion.

Type 8 echo character is encountered in two main areas of the rise. The larger zone intervenes



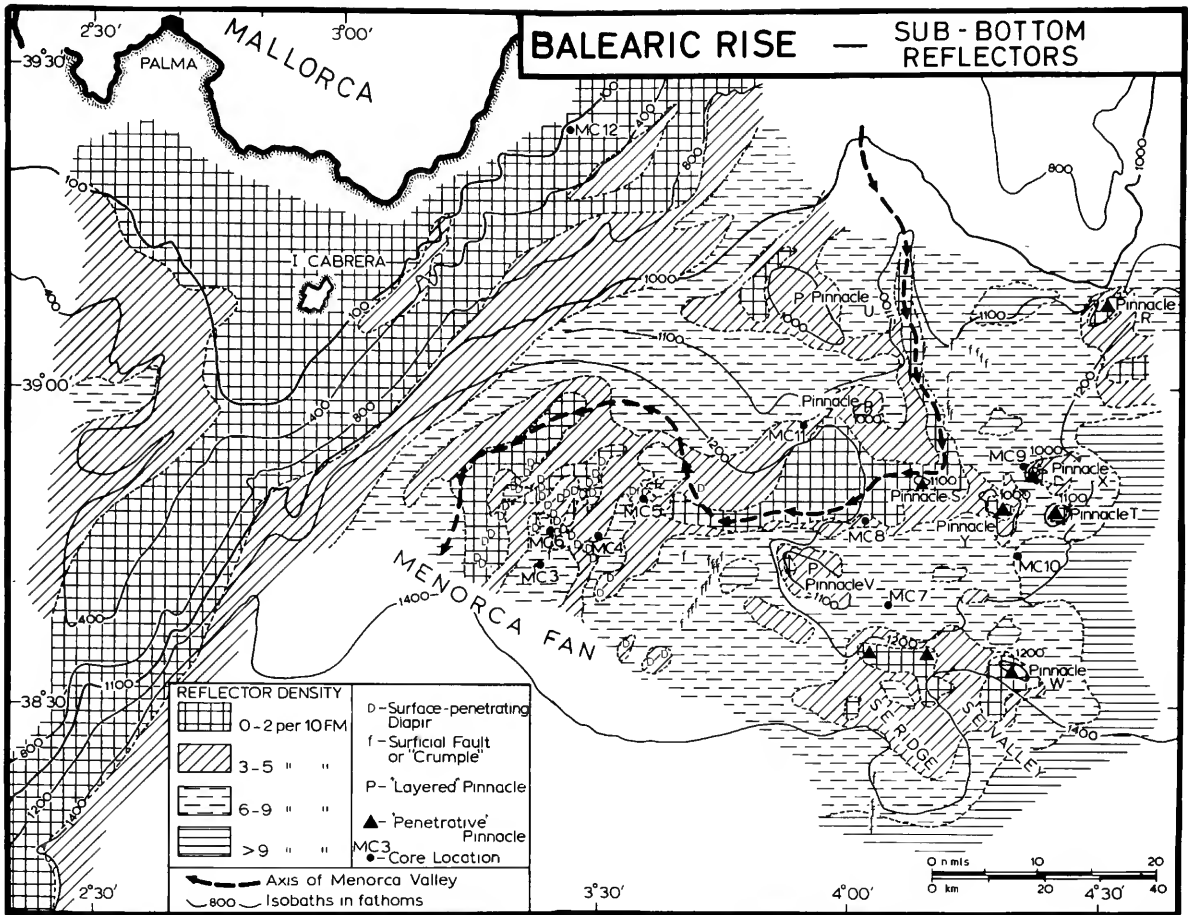


FIGURE 8.—Map showing generalized distribution of sub-bottom reflector density, determined from 3.5kHz profiles; locations of sediment-cores obtained on *Lynch-I* cruise are indicated, together with the Layered and Penetrative Pinnacles, surface-penetrating diapirs, and surficial "crumples" (probably related to sediment creep or slumping; see text for explanation).

between the eastern margin of the Menorca Fan and the western slope of the Southeast Ridge, while the other region occurs on both flanks of Menorca Canyon, immediately north of the abrupt westward change in trend. Smaller areas of type 8 echos occur within the Menorca Valley, near the apex of the fan, and on the gently dissected margin of the basin plain where it abuts against the southern flank of the Southeast Ridge (Figure 7). Thus this echo type appears to be developed mainly on the gently sloping levee-like areas adjacent to the presently active canyon-fan system and also appears to be gradational laterally into the type 4 category (Figure 5G, H). The individual surface undulations

vary from 5 to 15 m in height and from 0.3 to 1.5 km (0.2 to 0.8 n mi) in width and generally display an upslope facing asymmetry. Unlike more typical deep-sea dune forms (Jacobi et al., 1975), the sub-bottom reflectors in the type 8 hyperbolae do not display a laterally migratory internal geometry but tend to be separated by subvertical planes of acoustic "shadow" (Figure 5H). Although these planes present a superficial resemblance to minor faults and have been indicated as such on Figure 8, there is no physical displacement of the reflectors on either side. Thus it is considered that the type 8 undulations represent either superficial "crumples" formed during incipient stages of slump deforma-

tion (similar to the features described by Jacobi, 1976) or large-scale constructional bedforms similar to those reported by Damuth (1975), Damuth and Hayes (1977), and Jacobi et al., (1975). At present it is not feasible to distinguish between these two possibilities. The consistent occurrence, however, of these undulatory features on sloping regions subject to relatively high sedimentation rates and the lateral attenuation of this acoustic facies against rocky, more steeply inclined elevations, such as the Southeast Ridge Pinnacles (Figure 7), favors a slumping origin.

#### DISTRIBUTION OF REFLECTOR DENSITY

A more quantified appraisal of the variations in acoustic response recorded in the 3.5 kHz profiles is provided by a map that depicts the distribution of the relative density of subbottom reflectors across the south Balearic margin (Figure 8). This diagram

is based on the number of reflectors observed within (or extrapolated to) an arbitrary 10-fathom (18 m) standard. The relative frequency of subbottom reflectors depends to some extent on instrumental performance that is influenced, in turn, by a number of external factors such as sea-state, ship's speed, etc. Thus an element of subjectivity is present even in this ostensibly quantitative measure of acoustic response. In particular, the distinction between the two highest reflector density classes (6-9 and >9) must be regarded as tentative since the seismic configuration used is capable of this degree of resolution only under optimum conditions. Moreover, as indicated in the discussion of the type 4 echo character (p. 13) the nature of the sedimentary controls governing generation of close-spaced reflectors remains obscure. Comparison with the lithologies revealed in piston and gravity cores suggests, however, that there exists a crude inverse correlation between total sand/silt content and reflector

TABLE 6.—Balearic Rise sediment sequence associations A-D (defined in Table 5) in relation to 3.5kHz echo character type, reflector density, sequence density and layer density

CORE	SEQUENCE ASSOCIATION	ECHO CHARACTER TYPE	REFLECTOR DENSITY	SEQUENCE DENSITY (*)		LAYER DENSITY (+)	
				<u>Seismic Profiles</u>		<u>Cores</u>	
MC1	D	4	>9	(9)	30	(1)	3
MC2	D	4	>9	(7)	51	(2)	15
MC3	C	7	6-9	(6)	19	(3)	9
MC4	B	6	6-9	(0)	0	(0)	0
MC5A	A	5	3-5	(2)	15	(2)	15
MC6	A	5	3-5	(15)	66	(4)	18
MC7	C	4	6-9	(4)	15	(0)	0
MC8	A	3	3-5	(6)	25	(3)	12
MC9	B	3	3-5	(4)	22	(4)	22
MC10	C	4	>9	(4)	20	(1)	5
MC11	B	3	3-5	(4)	69	(1)	17

(\*) Extrapolated from core length to 10 fm of stratigraphic section and calculated for turbidite plus channel sequences

(+) Only sand layers considered and extrapolated from core length to 10 fm of stratigraphic section

The number in parentheses shows the actual number of layers and sequences observed in the core

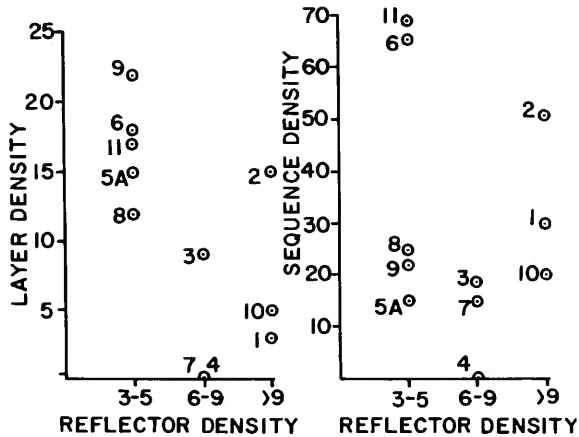


FIGURE 9.—Graphs illustrating relationships between relative density of subbottom reflectors (determined from 3.5kHz records and related to an arbitrary 10 fm or 18 m, vertical interval), (left) density of well-defined sand or coarse silt layers (actual frequency of layers encountered in cores, extrapolated to an arbitrary 10 fm stratigraphic section), and (right) density of turbiditic plus channel sequences (actual frequency encountered in cores, extrapolated to an arbitrary 10 fm stratigraphic section; numbers adjacent to plotted points refer to relevant cores; see Figures 1B, 8, Table 6).

density (Tables 4 and 6) and there appears to be a similar inverse correlation between the frequency of well-defined sand/silt layers and reflector frequency (Figure 9). Thus the reflector density map (Figure 8) may be regarded as crudely indicating the lateral distribution of sand and silt within the near-surface sediments (bearing in mind that areas of outcropping rock will be included also in the lowest category (0 to 2) of reflector density).

Not surprisingly, the broad pattern revealed by Figure 8 is comparable with that revealed by the distribution of echo character (Figure 7). The highest reflector densities are encountered on the Balearic Basin plain and in a few small areas perched on the Pinnacles/Southeast Ridge province-zones that appear to be dominated by hemipelagic sedimentation. Low reflector densities occur on the Mallorca Shelf and the Emile Baudot Escarpment and also characterize the Menorca Canyon, Valley, and Fan complex. The south- and southwest-trending linear belts of differing reflector density encountered on the Menorca Fan (Figure 8) provide graphic evidence for the existence of a system of distributary fan-channels, formerly active but now

bypassed to the north and west by the main Menorca Channel (Figures 2 and 3).

Smaller areas of low reflector density occur around both the Penetrative and the Layered Pinnacles. These pinnacle types are distinguished not only by minor physiographic differences but also by contrasting subbottom characters. The Layered Pinnacles are mantled by a substantial thickness of layered sediments (Figure 6A, B) whereas Penetrative Pinnacles display only a thin veneer of sediments above acoustically confused rock-basement (Figure 6D, F). The lateral extension of such zones of low reflector density into flatter areas such as the Southeast Valley or the "moated" depression northwest of Pinnacle U (Figure 8) suggests that in addition to outcropping rock such areas may also include regions of sand- or silt-covered seafloor, presumably derived either (a) from localized erosion of rock forming the pinnacles, or (b) from reworking and displacement of fines, leaving a coarser sediment lag.

#### Major Sediment Types on the Balearic Rise

The preceding analysis of seismic and morphologic attributes has been supplemented by a study of 131 unconsolidated sediment samples from 11 piston and gravity cores (1 to 6 m in length) collected on the Balearic Rise and adjacent Balearic Basin plain (Figure 8). Representative samples were collected from each of the major sediment types identified in split cores and core X-radiographs. Sample thickness ranges from 2 to 5 mm; it was not possible to sample thin (<2 mm) laminae without collecting material from adjacent laminae. The sample position in each core is indicated by a letter-number code to the left of the lithologic logs in Figure 10.

The organic matter in each sample was removed with hydrogen peroxide, and the fraction coarser than 63 microns was separated by wet sieving. Grain counts (300 to 400 grains per sample) of the sand fraction were made by unit area measurement. Fourteen major sand-sized components have been grouped into three categories: (A) pteropods and planktonic foraminifera; (B) shells (molluscan), shell fragments, benthonic foraminifera, ostracods, bryozoa, others (echinoderms, sponge spicules, etc.), plant fragments; and (C) heavy minerals, mica, pyrite (used here as a general term for any form of

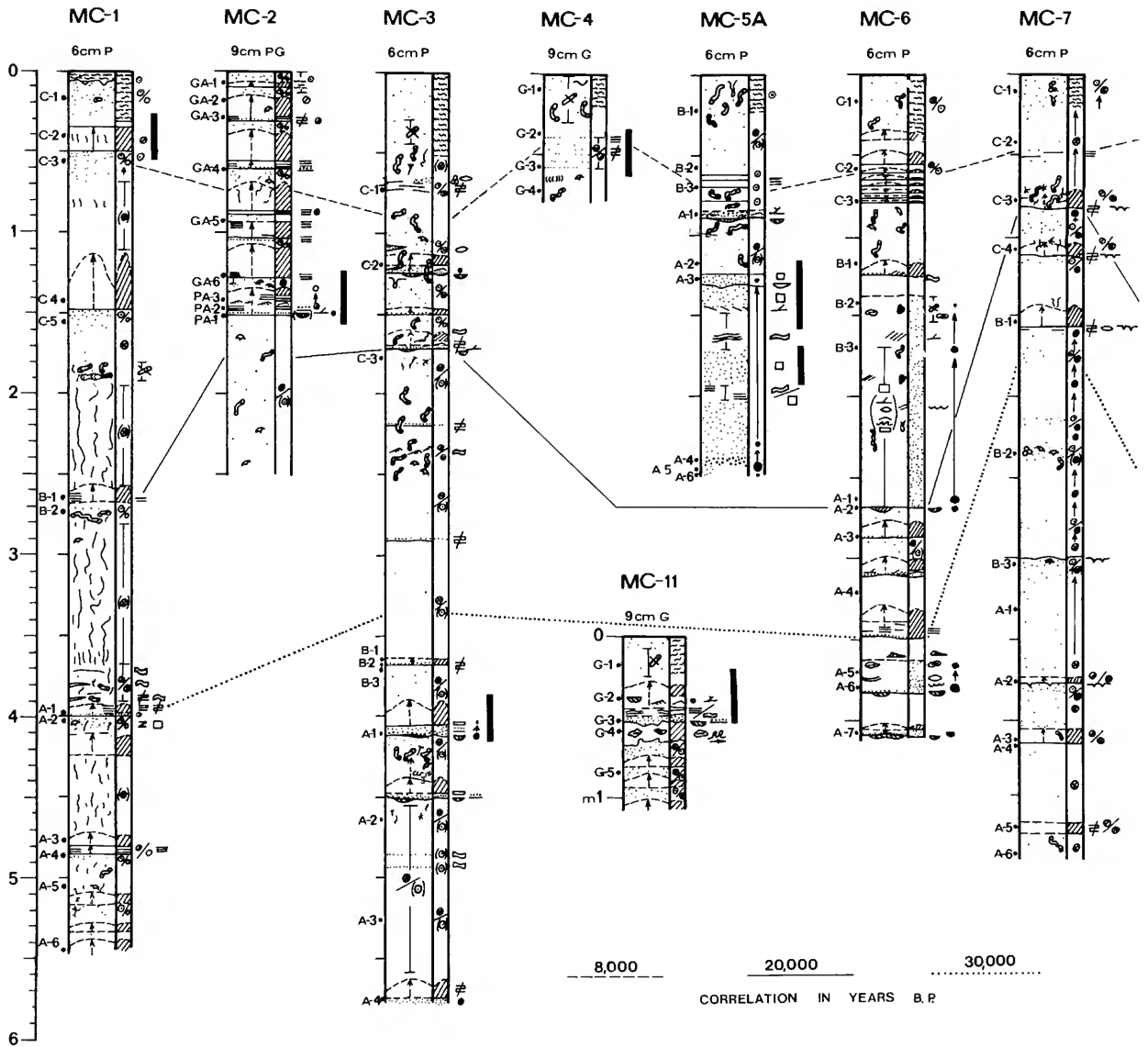
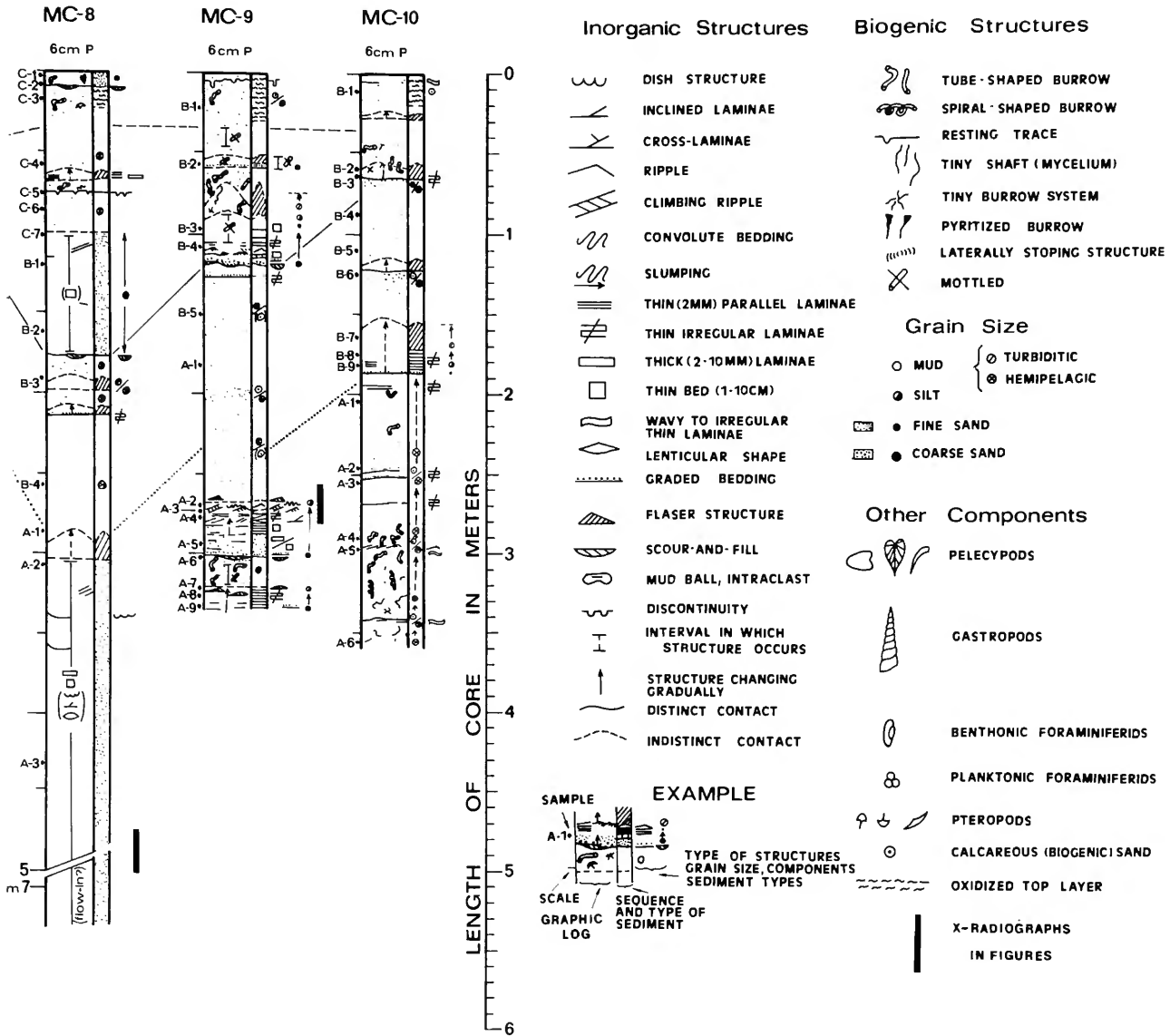


FIGURE 10.—Lithologic logs of 11 Balearic Rise cores (location of cores shown in Figures 1B and 8).

ferrous sulphide), light minerals, and volcanic ash. The results of the grain count analysis of each core sample are plotted on compositional triangles (Figure 11). All grain counts also are plotted in the upper compositional triangle in Figure 12 and the data are summarized in Table 3. The grain count data used to prepare Figures 11 and 12 have been listed in two tables in the Appendix.

Five main sediment types are recognized in

Balearic Rise cores: (1) bioclastic (terrigenous) sand; (2) silt; (3) turbidite mud; (4) hemipelagic mud; and (5) calcareous ooze (sandy mud). These are distinguished by the amount and composition of the sand fraction, and by sedimentary structures observed in split cores and in core X-radiographs. Each sample is assigned to one of these five types on Figures 11 and 12; the legend for the symbols used is given in Figure 12. The five sediment types are



compositionally gradational as noted on the lower triangular diagram in Figure 12.

The *bioclastic (terrigenous) sand* type is present to dominant in seven of the cores examined, but is absent in cores MC1, MC7, and MC10 (Figure 11, Table 4). The total sand fraction content is generally the highest of all the sediment types (Table 3), but is highly variable (14% to 95%). Planktonic (A) and inorganic (C) components are

low. The benthonic biogenic fraction (B) is predominant, comprising at least 60 per cent in all sand samples that are thus concentrated at the B component apex of the two triangular diagrams in Figure 12. Two sand subtypes are recognized: (a) channel sand, and (b) turbidite sand.

The first subtype, *channel sand*, is generally thick (>70 cm), coarse-grained units that contain a mix of sand-sized components. Lithologic breaks

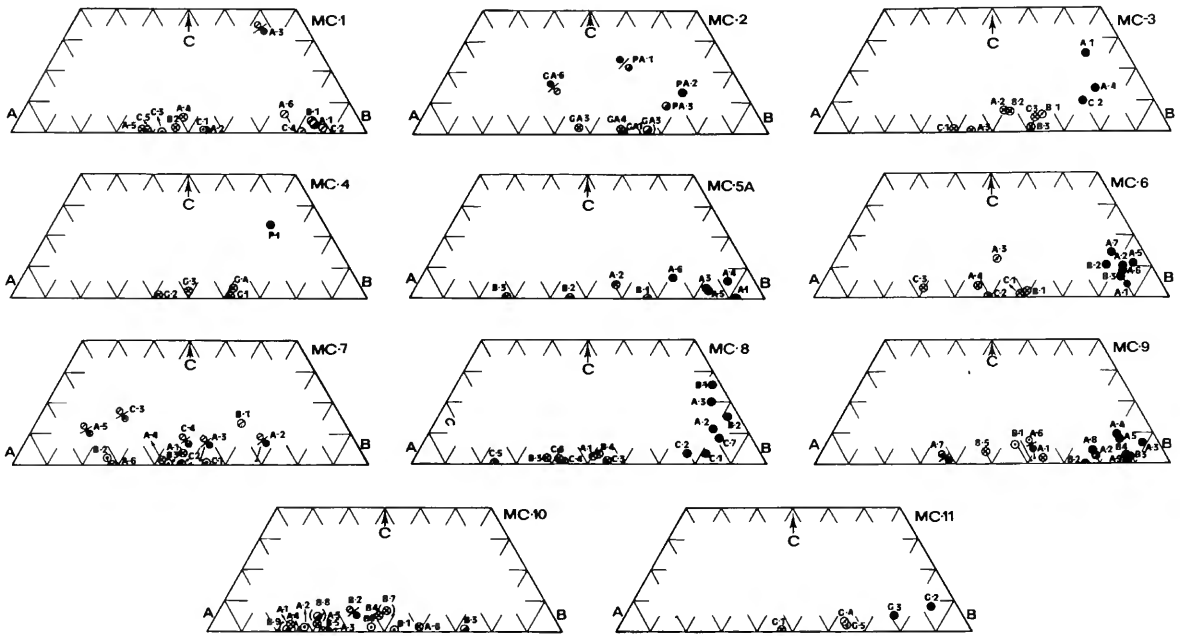


FIGURE 11.—Composition of sand-size fraction ( $> 63\mu\text{m}$ ) of selected samples from 11 cores collected in Balearic Rise and plotted on triangular diagrams (letter-number code of each sample is shown on core logs in Figure 10; compositional end-points on triangles: A, pteropods and planktonic foraminifera; B, shells (molluscs), shell fragments, benthonic foraminifera, ostracods, bryozoa, others (echinoderms, sponge spicules, etc.), plant fragments; c, heavy minerals, mica, pyrite, light minerals and volcanic ash; symbols of sediment type given in Figure 12.)

within a single channel sand unit are generally emphasized by the presence of erosional contacts and marked differences in texture (Figures 10 and 13; cores MC5A:125–132 cm, MC8:587 cm). The most abundant components are shell fragments (usually  $>70\%$ ), planktonic foraminifers (5% to 10%), and light minerals ( $\cong 5\%$ ) (Tables 3). Mica and pyrite are absent or present in trace amounts only. Sand-size material shows different states of preservation; some bioclastic particles are stained with iron oxide and grain edges are rounded and worn. The shell fragments represent mixed thanatocoenoses, i.e., residual biogenic material of variable age from different environments. The light mineral fraction includes very well-rounded and pitted limestone grains, probably derived in part from calcareous Mesozoic and Tertiary formations on the islands of Mallorca and Menorca (cf. Obrador et al., 1971) and the adjacent submerged Balearic Platform. The sand samples contain only a minor amount of siliceous grains and a negligible amount of (or no) lutite matrix. These channel sand strata

have sharp erosional bases and well-defined tops and generally comprise alternating structureless and cross- or wavy-laminated layers (Figure 13). These strata sometimes display poorly defined concave-upward laminations, possibly dish structures (Stauffer, 1967). Upward grading to finer sediment is not common (Figure 10; core MC5A, MC6, and MC8; see non-gradational groupings in Figure 11: cores MC6 and MC8).

The typical *turbidite sand*, the second subtype, generally grades upward to the silt sediment type, and displays a wider range of sand content. The content is usually lower than in channel sands; a sand content of at least 15% is used to distinguish turbidite sands from the silt type. Sorting of the turbidite sands is poorer than in channel sands. The proportions of components (A), (B), and (C) are roughly similar to those of channel sands, but relative percentages are more variable (Table 3). Turbiditic sands usually display the most pronounced suite of sedimentary structures of all the sediment types in the study area. The Bouma

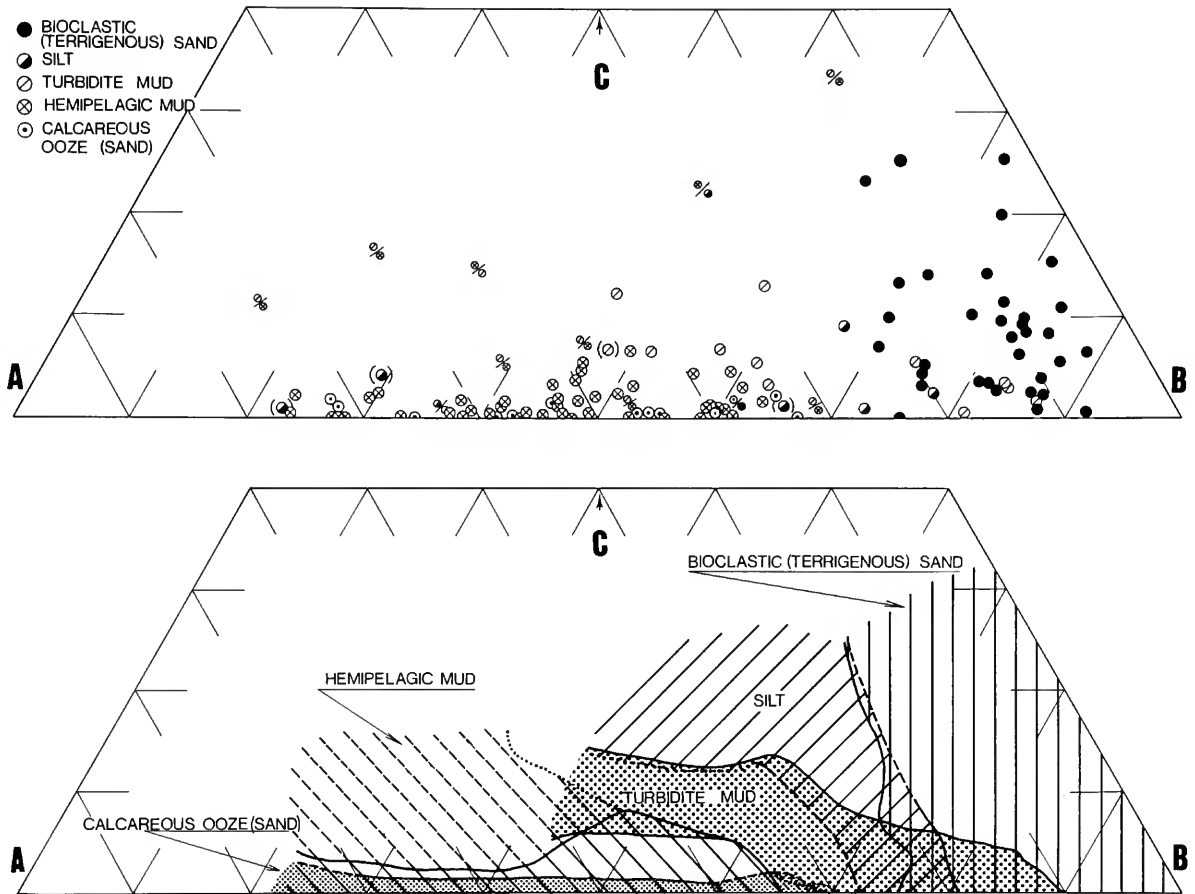


FIGURE 12.—Compositional plots on triangular diagrams of sand-size fraction ( $> 63 \mu\text{m}$ ) of selected samples from 11 cores collected on Balearic Rise (composition end-points on both triangles as in Figure 11; upper triangle shows distribution of 5 major sediment types defined in this study; lower triangle depicts sediments type distribution—explanation in text; data are summarized in Table 3).

(1962) divisions, including graded bedding and cross- and ripple-lamination, as well as flaser structures and starved ripples, are commonly observed (Figure 14).

The *silt* sediment type is the least common type in Balearic Rise cores (Table 4). Sand content ranges between 0.1% and 15%, with a median of 7% (Table 3). The sand fraction composition is highly variable; shell fragments usually comprise more than 50 per cent of the total sand fraction. Planktonic foraminifera are also abundant, and benthonic foraminifera are present or absent. Other biogenic components include echinoderm spicules, bryozoa, ostracods, plant fragments, sponge spicules, and others. The proportion of the inorganic (C)

component is low (mean of 3%) and generally includes traces of mica and pyrite. This sediment type plots toward the right half of the lower compositional triangle in Figure 12 and shows continuity with sand types described earlier.

Sedimentary structures include inclined laminae, wavy to irregular thin lamination or parallel lamination, and flaser structures (Figures 10, 14, 15: cores MC2, MC3, MC9, and MC11). Well-developed laminae occur at the base of silt layers; these disappear upward as these units grade texturally to mud (cf. Figure 14, core MC11GL, from 45 to 37 cm).

The *turbidite mud* type is present in most cores (Table 4), but is relatively less abundant than in

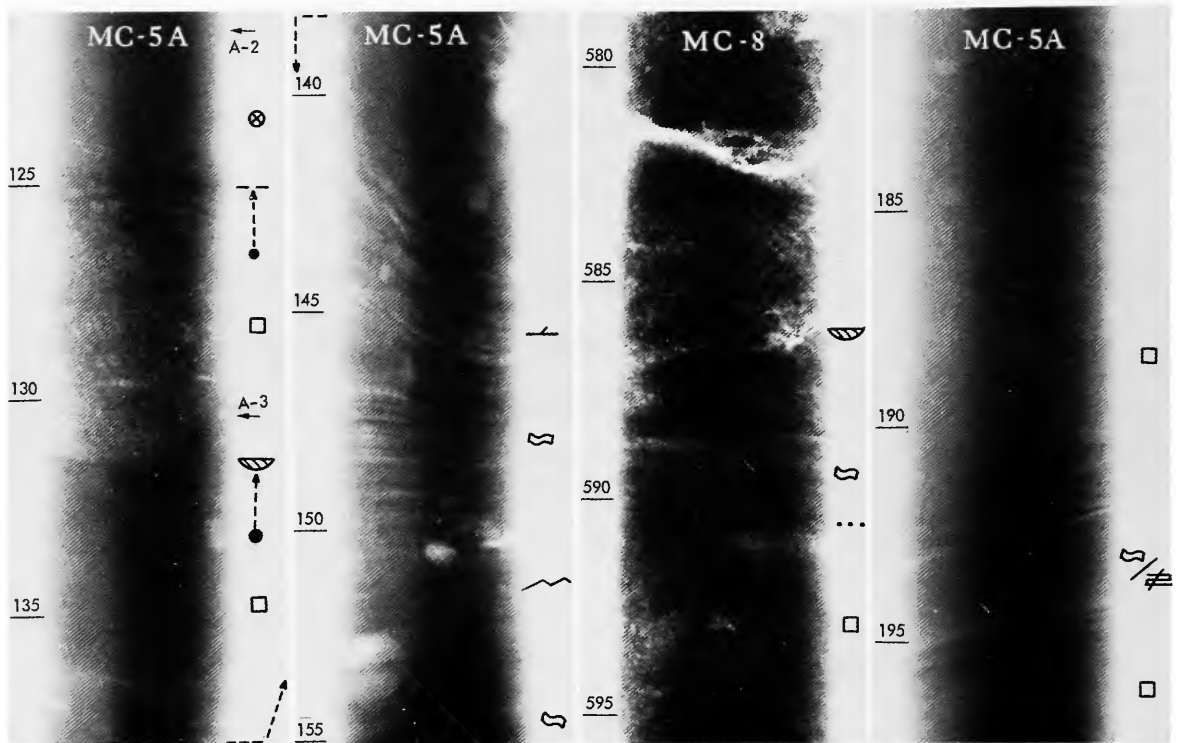


FIGURE 13.—Selected X-radiographs (positive prints) of sands interpreted as channel sequences (scale on left of print shows depth in centimeters from top of core; sections illustrated and legend of symbols used are show in Figure 10; explanation in text).

cores collected in other areas of the Mediterranean (cf. Rupke and Stanley, 1974; Maldonado and Stanley, 1976b). It contains the lowest proportion of sand (0.1% to 3.0%) of all the sediment types (Table 3). The sand fraction is dominated by high proportions (45% to 86%) of component (B). Shell fragments, which predominate, show a mixed origin from different environments as attested by marked differences in the state of faunal preservation. Benthonic foraminifera account for only about 1% to 5%. The planktonic fraction (A) is common to abundant (11% to 45%), with a median of 29%; the proportion of planktonic foraminifera is high in this fraction. The inorganic fraction (C), generally low (1% to 12%), is dominated by heavy and light minerals that usually include angular and flaky grains. Mica is present in most samples. X-radiography usually reveals this mud to be structureless; however, delicate lamination is sometimes observed at the base of the layer. Bioturbation structures are poorly developed, and generally

represented by individual subvertical burrows. Small subvertical tube-shaped burrows, termed *Mycellia*, are observed. In split cores, this mud type is distinguished by its very smooth, uniform aspect due to the low sand content.

Layers of the *hemipelagic mud* type, the predominant sediment in most cores, usually constitute more than 50 per cent of the total core section (Figure 11, Table 4). Sand content (3% to 9%) is higher than in turbiditic mud; the planktonic fraction (A), mainly planktonic foraminifera, predominates (35% to 76%). Component (B), also important (22% to 68%), is dominated by shell fragments (mainly broken tests of planktonic foraminifera and pteropods). The percentage of benthonic foraminifera ranges from 2% to 15%. The inorganic fraction (C) is low (trace to 6%) and usually includes light minerals and traces of heavy minerals, mica, and rarely pyrite. These muds are generally homogeneous in X-radiographs and split cores; they do not display well-defined primary sedimentary struc-



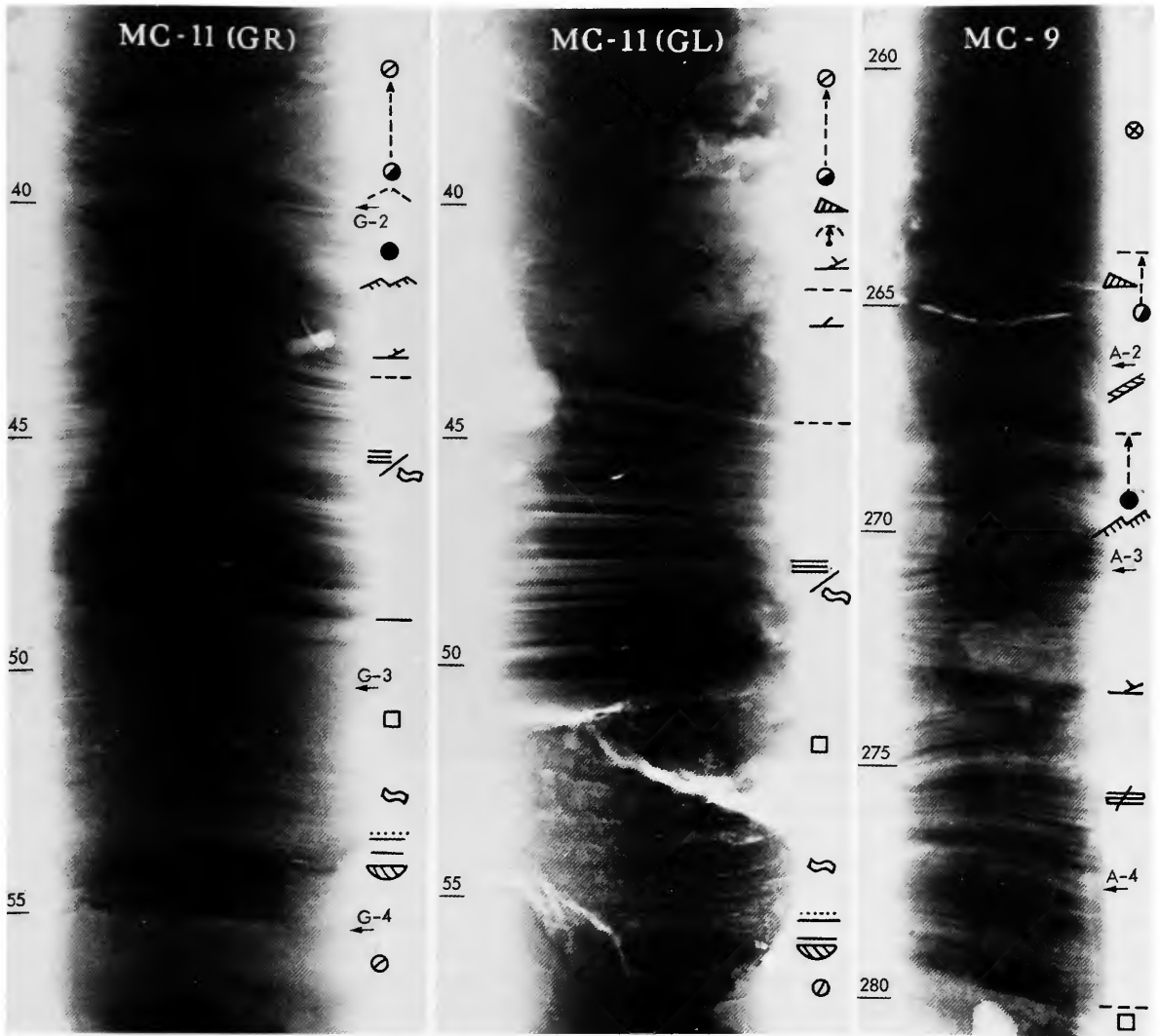


FIGURE 14.—Selected core X-radiographs (positive prints) showing turbiditic sequences; cores MC11 (GR) and MC11 (GL), collected at same station, show slight differences in same turbidite layer (symbols as in Figure 10).

tures, but generally reveal evidence of vertical bioturbation. Moreover, subtle textural, compositional, and color changes are observed (these are discussed in a later section on the hemipelagic-turbidite mud association). This mud type is distinguished in X-radiographs by light speckling produced by tests of planktonic foraminifera, pteropods, and small pteropod fragments that appear to float in a mud matrix (Figure 15 and core MC3, section from 412

to 421 cm; core MC1, section from 50 to 55 cm depth).

The *calcareous ooze* (sandy mud) type, also present in most cores (Figure 11, Table 4), is a variant of the hemipelagic mud type with which it is transitional (lower compositional triangle, Figure 12). Calcareous ooze has a minimum sand content of about 10 per cent, and a maximum of 21 per cent (Table 3). Thin layers composed almost entirely

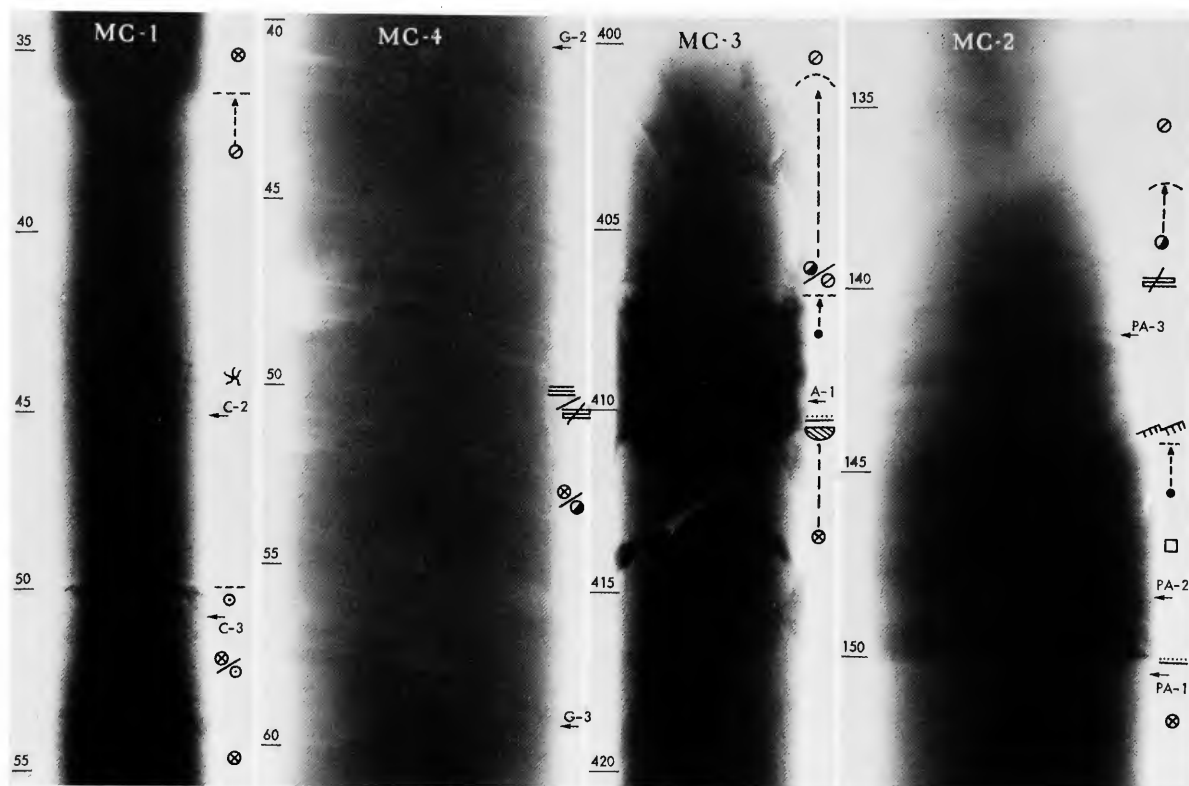


FIGURE 15.—Selected core X-radiographs (positive prints) showing hemipelagic sequence (MC1), laminated mud (MC4), and turbiditic sequences (MC3 and MC2) (symbols as in Figure 10).

of sand-sized planktonic components are also observed (e.g., Figure 15, core MC1, 50 cm). The sand fraction composition is similar to that of the hemipelagic mud, but shows a lower amount of inorganic components (0% to 2%) and an absence of pyrite; the benthonic foraminiferal content also is generally lower (2% to 5%). Sedimentary structures are usually absent; occasionally, poorly developed and thin, irregular laminae are observed. The split core and X-radiographic analyses reveal somewhat higher amounts of planktonic foraminifera and small fragments of pteropods dispersed in a mud matrix than in the hemipelagic mud type (Figure 15, core MC1).

#### Facies Distribution and Processes

The major Balearic Rise sediment types described above form natural assemblages that present distinct lateral and vertical lithologic affinities. Three major sediment associations, or sequences, are rec-

ognized: (a) channel sand sequences; (b) turbiditic sequences, consisting of a variable association of turbiditic sand, silt, and mud; and (c) hemipelagic sequences, consisting of hemipelagic mud and calcareous ooze (sandy mud). Similar sequences have been recognized elsewhere in the Mediterranean, such as the Strait of Sicily (Maldonado and Stanley, 1976b) and the Nile Cone (Maldonado and Stanley, 1976a).

There appears to be a good correlation between the Late Quaternary sediment distribution and the Balearic Rise physiography. Four distinct core assemblages, defined predominantly on sediment type and sequence, are distinguished.

#### CHANNEL SAND ASSEMBLAGE (A)

Assemblage A (Tables 4 and 5) is characterized by a predominance of sand sequences. These sequences include relatively thick (some >1 m) layers of clean, fine- to coarse-grained sands composed of

mixed bioclastic and terrigenous components. These are similar to sediments recovered on the Balearic Platform where a surficial cover of shelly sand and gravel prevails (U.S. Naval Oceanographic Office, 1965; Frazer et al., 1970).

In general, sand layers retrieved in rise cores are not well-graded and their most diagnostic feature is the presence of cut-and-fill structures within the sand units. The composite nature of sand layers is revealed in X-radiographs by marked changes in texture as well as sharp, basal erosional contacts (cores MC5A, 125 to 132 cm; MC8, 587 cm, Figure 13). No consistent vertical sedimentary trends in grain size, mineralogy, or faunal composition are observed within the sand layers. These units do not grade upward to turbidite layers, but are sharply topped by hemipelagic mud (Figure 10, cores MC5A, MC6, MC8). Structureless sand commonly alternates with sand displaying high-angle cross-lamination (Figure 13, core MC5A). Channel sand units are interbedded with hemipelagic mud and turbiditic sequences that show poor (or no) development of  $T_{a-e}$  Bouma turbidite divisions (Figure 10, cores MC5A, MC6).

Cores comprising this sediment assemblage in the Balearic Rise are recovered only close to the Menorca Valley on the upper Menorca Fan (MC8) and on lobes (i.e., MC5A, MC6) of the middle fan (Figure 8). The sand size and texture are remarkably similar in different cores; only small differences in maximum grain size are observed. Minor differences in texture and sand unit thickness in the Menorca Fan sector are more closely related to the position of cores relative to the Menorca Valley than to overall distality from the Balearic Platform shelf edge.

It is probable that many of these thick sand units have been deposited by processes other than classic turbiditic mechanisms. Two main types of transport mechanisms are postulated: (a) gravity flows, including mainly sand flow (i.e., fluidized and/or grain flow; cf. Middleton and Hampton, 1973) and high-density turbidity currents, and (b) bottom traction.

Sand flows are identified by the presence of diffuse plane lamination, possible but obscure dish structures, low matrix, and the almost structureless nature of some sand layers. There are some observations, however, that suggest other mechanisms also are involved: (1) the slope of the rise surface, in-

cluding the Menorca Fan surface and channel system, is much less than the  $10^\circ$  minimum inclination postulated for sand flow mechanisms (Middleton and Hampton, 1973); (2) X-radiographs show that the structureless layers are often interbedded with sands displaying well-defined high-angle cross-lamination (Figure 13). Stratification of this type is usually related to migrating bed forms resulting from bottom-traction mechanisms. In some ancient deep-water facies models, similar well-developed cross-bedded sands have been observed in association with pebbly facies (Walker, 1975). Bottom currents of the type recorded in some modern canyons (Shepard and Marshall, 1973) may be responsible for some lamination of sand, particularly in the upper channel area.

Turbidity currents also may be important in the transport of the coarse sands. Most thick sand units do not display the complete sequence of Bouma divisions, but a few reveal what may be a poorly developed lower ( $T_a$ ) graded division. This type of composite sand layer may have accumulated by the stacking of the coarse lower part of several turbidites, although this explanation requires that each succeeding flow eroded the  $T_{c-d}$  divisions of the previous deposit. Core analysis does not lend strong support to this hypothesis inasmuch as: (1) succeeding sand layers are generally not graded, (2) the upper section of sand units do not show upper turbidite divisions, and (3) coarse sands are capped directly by hemipelagic muds.

Elsewhere on the rise, in sectors away from channels, turbidites are commonly found (Table 4). The  $T_{c-d}$  divisions are poorly developed, however, as in the channel sequence. This, in large part, is attributed to the nature of the source materials shed from the Balearic Shelf, which are largely coarse bioclastic sands with a very subordinate fine-grained component. Moreover, the absence of major rivers and the much-reduced sediment cover on the marginal slopes also have minimized the amount of fines likely to be entrained in downslope flows. The paucity of pelitic layers in channels such as the Menorca Valley may result from mechanisms that have removed the fine fraction from turbidity flows in the channel, i.e., either (a) overbank flow and lateral spreading away from the main flow, or (b) longitudinal transport through the main channels and by-passing to more distal lower fan and Balearic Basin plain environments. High-density

turbidity flows may have deposited primarily the basal  $T_a$  division in the main channel; the absence or poor development of grading of the coarse sand layers may result from some final stage of post-depositional grain reorganization (i.e., fluidization and/or water escape mechanism).

The features observed in the channel sand sequence suggest that several processes have been involved and that the cores record transformation from one flow mechanism to another, i.e., from grain/fluidized to turbiditic flow (Middleton and Hampton, 1973; Kelling and Stanley, 1976; Stanley et al., 1978) or from turbiditic to fluidized flow during the final brief period preceding deposition (Walker, 1976). Each sand layer in a core represents a different combination of gravity processes. Without available near-bottom physical oceanographic measurements we cannot evaluate the role of traction currents that also appear to have been important in channel sand deposition. These sequences are dated younger than 23,000 but older than 16,000 years BP (Figure 10) which corresponds to the lowering and maximum low stand of sea level during the last glaciation. The 3.5kHz echo character in sectors where sand-rich cores are collected is of type 5 in the Menorca Fan lobes and type 3 near the main fan channel system. The 3.5kHz reflector density (3 to 5) in these areas is low (Table 6).

#### PROXIMAL TURBIDITIC-HEMIPELAGIC ASSEMBLAGE (B)

Assemblage B (Tables 4 and 5) is characterized by abundant sand turbidites (10 to 45 cm) that alternate with thick (to 150 cm) sequences of hemipelagic mud (e.g., cores MC9, MC11, Figure 10). Turbidite sequences are of the type  $T_{a-c}$ ,  $T_{a-e}$ ,  $T_{d-e}$  (Bouma, 1962) and  $T_{e,t}$  (Rupke and Stanley, 1974); the  $T_d$  (laminated fine sand to silt) division is poorly developed, and turbidite mud ( $T_{e,t}$ ) is absent or poorly represented (Table 4). This contrasts with the Balearic Basin sequences, south of the rise, which display a high proportion of mud turbidites (see Rupke and Stanley, 1974, their cores LYII-8, 8A, 9, 9A).

Core assemblage B occurs on the margins of the Menorca Fan valley and fan lobes; the characteristic graded sandy units result from two related processes. The thin, fine-grained turbidites have been deposited from the fine tail of density currents. This material, presumably transported be-

yond the channel by overbank flow, is characterized by alternating fine-sand layers (displaying small flaser structures and thin layers of wavy-laminated or climbing ripples, and starved ripples) and mud. Thicker, coarser turbiditic sequences were transported by the main body of density flows within channels and also by crevasse-splay processes along the channel margins. The structures of both fine- and coarse-grade turbidites indicate a rapid diminution of turbulence during crevasse-splay and overbank flows. Mud rip-up clasts and deformed layers are occasionally noted (e.g., core MC11, Figure 10); these are attributed to slumping of the channel wall. The proportion of hemipelagic versus turbiditic sequences at each core site is a function of its distance from the Menorca Fan valley. Core MC9 is characterized by a relatively high percentage of thick hemipelagic units, whereas core MC11, closer to the channel, displays a higher proportion of turbidites (Figures 7 and 10).

Assemblage B is associated with 3.5kHz type 3 echo character; the reflector density (3 to 5) in the vicinity of these cores is low (Table 6).

#### HEMIPELAGIC-TURBIDITIC MUD ASSEMBLAGE (C)

This assemblage (Tables 4 and 5) is characterized by a low proportion of turbidite sequences relative to hemipelagic mud. Two subtypes are distinguished, the first characterized by somewhat higher amounts of  $T_{c-e}$  and  $T_e$  turbiditic ("distal") sequences (core MC3, Figures 10, 15; Table 4), and the second characterized by a preponderance of hemipelagic mud alternating with a few thin mud ( $T_{e,t}$ ) turbidites. Silt turbidite sequences ( $T_{d-e}$ ) are sometimes noted (e.g., core MC10). This hemipelagic-rich subtype occurs on smooth, elevated areas away from the main channel systems, and is associated with 3.5kHz echo types 4 and 7. The 3.5kHz echo character chart (Figure 7) indicates that this is the predominant facies on the Balearic Rise.

The main sedimentary process involved in this core assemblage is settling from suspension. The hemipelagic deposits are modified by fluctuations of fine-grained input, bottom currents, and biogenic productivity. Sporadic incursions of turbidity flows modify the accumulation of fine-grained suspensates. This relatively uniform mud facies displays variations in the proportion and amount of planktonic

(foraminiferal and pteropod) components. Hemipelagic variants include (1) muds that display a gradual upward increase or decrease in the amount of biogenic constituents and (2) alternations of light yellowish orange, calcareous (biogenic) muds covered by gray, biogenic-poor muds. In the latter case, the two mud types are separated by a sharp contact, and these alternating sequences display a cyclic pattern in cores (e.g., MC7, Figure 10 and RC9-199, 200, Figure 16).

The only sedimentary structures observed in

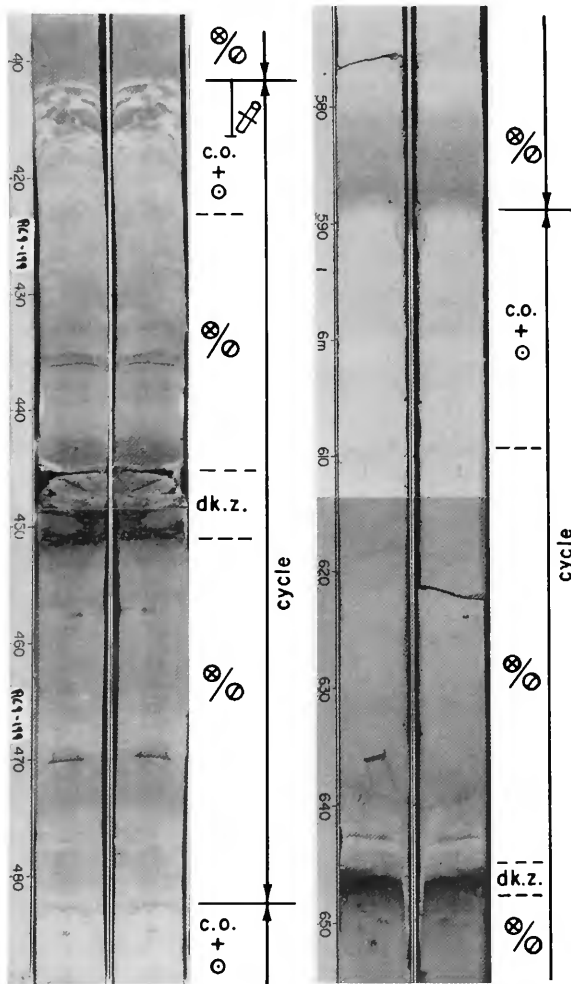


FIGURE 16.—Selected photographs of split cores (Conrad RC9-199 and RC9-200) showing well-developed carbonate cycles in Balearic Rise (c.o. = calcareous ooze; dk.z. = dark mud; other symbols as in Figure 10; scale on side of cores in centimeters from top of core; explanation in text)

either mud types (1) or (2) are faint parallel to irregular thin lamination or poorly developed grading; more often the mud is structureless. Locally, planktonic foraminifera are concentrated in thin, irregularly laminated layers; similar facies elsewhere have been attributed to biogenic blooms that subsequently have been concentrated as thin lag deposits by bottom currents (Huang and Stanley, 1972). The relatively shallow nature (< 2500 m) of the Balearic Rise suggests that carbonate compensation depth (CCD) effects have been negligible in the development of the cyclic pattern of these Late Quaternary cores. The features observed in (1) are better explained by changes in bottom currents and productivity. Evidence for bottom currents on the rise is provided by the irregular lamination of silt-size material in hemipelagic mud units (e.g., cores MC4, MC7, Figures 10 and 15). Earlier in this study, evidence of bottom currents was cited (i.e., the asymmetric scouring and, elsewhere, ponding of sediment around topographic features and pinnacles, Figures 2 and 4). Although bottom photographs suggest that present bottom currents are weak (Figure 17), structures such as the laminae observed on X-radiographs (core MC4, Figure 15) show that periodically the currents have been sufficiently strong to rework and redistribute fine-grained sediment. Evidence of sporadic biogenic blooms is provided by high concentrations (to 80% of the total sediment) of planktonic components in some thin layers; these blooms are typified by an enhanced foraminiferal content, consisting of a few species only. The interaction of sediment input, bottom current energy, and changes in biogenic productivity has resulted in the spread of a fine-grained sediment cover across the Balearic Rise. Bioturbation of the hemipelagic facies is noted on most bottom photographs (Figure 17), but the degree of reworking appears considerably less intense than in some other sectors of the Mediterranean (cf. Huang and Stanley, 1972; Maldonado and Stanley, 1976b).

In the case of hemipelagic subtype (2), the two muds, separated by a sharp contact, are attributed to large-scale Quaternary climatic changes that triggered sea level oscillations and physical oceanographic variations of the type recorded elsewhere in the Mediterranean (cf. Huang and Stanley, 1972; Stanley et al., 1975; Maldonado and Stanley, 1976a, b). The cyclic nature of Balearic Rise cores prob-



FIGURE 17.—Bottom photographs collected on Balearic Rise showing typical surficial sediment cover consisting of bioturbated hemipelagic mud and fecal pellets; small volcano-like mound with apical vents are most characteristic biogenic structures observed as well as short trails: A, Conrad-9 camera station south of Pinnacle R, 2085m; B, Conrad-9 station west of Southeast Ridge, 2550m (photos courtesy Lamont-Doherty Geological Observatory, Columbia University).

ably results from the effects of changes in sediment input as well as in water mass movement, stratification, and possible current reversals, but does not indicate anaerobic conditions, as interpreted in the eastern Mediterranean (cf. Van Straaten, 1972).

Cores recovered from the smooth elevated areas, and particularly the long Conrad RC9-119 and RC9-200 cores and MC7, reveal well-developed carbonate cyclic patterns. Each cycle is formed by (a) a basal gray hemipelagic-terrigenous mud division, followed by (b) a light cream-colored calcareous-biogenic ooze division (Figure 16). The basal

(a) division occasionally incorporates a dark gray zone (less than 10 cm thick) that may possibly be the equivalent of the dark-streaked, mottled mud zone in the Alboran Sea (Huang and Stanley, 1972, fig. 7) and also of the organic ooze-sapropel division commonly encountered in eastern Mediterranean cores (Maldonado and Stanley, 1976a). The average thickness of the cycles as measured in long cores such as RC9-199 (total length > 9 m) is on the order of 1 m. These cycles may represent an incomplete cyclothem sequence as defined in the eastern Mediterranean and probably formed during phases of stratification and partial ventilation associated with current reversals, as proposed by Huang and Stanley (1972) and Stanley et al. (1975).

One area where the hemipelagic trends are well displayed is the smooth elevated platform around pinnacles T, V, and Y east of the Menorca Valley, an area relatively protected from turbidity current and other gravity flow incursions. The three uppermost light-colored, carbonate-rich layers (for example, core MC7, Figure 10) have yielded radiocarbon dates. The two lower layers were deposited about 28,000 and 21,000 years BP (Table 7); these are followed by gray terrigenous layers attributed to a marked increase in fine sediment input accompanying the postglacial sea level rise. An upper calcareous ooze layer is dated between 3000 years BP and the present. It is possible that during either low or high sea-level stands, type 1 hemipelagic sequences accumulated as a result of changes in bottom current activity and/or productivity; type 2 hemipelagic sequences are more closely related to marked changes in fine-grained terrigenous input and reflect changes in offshelf transport resulting from the rise or fall in sea level. Similar sequences of about the same age have been recorded from the eastern Mediterranean (Stanley and Maldonado, 1977).

The 3.5kHz echo character of seafloor sectors associated with levee deposits (core MC3) is type 7, with a reflector density of 6 to 9, and that of the smooth elevated areas is type 4, with a reflector density of over 9 (Table 6).

#### BASIN PLAIN ASSEMBLAGE (D)

Assemblage D (Tables 4 and 5) includes rare to abundant mud turbidite sequences and a high proportion of hemipelagic mud (e.g., cores MC1 and

MC2 recovered south and west of the Balearic Rise, Figure 10; see also cores described by Rupke and Stanley, 1974, figs. 6 and 7). The Balearic Basin plain assemblages records the prevalence of suspension processes interrupted by distal turbidity current incursions; sedimentation is thus similar to the regime existing on the smooth, elevated areas of the rise as discussed in the previous section, but the basin plain sequences include enhanced proportions of mud turbidites and a few sand and silty turbidite sequences. Some of the thinner laminated and biogenic-poor hemipelagic layers appear to have been modified by weak bottom current activity, but this effect is minor in terms of the total sediment section. The 3.5kHz profiles show that the seafloor in this sector beyond the rise has a subbottom character [echotype 4; high (>9) reflector density] similar to that of the smooth, elevated areas of the Menorca Rise.

### Sedimentation Rates

Eight radiocarbon dates (Table 7) were obtained from selected Balearic Rise cores (R. Stuckenrath, Smithsonian Carbon Dating Laboratory, pers. comm.). The samples are representative of the several core associations and environments identified in this study. Calculated sedimentation rates based on these dates are shown in Figure 18.

Three samples from core MC7 (Figure 10), collected on the smooth, elevated area of the Balearic Rise south of the Menorca Valley and east of Pinacle V, yield an average sedimentation rate of 6 to 7 cm/10<sup>3</sup> yrs (Figure 18). The rates in this core also show a general decrease upward in the stratigraphic section, from more than 9 cm/10<sup>3</sup> yr be-

tween 20,000 and 30,000 years BP to 5 cm/10<sup>3</sup> yr between 20,000 to 3,000 years BP, and about 2 cm/10<sup>3</sup> yr during the last 3,000 years BP. Core MC3, within the same core group association, shows a slightly higher rate (10 to 11 cm/10<sup>3</sup> yr) in the Menorca Fan lobes; this reflects the enhanced proportion of distal turbiditic incursions on this active depositional area of the rise.

The highest sedimentation rates in the study area are recorded in core MC1, on the basin plain southwest of the rise (Figure 18). Lithological correlation shows that some channel sand associations also may have accumulated at rates similar to core MC1 during the Late Quaternary (e.g., cores MC5A and MC6, Figure 10). Average sedimentation rates of 12 to 13 cm/10<sup>3</sup> yr are calculated for the Late Quaternary (Figure 18) in these cores.

The Balearic Rise channel sand association reveals low rates during the Holocene (about 5 cm/10<sup>3</sup> yr in core MC5A), an average rate >10 cm/10<sup>3</sup> yr is calculated for the Late Quaternary on the basis of lithostratigraphic correlation (Figures 10, 18). The thick channel sands appear best developed between 23,000 and 16,000 years BP. An estimated average age of 19,000 years BP is assigned to the base of the coarse channel sand for correlation purposes.

These rates enable us to estimate that the unconsolidated sediment section traversed on the 3.5kHz profiles (about 30 to 80 m penetration) probably includes deposits of Upper Pleistocene age. This is based on an overall average sedimentation rate ranging from 5 to 10 cm/10<sup>3</sup> years, which would cover a time span of about 250,000 to 500,000 years.

Overall, Balearic Rise sedimentation rates are lower than those recorded in other studies of the western Mediterranean. Rupke and Stanley (1974) calculate a rate of about 10 cm/10<sup>3</sup> yr for hemipelagic sedimentation and an average rate of 23 cm/10<sup>3</sup> yr for the total sediment thickness in the southern Algéro-Balearic Basin. In turn, these are somewhat lower than the 30 cm/10<sup>3</sup> yr and the higher rates calculated by Gennesseaux and Thommeret (1968) in the northern Balearic Basin. JOIDES core Site 124, east of the Balearic Rise, yields an average long-term Plio-Quaternary sedimentation rate of 9 cm/10<sup>3</sup> yr consistent with our results, and a rate in excess of 13 cm/10<sup>3</sup> yr at core Site 133 west of Sardinia (Ryan, Hsü et al., 1973).

TABLE 7.—Radiocarbon dated samples from cores in different Balearic Rise environments

CORE	DEPTH (cm)	SEDIMENT TYPE	RADIOCARBON DATE (in years B. P.)
MC-1	159-174	Hemipelagic mud	13,980 ± 140
MC-3	248-261	Hemipelagic mud	24,650 ± 380
MC-5A	92-110	Hemipelagic mud	16,200 ± 150
MC-7	0-10	Oxidized top layer	2,850 ± 70
MC-7	91-103	Calcareous ooze	21,030 ± 240
MC-7	190-204	Hemipelagic mud	32,100 ± 1100
MC-8	214-230	Hemipelagic mud	23,380 ± 325
MC-9	196-213	Calcareous ooze	28,200 ± 600

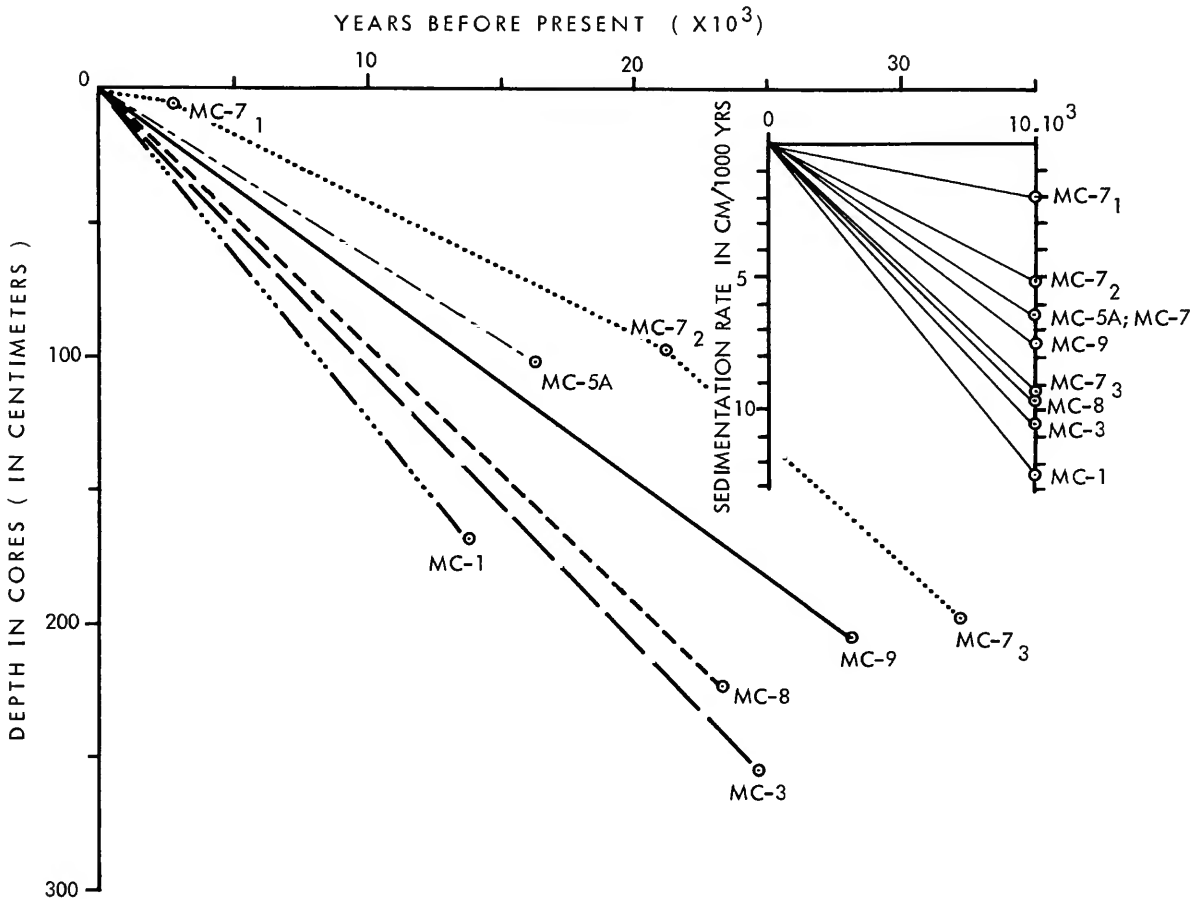


FIGURE 18.—Sedimentation rates based on radiocarbon dating of samples from cores in different Balearic Rise environments (Table 7); graph in upper right corner shows calculated rates in  $\text{cm}/10^3 \text{ yr}$ ; in the case of core MC7, average overall sedimentation rate is depicted as well as rates during three periods of time since 32,100 years BP.

Much higher rates have been calculated in the Alboran Sea (from 26 to  $30 \text{ cm}/10^3 \text{ yr}$ ; Huang and Stanley, 1972). Deposits in the small, deep basins of the Strait of Sicily have accumulated at an average rate of 20 to  $25 \text{ cm}/10^3 \text{ yrs}$  (Maldonado and Stanley, 1976b).

Sedimentation rates in submarine fans elsewhere in the world during the Upper Holocene, largely dominated by hemipelagic sedimentation, also are low in most cases. The Amazon Cone (Damuth and Kumar, 1975) yields a rate of 4 to  $6 \text{ cm}/10^3 \text{ yr}$ , the Nile Cone (Stanley and Maldonado, 1977) has extensive areas with rates of 4 to  $8 \text{ cm}/10^3 \text{ yr}$  during the past 6000 years, the Astoria Fan provides a rate of  $8 \text{ cm}/10^3 \text{ yr}$  (Nelson, 1976) and the La Jolla

Fan (Shepard et al., 1969) is characterized by slightly higher rates. The Mississippi Cone yields a significantly higher sedimentation rate ( $>22 \text{ cm}/10^3 \text{ yr}$  during the Late Holocene (Huang and Goodell, 1970).

The consistently low Balearic Rise sedimentation rates during the Late Quaternary are attributed to the limited terrigenous input of fine-grained material in this sector, and the relatively low proportion of mud turbidites compared to other fans (e.g., the Nile Cone; Maldonado and Stanley, 1976c). Even in the Menorca Fan lobes, where more active deposition might be expected, sedimentation rates are reduced. Another factor is the bottom current activity that has eroded some rise surface sediments



and transferred these onto the Algéro-Balearic Basin plain. This seaward bypassing phenomenon may be responsible for the much higher rates recorded on the more distal Basin.

### Structural and Physiographic Controls on Recent Sedimentation

Previous studies based on intermediate- to deep-penetration seismic profiles (Mauffret et al., 1972; Stanley et al., 1974a, 1976; Mauffret, 1976) have demonstrated that the Balearic Rise is a complex feature created by foundering of a portion of the Balearic Platform in Late Miocene and post-Messinian time along a series of NE-SW faults that are parallel to the main trend of the Betic chain. The principal expression of this defining set of fractures in the Balearic region is provided by the Emile Baudot Escarpment. The virtual absence of sediment cover on this feature indicates that the subsidence along this line probably has continued until very recent geological time. The foundered block of the Balearic Rise has been broken into a series of smaller horsts and troughs as the result of faulting that occurred along both the NNW-SSE and, later, predominantly NE-SW trends. The former set of faults is exemplified by the fractures bounding the Menorca Ridge.

#### MORPHOLOGIC AND SUBBOTTOM CONSIDERATIONS

Consideration of the thickness and nature of the Plio-Quaternary sequences on the rise demonstrates that the underlying structure has exerted a dominant control on the distribution of physiographic environments and hence on the distribution and the relative vertical persistence of different sediment types. Thus, thick pods or lenticular bodies of Plio-Quaternary sediments, which are represented in sparker or air-gun records by lensoid, thick, cross-cutting (channeled) sequences of reflectors (Figure 6, profiles A, E) are encountered in the Menorca Valley and Fan regions. A second type of thick, flat-topped, and ponded channel-fill is encountered on the eastern flank of the rise, locally forming a facies marginal to that of the basin plain (Figure 6, profiles A, F; cf. Figure 7).

The lower part of the Menorca Valley within the rise is a morphologically complex area (Figure 3) underlain by a stacked and mutually cross-cutting

system of broadly lensoid units that represent the migrating lobes of the Menorca Fan. A similar sequence is recognized below the eastern margin of the Cabrera Canyon (Figure 1A).

The lower Menorca Valley and Menorca Fan regions are also characterized by the presence of abundant salt-diapirs that originate below the M reflector zone (in the "couche fluante") and displace older channel, interchannel, and levee fan deposits of the Plio-Quaternary sequence (Figure 6, profiles A, E). Many of these diapirs penetrate the present seafloor in this region and, through their topographic expression, exert a significant influence on present-day sediment distribution and sedimentary processes both on the rise and on the Balearic Basin plain beyond (cf. Stanley et al., 1974b, 1976).

Relatively thinner sequences identified by continuous and multiple, parallel reflecting layers, occur on the more elevated portions of the rise, and generally form smooth, gently sloping platform regions.

Abrupt and relatively steep prominences, here termed "Pinnacles," also occur on more elevated parts of the rise. The features termed "Layered Pinnacles" are essentially up-faulted blocks, or horsts, of the sub-M reflector acoustic basement that have acquired a partial cover of multiple-layered Plio-Quaternary sediments, whereas "Penetrative Pinnacles" are either similarly faulted masses, lacking any significant sediment cover, or are volcanic in origin (Gonnard et al., 1975; Stanley et al., 1976, Fig. 28). The lack of any appreciable sediment veneer on these Penetrative Pinnacles, together with the fact they penetrate the most superficial reflectors, of presumed Late Quaternary age, on the 3.5kHz records demonstrates that, whatever their origin, these are geologically young features. These recently developed eminences have influenced the sediment distribution in their vicinity, as indicated in the 3.5kHz profiles by the consistent ponding of sediment on their upslope flanks and the presence of narrow sand-floored "moats" or depressions on the downslope flanks (Figure 4B, 4J, 5A).

The 3.5kHz records indicate that the overall distribution of young sediments on the rise also has been modified to varying degrees by post-depositional slumping and mass-movements. Slump features are most pronounced and volumetrically most important in the immediate vicinity of the Emile Baudot Escarpment (Figure 2), but other structures

attributed to slumping affect the recent sediments on the sloping flanks of the Menorca Valley and on the eastern margin of the Menorca Fan (Figures 4E, 5G, 5H, and Figure 8, letter f).

The principal physiographic control on the nature, distribution, and thickness of sediments on the Balearic Rise throughout the Plio-Quaternary has been the Menorca Valley. In its upper course the location and trend of this feature is governed by faulting of NNW-SSE trend, approximately parallel to the fractures bounding the Menorca Ridge, to the east (Stanley et al., 1976). The thick channel-fill sequence encountered below the SE Valley probably represents a former distributary of the Menorca Valley that extended onto the Balearic Basin plain. The nature of the fill in the Southeast Valley, however, indicates that this sediment path was abandoned during Plio-Quaternary times, presumably through the elevation of an intervening up-faulted block (the Pinnacle V-Pinnacle W ridge). This feature forms a part of the complex tectonic barrier that is deemed responsible for the westward diversion of the Menorca Valley system.

At the present time the Menorca Valley debouches onto the Balearic Basin plain in the form of a broad deepsea fan that, with a radius of about 80 km and a width of about 50 km, is appreciably smaller than most analogous features, probably because of the tectonic constraints that have restricted lateral fan-valley migration and fan-lobe development. Thus, the Menorca Fan is a topographically complex region created by a series of overlapping lobes of sediment, with small interfingering channels, separated by wider, flat or gently undulating, more elevated zones of levee-type. The morphology of the fan region is further complicated by the presence of shallow faults that displace even superficial sediments (Figure 2) and also by active salt diapirs. Some of the salt domes penetrate to the surface and form minor elevations, while other buried salt structures are responsible for doming up the overlying sediment veneer (Figure 3). By their influence on fan topography these faults and salt diapirs clearly exert a powerful control on the distribution of coarser sediments. Moreover, even areas of fine sediment accumulation on the flanks of the fan are affected by post-depositional movements in the form of localized slumping (Figure 8, letter f) that eventually may produce significant modification of the gently sloping inter-channel areas. The

interaction of shallow tectonics with sedimentary processes and the complex physiography that is thus created clearly distinguishes the Menorca Fan from other described examples in which sedimentation has been the sole, or at least the predominant, factor in development of the fan morphology. It is noteworthy that at present the largest and most active channel in the lower course of the Menorca Valley system follows a circuitous route that effectively bypasses the most complex and topographically diverse central portion of the fan (Figures 2, 3, 7). It is possible that this westward diversion of the active channel was achieved simultaneously with the cut-off of the original southeast-trending valley system through uplift of the fault-bounded northwest-southeast trending blocks, exemplified by Pinnacles V and W.

#### LITHOFACIES CONSIDERATIONS

The core data obtained from the Balearic Rise demonstrates that, at least for the geologically young sediment section, there exists a close correlation between the predominant sediment type and sequence and the present physiographic setting of the cores. In general, coarser sediments occupy topographic depressions and finer sequences are typical of more elevated regions. Thus, cores characterized by channeled sequences and thick sands of the channel sand assemblage (i.e., MC5A, MC6, MC8) occur in active channels in both the Menorca Valley proper and the fan region. In contrast, topographic highs are dominated by hemipelagic muds (part of the hemipelagic-turbiditic mud assemblage), both in the leveed interchannel areas of the fan (core MC3) and on the broader elevated platform regions of the tectonic barrier region (MC7 and MC10). Despite their broad similarities to the elevated platform successions, the levee sequences can be identified because of the higher proportion of thin silt to sand turbidite layers that they contain (Figure 15).

A further category of sediment-sequence (proximal turbidite assemblage) is composed of interbedded, well-defined sandy turbidites and hemipelagic mud layers (e.g., cores MC9 and MC11). These sandy sequences are attributed to proximal turbidite deposition on the flanks of active channels (core MC11). Core MC9 is somewhat anomalous since it is located on the elevated platform between

Pinnacles X and Y and is more than 60 meters higher than the floor of the nearest appropriate section of the Menorca Valley (Figure 8). It comprises several turbidite layers (Figures 10, 15) and the presence of such turbidite beds in this core furnishes the sole exception to the general rule concerning sediment type and physiographic locale that was established earlier. Three possibilities exist to explain this anomaly: (a) the turbidites were conveyed to this point through a former channel, for which there is no evidence in the shallow seismic records; (b) the turbidity currents responsible for deposition of the sands in core MC9 were capable of ascending out of the Menorca Valley through the observed height-difference of 60 meters or more; however, there is no supporting evidence in any of the other cores from comparable physiographic locales on the Balearic Rise. A third possibility (c) is that the turbidite sands represent recently uplifted materials from a former channel-bank environment. There is some evidence for the existence of young faults in this vicinity (Figure 2). On available information it is not possible to state categorically which, if any, of these alternatives is correct. The abundant evidence for active tectonic displacement throughout the rise region, however, suggests that recent uplift may account most readily for this apparent anomaly.

Basin plain assemblage cores (MC1 and MC2) are characterized by interlayering of mud turbidites with hemipelagites and occasional fine, sand- or silt-grade turbidites. This type of sequence reflects deposition from occasional dilute or "spent" turbidity flows. Similar sequences that have been described from adjacent portions of the Algéro-Balearic Basin plain by Rupke and Stanley (1974) contain a substantially higher proportion of mud turbidites, probably reflecting the multiple sources of fine-grained detritus available in the more central parts of this basin.

Moreover, the northwest-southeast trending physiographic and tectonic barrier embracing Pinnacles V, W, X, Y, and T has been particularly effective in preventing the access of mud turbidites to the eastern parts of the Basin plain, as attested by the depleted proportions of such layers in cores MC7 and MC10. Cores obtained by the Lamont-Doherty Geological Observatory (RC9-199, RC9-200, and V10-4) from the southern and eastern

margins of the rise are lithologically similar to those described above (see p. 31 and Figure 16).

#### SUBBOTTOM AND LITHOFACIES CORRELATIONS

A strong correlation can be recognized between both the echo character and reflector densities exhibited by shallow seismic (3.5kHz) records and the structural-physiographic provinces determined from deep seismic methods (Table 2). Low reflector densities appear in two contrasting physiographic settings, namely within the channel regions and on some pinnacles and steep slopes. The echo character, however, provides a means of distinguishing between these different physiographic environments. An intermediate reflector density is a general feature of the fan lobe regime but again echo character facilitates distinction of several important environments, such as the active channels and the interchannel levee regions. High reflector densities characterize the more elevated regions of the rise (apart from the Penetrative Pinnacles), and areas of active or past slumping. The maximum reflector densities are found almost exclusively on the basin plain.

The core data greatly assist interpretation of the echo character and reflector density distributions in terms of dominant sediment character within different physiographic provinces. Cores that yield the highest proportions of sand and silt in channeled sequence units (assemblage A) fall into echo character types 3 and 5 (Table 6). Type B assemblages with abundant sandy turbidite sequences occur in regions characterized by echo character type 3 (Table 6). Thus, the core evidence substantiates the conclusion that rise regions exhibiting type 3 and type 5 echo characters, with low reflector densities, represent the axes or proximal flanks of active channels, through which coarse detritus has been conveyed in the geologically recent past. Type C core sequences, dominated by hemipelagic muds, with rare, thin, silt-to-sand turbidites, occur in association with echo character types 4 and 7 and generally display high reflector densities (Table 6). These sediments are interpreted as the sequences developed on interchannel levees or on more elevated, gently sloping platforms, isolated from active channels. Type D core sequences (dominantly hemipelagites but with some silt and mud turbidites) are

found only on the Balearic Basin plain where they fall into echo character type 4 and display the highest reflector densities encountered (Table 6).

In general, the reflector density appears to correlate inversely with the frequency of well-defined sand-to-silt layers that are interbedded with mud in cores (Figure 9, left side). In contrast, there appears to be little correlation between reflector density and the frequency or density of discrete sequences within the cores (Figure 9, right side). The inverse relationship that exists between reflector density and the frequency of reflecting coarse layers is probably attributable to the nature of the acoustic pulse emitted by the 3.5kHz system used in this survey. Reflecting layers superposed at small vertical intervals (less than approximately 1 meter apart) will give rise to mutually interfering multiples unresolvable on the 3.5kHz records, producing a vertically prolonged, continuous trace. Conversely, the absence of a clear correlation between reflector density and the frequency of sequences in the cores is ascribed to the relatively subtle nature of the lithologic changes represented in these sequence-units. For example, it is improbable that the acoustic response of mud turbidites and hemipelagic muds is sufficiently contrasted to be recorded as a reflector in our records. Only the more marked lithologic contrasts offered by an alternation of coarser layers with such muds appear to be resolvable by this system.

#### Sediment Transport and Dispersal on the Balearic Rise

On the basis of the available core data and the close correlation with the shallow subbottom 3.5kHz records that is demonstrated above, it is now possible to summarize the general character of sedimentary processes operating in geologically recent times throughout the Balearic Rise and adjacent regions (Figure 19).

Three main sedimentary processes appear to influence sediment distribution on the Balearic Rise: sediment gravity flows (Middleton and Hampton, 1973), suspension primarily from hemipelagic settling, and bottom currents (in the channel system and around some pinnacles). The distribution and relative importance of each of these main process categories are controlled by the boundary condi-

tions of the depositional system. Thus, sands, silts, and occasional mud layers attributable to turbidity flow and other forms of sediment gravity flow and to bottom currents are most commonly encountered in the active and abandoned channel systems associated with the Menorca Valley and Fan. The bank sediments of these channels are dominated by well-developed, classic sand-to-silt turbidite units (e.g., core MC11), in some cases modified by mass flow mechanisms.

Turbidites composed of more fine-grained material and of more distal character (lacking the basal erosion surface and lower  $T_a$  and  $T_b$  intervals of the Bouma sequence) occur on the natural levees bordering fan channels, on the adjacent Basin plain, and also on the gently sloping platform that constitutes the more elevated parts of the rise. Some of these materials were carried into the system by shelf-edge spillover and by failure on the slope.

Sedimentation in the three regions cited above is at present dominated by settling of hemipelagic mud, which represents a universal motif throughout the rise region. Such finer-grained deposits, however, are proportionately less significant in the channeled areas, partly because of the erosive removal of such material and partly because of the more important depositional role of sediment gravity flows and tractional processes as outlined above.

Indirect evidence for the existence of other sedimentary processes on the rise is provided by the presence, within the hemipelagic muds of some cores (e.g., MC4) of parallel to irregular, thin laminations that may be attributed to weak bottom currents. Additional evidence for these bottom currents is provided by the shallow, scoured hollows or "moats" commonly observed on the downslope flanks of major pinnacles (Figure 4B), with concomitant accumulation of sediment on the opposite flanks. The occurrence of high-angle cross-lamination in the upper parts of some channelized sands also suggests the operation of tractional bottom currents.

Furthermore, post-depositional mass movements have demonstrably operated on more steeply inclined surfaces within the rise. Two main categories of slump movement may be distinguished: (a) the relatively rapid displacement of substantial masses of sediment along a single or a few curved glide planes (Figure 4E) and, (b) the more continuous and slow downslope creep of large, more gently

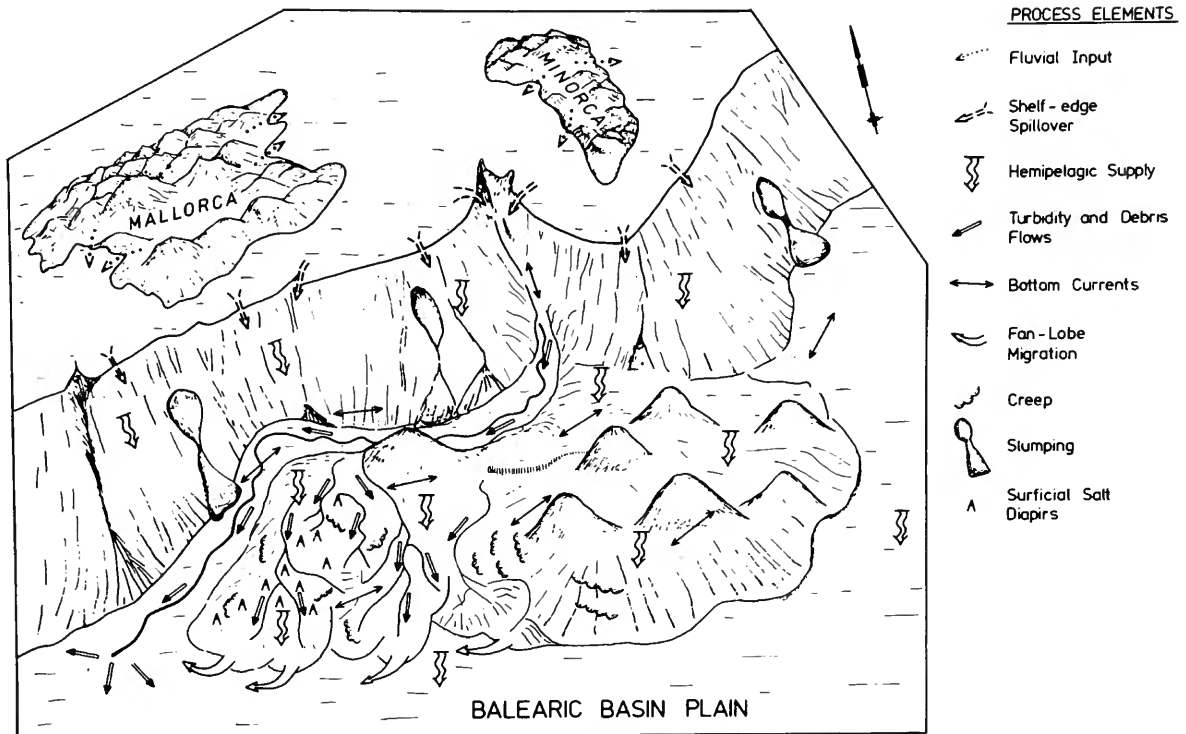


FIGURE 19.—Interpretative diagram illustrating principal sedimentation processes contributing to Plio-Quaternary sequence on structurally active Balearic Rise (see text for explanation).

inclined sediment bodies, moving along multiple, parallel shear planes (Figure 5G, 5H). Type (a) slumps appear to be more common at the base of steeper slopes, where large blocks of sediment have been displaced suddenly, producing curved slump-scars. Features of this type occur along much of the lower part of the Emile Baudot Escarpment, at the foot of several of the pinnacles on the rise and, on a smaller scale, modifying the surface of the fan lobe complex of the lower Menorca Valley. Type (b) slumps give rise to a tightly undulatory surface topography that is encountered mainly on the eastern margin of the Menorca Valley (Figure 8).

The relative importance of the above described processes has not been constant in time. This largely reflects changes in sediment input that were controlled by large-scale Late Quaternary climatic oscillations. These climatic changes induced major eustatic fluctuations that directly modified sediment input, affecting the source area, nature and amount of sediment, and submarine processes.

The Balearic Platform, for the most part shallower than 100 meters, was subaerially exposed during the Quaternary eustatic low sea level stands. This exposure of the broad sector around the islands of Mallorca and Menorca effectively doubled the area of the source terrain that shed sediment onto the Balearic Rise below. Rivers on Mallorca, draining the mountainous northwest sector, flowed both to the northeast and southwest of the island and carried enhanced volumes of clastic and carbonate sediment largely eroded from Mesozoic and Tertiary rocks. During the eustatic low stands the smaller rivers on Menorca also conveyed to the Balearic Platform margin and the steep slopes beyond substantial amounts of detritus eroded from the Miocene calcarenites that form the southern half of Menorca (Obrador et al., 1971). It is doubtful that even this enhanced fluvial system, draining such a limited source area during lower sea level stand, would have carried large volumes of fine-grained material, and it is surmised that much of

the sediment transferred beyond the platform edge was of a coarse, bioclastic nature.

This phase of direct, enhanced transport to the shelf edge and onto the upper Emile Baudot Escarpment favored mass gravity processes. Some materials were transported downslope on the Emile Baudot Escarpment and Menorca Ridge and some were channelized within submarine valleys (including the Menorca Valley) and thus transferred to the southwestern sector of the Balearic Rise, presumably by sand flows, turbiditic processes, and bottom currents. The effects of bottom currents within the channel system may explain the lack of a distinct downslope trend in sand texture and layer thickness within the fan system.

Subsequently, the rise in sea level has resulted in a decrease in sediment input and in a relatively more important role for suspension-related processes. This is effectively demonstrated by the decrease in sedimentation rates noted in the upper parts of cores.

#### Evolution of the Menorca Fan

Analysis of the high-resolution subbottom profiles and the cores enables the Plio-Quaternary history of the Menorca Fan and of the Menorca Canyon-Valley-Fan depositional system to be traced in some detail. The combined effects of (1) strong tectonic overprint controlling channel migration and fan morphology, (2) the relatively low input of fine-grained sediment, and (3) the role of bottom currents, have resulted in formation of a somewhat unusual submarine fan. The effects of overbank flow of fine-grained sediment and of channel migration, normally two major mechanisms of fan lobe development (Normark, 1970, 1974) appear reduced in the case of the Menorca Fan. This appears to arise from two factors: (a) the structurally controlled Menorca Valley, the major channel, which apparently has not been able to meander freely, and (b) the downslope channelization of sediment that consists largely of coarse-grained material. Much of this sediment is not likely to have been carried much beyond the channel levees by sheet flow. The fine-grained deposits recovered on different parts of the fan surface consist mainly of hemipelagic units while the proportion of fine-grained turbidites is reduced. Calculated rates of

hemipelagic sedimentation (approximately 6 to 7 cm/1000 years) based on radiocarbon dating are slightly lower than hemipelagic depositional rates in the adjacent Balearic Basin (Rupke and Stanley, 1974, fig. 21) and in other fans (Shepard et al., 1969; Nelson, 1976).

The Late Quaternary sedimentary evolution of the Menorca Fan is summarized as follows (cf. Figures 7, 8, and 19).

The distribution of sediment types and sequences is closely related to the Menorca Fan Valley-Fan lobe setting on the Balearic Rise surface. Relatively thick layers of sand (e.g., core 5A, Figure 10A) characterize the main channel assemblage on the middle and upper fan. The 3.5kHz survey shows that this facies association extends downslope and across the fan all the way to the Balearic Basin plain (Figure 7). This phenomenon is not unique to the Menorca Fan since similar thick pods of sand have been observed in other modern fans (cf. La Jolla Fan, Shepard et al., 1969; Nile Cone, Maldonado and Stanley, 1976a). These coarse sand layers were deposited between about 23,000 and 16,000 years BP (Table 7).

Turbidites ("distal") without the  $T_a$  and  $T_b$  Bouma divisions are found in all of the fan provinces as well as in the Balearic Basin plain. Complete ( $T_{a-e}$ ) turbidites tend to be concentrated on the upper and middle fan, and also are present in the basin plain (e.g. core MC2, Figure 15). Complete turbidites are generally absent in cores collected in the middle fan interchannel sectors. The absence of turbidite thinning on the lower Menorca Fan is a characteristic found elsewhere (Shepard et al., 1969; Nelson, 1976).

The core analysis shows that on the Menorca Fan hemipelagic muds account for more than 50 percent of the cored series, except in the channel assemblage where they represent as much as 30 to 50 percent of the section. This high proportion in both Pleistocene and Quaternary series throughout the fan area is in contrast to most open fan models where turbidite mud is regarded as the dominant fine-grained sediment type (Curry and Moore, 1971, 1974; Normark and Piper, 1972; Nelson, 1976). The reduced importance of mud turbidites on the Menorca Fan may be accounted for, in part, by (1) the lack of major adjacent sources of fine-grained detrital material, and (2) by-passing onto the Balearic Basin plain.

The hemipelagic suspensates probably settled

slowly through moving water masses. Bottom currents, such as those in the Menorca Valley, at times may have been strong enough to move and concentrate medium- to coarse-grained sand and to prevent the accumulation of fines. The nature of such currents in the Menorca Valley is not known, but perhaps may have been similar to channelized currents along canyon floors observed in other regions (Keller et al., 1973; Shepard and Marshall, 1973; Keller and Shepard, 1978).

Some modification of the sediment distribution in fan lobes appears to have been achieved by downslope creep and large mass-gravity failure such as slumping (the latter triggered by tectonic activity) that resulted in channel cut-off and subsequent diversion and migration. This channel modification phenomenon resulted in the lateral shift of fan lobes and in the areal facies distribution observed on the fan. It is noteworthy that similar sedimentary processes, including differential hemipelagic settling, low-flow regime bottom currents, and mass movements by sliding or slumping, have been identified as the major sediment mechanisms for the development of the Mississippi deep sea fan (Huang and Goodell, 1970).

In time, the lower Menorca Valley and middle fan lobes have shifted westward on the rise. Looking down-channel, this displacement does not conform to the pattern of levee-fan evolution toward the left as a result of Coriolis force (cf. discussions by Menard, 1955, and Menard et al., 1965). This pattern of fan lobe migration tends to support the conclusion that the Menorca Fan morphology and facies more closely reflect tectonic control than sedimentation patterns *per se* (Figure 8).

The main factor controlling the present locus of more powerful sedimentary processes, and hence the rate of sediment accumulation, is the position of the active Menorca channel and its distributaries. It was shown earlier that the diversion of the main Menorca channel system has been produced by transverse faulting, imposing a barrier to the more direct route of the initial canyon system, itself fault-defined. A process that may further effect localized diversion and impedance, at least of active distributary channels, is slumping or slope-creep of large areas of the interchannel lobes. This process may be substantially reinforced and accelerated by the diapirism that is an important element of the Menorca Fan region (see Figures 3, 5D, E, I).

In more general terms, it is significant that the area in which Plio-Quaternary sediments attain their maximum thickness on the rise is coincident with the topographically lower portion of the Menorca Valley and Fan. As demonstrated earlier, this is also the region in which the most active sedimentary processes have operated, supplying substantial volumes of sand, silt, and mud. Since this region of thick sediment accumulation remains topographically depressed in relation to adjacent areas, it is necessary to conclude that this area is undergoing active subsidence at a rate that broadly matches the rate of sedimentation. The present data are inadequate to decide whether this subsidence is attributable to sediment-loading, to continued down-faulting of this region, or to a salt-withdrawal mechanism analogous to that proposed for the Catalanian margin by Stanley et al. (1976).

The facts elicited above clearly demonstrate that a generalized model of canyon-fan sedimentation in broad terms can be applied to explain the present and past distribution of sediments on the Balearic Rise. The unique combination of foundering-tectonics and salt-diapirism, however, has exerted a degree of control, on both a regional and a localized level, that has significantly modified the nature and paths of sediment distributing processes operating in this region. At the present time, these effects are most clearly displayed in the Menorca Fan, where the morphology and sediment distribution are primarily controlled by such tectonic and diapiric factors, rather than the purely sedimentary processes (such as lateral migration or avulsion of channels) that provide the dominant controls in more conventional submarine fans.

### Summary and Conclusions

The Balearic Rise is identified as a recently subsiding block of the South Balearic Platform, depressed by two intersecting sets of major faults: an earlier system of NNW-SSE trend (Menorca Ridge and the eastern boundary fault), and the later NE-SW fractures (Emile Baudot Escarpment). Contemporaneous and subsequent faulting mainly along N-S and WNW-ESE trends, and possibly associated with some volcanicity, has generated the irregular pinnacles-and-platform topography of the more elevated eastern sector of the rise. The uplift of

this horst-style domain may have induced the abrupt westward diversion of the Menorca Canyon-Valley, which it is suspected originally may have debouched onto the Balearic Basin plain through the Southeast Valley.

Additionally, salt tectonic effects are identifiable on the Balearic Rise and are conspicuous on its major constructional element, the Menorca Fan, where many salt domes find topographic expression on the seafloor. The coincidence of these halokinetic structures with the zone of maximum Plio-Quaternary thickness suggests that superincumbent loading may be the causative mechanism for the diapiric upwelling. At present the main channel of the Menorca Valley system has been diverted along the northern and western peripheries of the Menorca Fan, which thus appears to be bypassed by the more active channelized flows. This situation may be a further result of halokinetic doming of the fan area and/or peripheral withdrawal of salt.

Echograms derived from 3.5kHz profiling of the Balearic Rise are divisible into 8 categories of echo character, which can be related both to physiographic locale and to the distribution of sediment types revealed by piston and gravity cores. Acoustic mapping confirms that the Menorca Canyon, Valley, and Fan are the main repositories of coarse sediment on the Balearic Rise, although localized zones also occur in the vicinity of some Pinnacles and in some of the marginal re-entrants of the Balearic Basin plain into the faulted eastern margin of the rise.

Five major sediment types are distinguished in Balearic Rise cores: (1) bioclastic (terrigenous) sand; (2) silt; (3) turbidite mud; (4) hemipelagic mud; and (5) calcareous ooze (sandy mud). The sediment types are defined on the basis of the sand fraction content and composition, and sedimentary structures observed in split cores and in core X-radiographs.

The sediment types are grouped into sequences, each of which is defined on the basis of a succession of sediment types. The three major sequences distinguished are (1) channel sand sequence, (2) turbidite sequence, and (3) hemipelagic sequence.

Four distinct lithofacies assemblages based on sediment type and sequence are identified in the core: (A) channel sand assemblage; (B) proximal turbiditic-hemipelagic assemblage; (C) hemipelagic-turbiditic mud assemblage; (D) basin plain assem-

blage. There is a good correlation between Late Quaternary sediment distribution and Balearic Rise physiography.

The channel sand assemblage characterizes the Menorca Valley and fan lobes of the middle Menorca Fan. The thick, coarse sand layers included in this assemblage were deposited by gravity and bottom current processes. Sedimentary structures record possible transformation from one flow mechanism to another.

Balearic Rise cores are characterized by low proportions (or absence) of  $T_a$  and  $T_t$  turbidite sequences reflecting, in part, the reduced input of fine-grained sediments from the source area, and bypassing of finer-grained turbidites onto the Balearic Basin plain beyond the rise.

The hemipelagic-turbidite mud assemblage is the predominant facies on the Balearic Rise. Two hemipelagic mud variants are recognized. These record the interaction of sediment input, bottom current energy, and changes in biogenic productivity, as well as the effects of large-scale Quaternary climatic fluctuations that triggered changes in water mass movement, stratification, and possible current reversals. The hemipelagic units are best developed on smooth, elevated platforms of the rise and other areas relatively protected from turbidity currents and related gravity flow incursions.

The Menorca Fan is characterized by a main fan-channel, linked to the Menorca Valley, which can be traced from the Balearic Platform to the Balearic Basin plain, and an association of small fan lobes and shallow channels on the lower Balearic Rise.

Late Quaternary rates of sedimentation on the Balearic Rise average from 12-13 cm/10<sup>3</sup> yr to 6-7 cm/10<sup>3</sup> yr in the various sedimentary sections sampled. The highest rates occur in the adjacent Balearic Basin plain and in the main Menorca Fan channel, while the lowest rates are found in cores on the smooth, elevated areas of the Rise where hemipelagic sedimentation predominates. The three upper calcareous ooze layers developed at about 28,000 years BP, 21,000 years BP, and between 3000 years and the present. The thick channel sand sequences are dated between 23,000 and 16,000 years BP, i.e., coinciding with the last major sea level lowering and the maximum low stand.

The physiography and sediment distribution of the Menorca Fan contrast with those of some mod-



ern submarine fans as a result of the much reduced importance of overbank flow and channel migration. This has resulted from structural constraints (faulting, salt tectonics) on the channel, and the particularly coarse-grained nature of material carried to the fan. The fan sections show a significantly

enhanced content of hemipelagic mud.

Sediment distribution in the fan lobes also appears to have been affected by downslope creep and other forms of mass sediment failure mechanisms which have blocked fan-valleys and modified channel diversion.

## Appendix

TABLE A.—Petrologic data based on samples collected on the Balearic Rise (data is simplified in Table B)

<u>CORE</u>	<u>SAMPLE</u>	<u>% SAND</u>	<u>% A</u>	<u>% B</u>	<u>% C</u>
MC 1	C-1	11.0	44.44	55.30	0.26
	C-2	0.2	11.84	86.60	1.56
	C-3	15.5	58.72	40.99	0.31
	C-4	0.02	18.46	80.72	0.83
	C-5	3.9	61.24	38.25	0.24
	B-1	0.03	13.41	83.09	3.49
	B-2	6.5	52.83	45.48	1.70
	A-1	0.1	13.13	83.75	3.13
	A-2	7.1	44.35	55.65	0.00
	A-3	0.2	13.08	53.08	33.85
	A-4	6.8	49.35	45.76	4.90
	A-5	4.9	62.53	36.65	0.83
	A-6	0.3	19.95	74.65	5.42
	MC 2	PA-1	3.8	29.50	47.98
PA-2		14.1	17.69	68.95	13.38
PA-3		0.4	24.30	66.48	8.93
GA-1		14.9	39.35	59.68	0.97
GA-2		0.04	36.02	56.83	7.15
GA-3		6.8	33.43	65.42	1.16
GA-4		7.0	40.23	58.62	1.15
GA-5		6.0	52.68	45.44	1.90
GA-6		6.8	53.21	31.59	15.20
MC 3	C-1	6.5	60.83	38.58	0.60
	C-2	18.9	20.24	69.94	9.82
	C-3	4.0	36.21	59.13	4.65
	B-1	2.6	33.66	60.79	5.56
	B-2	2.7	42.15	51.16	6.69
	B-3	3.3	38.51	60.30	0.90
	A-1	66.1	11.48	63.14	25.38
	A-2	3.1	43.99	49.36	6.64
	A-3	4.2	56.03	43.33	0.66
	A-4	66.6	14.93	71.05	14.03
MC 4	G-1	7.6	38.41	61.29	0.31
	G-2	7.7	59.08	40.59	0.33
	G-3	4.1	49.19	48.54	2.28
	G-4	4.6	36.03	68.87	3.10
	P-1	43.2	15.66	61.08	23.27

TABLE A.—Petrologic data based on samples collected on the Balearic Rise (data is simplified in Table B)—(Cont.)

<u>CORE</u>	<u>SAMPLE</u>	<u>% SAND</u>	<u>% A</u>	<u>% B</u>	<u>% C</u>
MC 5A	B-1	11.9	33.01	67.00	0.00
	B-2	7.4	54.80	44.90	0.31
	B-3	5.2	72.55	27.13	0.33
	A-1	79.5	8.15	91.21	0.66
	A-2	4.6	39.65	55.98	4.37
	A-3	83.0	14.96	81.62	3.41
	A-4	91.0	7.83	86.67	5.51
	A-5	81.0	14.63	82.63	2.75
	A-6	19.5	22.51	70.38	7.12
MC 6	C-1	9.7	41.27	58.74	0.00
	C-2	7.1	50.74	48.97	0.30
	C-3	4.5	68.73	29.21	2.07
	B-1	4.6	39.32	59.14	1.55
	B-2	77.2	12.99	76.88	10.13
	B-3	82.5	10.82	82.96	6.24
	A-1	91.5	10.06	85.80	4.15
	A-2	82.0	8.76	81.51	9.74
	A-3	3.2	42.45	45.28	12.27
	A-4	3.9	52.12	44.30	3.59
	A-5	95.4	4.73	84.23	11.04
	A-6	92.4	9.07	81.87	9.07
	A-7	46.8	9.51	76.38	14.11
	MC 7	C-1	12.8	45.40	54.04
C-2		9.7	52.57	47.43	0.00
C-3		4.1	60.80	22.66	16.53
C-4		2.7	47.34	45.14	7.52
B-1		2.5	29.45	57.61	12.95
B-2		17.3	72.22	25.93	1.86
B-3		17.9	57.19	42.48	0.33
A-1		6.3	50.97	47.11	1.95
A-2		5.7	31.23	67.50	1.25
A-3		7.3	45.54	51.79	2.69
A-4		6.7	57.38	41.02	1.61
A-5		2.7	73.21	15.38	11.41
A-6		9.6	71.82	28.18	0.00
MC 8		C-1	70.4	15.47	80.80
	C-2	86.6	20.82	76.03	3.15
	C-3	7.6	47.47	52.22	0.32
	C-4	9.3	56.97	43.02	0.00
	C-5	6.3	76.42	22.99	0.60
	C-6	5.8	57.69	41.03	1.28
	C-7	91.8	9.10	82.42	8.49
	B-1	95.1	2.53	71.91	25.56
	B-2	93.6	3.51	81.02	15.51

TABLE A.—Petrologic data based on samples collected on the Balearic Rise (data is simplified in Table B)—(Cont.)

<u>CORE</u>	<u>SAMPLE</u>	<u>% SAND</u>	<u>% A</u>	<u>% B</u>	<u>% C</u>
MC 8	B-3	4.6	60.75	37.37	1.89
	B-4	3.1	45.50	51.16	3.32
	A-1	3.6	47.24	50.16	2.60
	A-2	93.6	9.72	78.72	11.55
	A-3	95.0	5.46	74.55	19.99
MC 9	B-1	15.4	38.32	60.74	0.93
	B-2	23.3	24.12	75.86	0.00
	B-3	70.1	10.97	86.78	2.26
	B-4	88.9	11.77	85.62	2.61
	B-5	8.0	50.16	45.92	3.93
	A-1	6.1	35.15	63.03	1.82
	A-2	5.5	20.11	77.13	2.75
	A-3	45.3	5.03	88.36	6.62
	A-4	69.8	10.70	79.44	9.86
	A-5	87.0	10.87	81.36	7.76
	A-6	17.2	37.72	60.54	1.75
	A-7	3.9	62.67	36.24	1.09
	A-8	31.4	19.08	75.39	5.54
	A-9	33.4	12.09	86.82	1.11
MC 10	B-1	11.2	46.97	52.40	0.64
	B-2	7.0	55.48	39.02	5.49
	B-3	14.3	26.67	72.47	0.87
	B-4	6.5	48.96	45.97	5.08
	B-5	9.4	66.78	32.90	0.33
	B-6	21.6	53.25	45.25	1.50
	B-7	3.3	45.87	47.27	6.85
	B-8	11.4	66.56	29.23	4.22
	B-9	15.9	76.65	22.37	0.99
	A-1	4.5	74.92	22.77	2.31
	A-2	10.7	72.04	26.74	1.21
	A-3	12.2	65.88	34.13	0.00
	A-4	5.2	72.81	27.19	0.00
	A-5	8.1	67.60	29.89	2.52
A-6	3.7	39.39	59.39	1.24	
MC 11	G-1	9.7	52.90	46.45	0.64
	G-2	64.4	7.42	84.28	8.31
	G-3	90.1	19.65	75.00	5.36
	G-4	1.9	33.72	62.83	3.46
	G-5	10.2	33.54	63.95	2.51

A = pteropods (1) + planktonic forams (4).

B = shells (molluscs) (2) + shell fragments (3) + benthonic forams (5) + ostracods (6) + bryozoa (7) + others (echinoderms, spongy spicules, ...) (8) + plant debris (9).

C = heavy minerals (10) + mica (11) + pyrite (12) + light minerals (13) + volcanic ash (14).

TABLE B.—Synthesis of sediment types and percentage of sand in cores collected on the Balearic Rise (based on data in Table A)

CORE	SAMPLE	SEDIMENT TYPE					% SAND
		●	◐	◑	⊗	⊙	
MC1	C-1					x	11.0
	C-2			x			0.2
	C-3					x	15.5
	C-4			x			0.02
	C-5				x		3.9
	B-1			x			0.03
	B-2				x		6.5
	A-1		x				0.1
	A-2				x		7.1
	A-3			x	x		0.2
	A-4				x		6.8
	A-5				x		4.9
	A-6			x			0.3
MC2	PA-1		x		x		3.8
	PA-2	x					14.1
	PA-3		x				0.4
	GA-1					x	14.9
	GA-2			x			0.04
	GA-3		(x)				6.8
	GA-4				x		7.0
	GA-5				x		6.0
GA-6			x	x		6.8	
MC3	C-1				x		6.5
	C-2	x					18.9
	C-3				x		4.0
	B-1			(x)			2.6
	B-2			x			2.7
	B-3				x		3.3
	A-1	x					66.1
	A-2				x		3.1
	A-3				x		4.2
A-4	x					66.6	
MC4	G-1				x		7.6
	G-2				x		7.7
	G-3				x		4.1
	G-4				x		4.6
	P-1	x					43.2

TABLE B.—Synthesis of sediment types and percentage of sand in cores collected on the Balearic Rise (based on data in Table A)—(Cont.)

CORE	SAMPLE	SEDIMENT TYPE					% SAND
		●	◐	◑	⊗	⊙	
MC5A	B-1					x	11.9
	B-2				x		7.4
	B-3				x		5.2
	A-1	x					79.5
	A-2				x		4.6
	A-3	x					83.0
	A-4	x					91.0
	A-5	x					81.0
A-6	x					19.5	
MC6	C-1				x		9.7
	C-2				x		7.1
	C-3				x		4.5
	B-1				x		4.6
	B-2	x					77.2
	B-3	x					82.5
	A-1	x					91.5
	A-2	x					82.0
	A-3			x			3.2
	A-4				x		3.9
	A-5	x					95.4
	A-6	x					92.4
	A-7	x					46.8
MC7	C-1					x	12.8
	C-2				x		9.7
	C-3			x	x		4.1
	C-4			x	x		2.7
	B-1			x			2.5
	B-2					x	17.3
	B-3					x	17.9
	A-1				x		6.3
	A-2			x	x		5.7
	A-3			x	x		7.3
	A-4				x		6.7
	A-5			x	x		2.7
	A-6				x		9.6
	MC8	C-1	x				
C-2		x					86.6
C-3					x		7.6
C-4					x		9.3
C-5					x		6.3
C-6					x		5.8
C-7		x					91.8



## Literature Cited

- Auzende, J. M., P. Bonnin, J. L. Olivet, and G. Pautot  
1971. Upper Miocene Salt Layer in the Western Mediterranean Basin. *Nature, Physical Science*, 230:82-84
- Biscaye, P. E., W.B.F. Ryan, and F. C. Wezel  
1972. Age and Nature of the Pan-Mediterranean Sub-bottom Reflector M. In D. J. Stanley, editor, *The Mediterranean Sea: A Natural Sedimentary Laboratory*, pages 83-90. Stroudsburg: Dowden, Hutchinson & Ross.
- Bouma, A. H.  
1962. *Sedimentology of Some Flysch Deposits, a Graphic Approach to Facies Interpretation*. 168 pages. Amsterdam: Elsevier.
- Burk, C. A., and C. L. Drake, editors  
1974. *The Geology of Continental Margins*. 1009 pages. New York: Springer-Verlag.
- Curry, J. R., and D. G. Moore  
1971. Growth of the Bengal Deep-Sea Fan and Denudation in the Himalayas. *Geological Society of America Bulletin*, 82:563-572.
- Curry, J. R., and D. G. Moore  
1974. Sedimentary and Tectonic Processes in the Bengal Deep-Sea Fan and Geosyncline. In C. A. Burk and C. L. Drake, editors, *The Geology of Continental Margins*, pages 617-627. New York: Springer-Verlag.
- Damuth, J. E.  
1975. Echo Character of the Western Equatorial Atlantic Floor and Its Relationship to the Dispersal and Distribution of Terrigenous Sediments. *Marine Geology*, 18:17-45.
- Damuth, J. E., and D. E. Hayes  
1977. Echo Character of the East Brazilian Continental Margin and Its Relationship to Sedimentary Processes. *Marine Geology*, 24:73-95.
- Damuth, J. E., and N. Kumar  
1975. Amazon Cone: Morphology, Sediments, Age, and Growth Pattern. *Geological Society of America Bulletin*, 16:863-878.
- Frazer, J. Z., G. Arrhenius, J. S. Hanor, and D. L. Hawkins  
1970. *Surface Sediment Distribution, Mediterranean Sea*. 8 pages. Defence Language Institute-Systems Development Agency.
- Genesseeux, M., and Y. Thommeret  
1968. Datation par le radiocarbone de quelques sédiments sous-marins de la Région Niçoise. *Revue de Géographie Physique et de Géologie Dynamique*, 10: 375-382.
- Gonnard, R., J. Letouzey, B. Biju-Dival, and L. Montadert  
1975. Apports de la sismique réflexion aux problèmes du volcanisme en Méditerranée et à l'interprétation des données magnétiques. In *Troisième Réunion des Sciences de la Terre, Montpellier (Avril 1975)*, 1 page.
- Heezen, B. C., and G. L. Johnson  
1969. Mediterranean Undercurrent and Microphysiography West of Gibraltar. *Bulletin de l'Institut Océanographique de Monaco*, 67(1382):1-95.
- Hollister, C. D., and B. C. Heezen  
1972. Geologic Effects of Ocean Bottom Currents: Western North Atlantic. In A. L. Gordon, editor, *Studies in Physical Oceanography*, pages 37-66. London: Gordon and Breach.
- Huang, T. C., and H. H. Goodell  
1970. Sediments and Sedimentary Process of Eastern Mississippi Cone, Gulf of Mexico. *American Association of Petroleum Geologists Bulletin*, 54:2070-2100.
- Huang, T. C., and D. J. Stanley  
1972. Western Alboran Sea: Sediment Dispersal, Ponding, and Reversal of Currents. In D. J. Stanley, editor, *The Mediterranean Sea: A Natural Sedimentation Laboratory*, pages 512-559. Stroudsburg: Dowden, Hutchinson & Ross.
- Hsü, K. J., L. Montadert, R. E. Garrison, and others  
1975. Glomar Challenger Returns to the Mediterranean Sea. *Geotimes*, August 1975:16-19.
- Jacobi, R. D.  
1976. Sediment Slides on the North Western Continental Margin of Africa. *Marine Geology*, 22:157-173.
- Jacobi, R. D., P. D. Rabinowitz, and R. W. Embley  
1975. Sediment Waves on the Moroccan Continental Rise. *Marine Geology*, 19:1761-1767.
- Keller, G. H., D. Lambert, G. Rowe, and N. Staresinic  
1973. Bottom Currents in the Hudson Canyon. *Science*, 180:180-183.
- Keller, G. H., and F. P. Shepard  
1978. Currents and Sedimentary Processes in Submarine Canyons off the Northeast United States. In D. J. Stanley and G. Kelling, editors, *Sedimentation in Submarine Canyons, Fans, and Trenches*, pages 15-32. Stroudsburg: Dowden, Hutchinson & Ross.
- Kelling, G., and D. J. Stanley  
1976. Sedimentation in Canyon, Slope, and Base-of-Slope Environments. In D. J. Stanley and D.J.P. Swift, editors, *Marine Sediment Transport and Environmental Management*, pages 379-435. New York: John Wiley and Sons, Inc.
- Maldonado, A., and D. J. Stanley  
1976a. The Nile Cone: Submarine Fan Development by Cyclic Sedimentation. *Marine Geology*, 20:27-40.
- Maldonado, A., and D. J. Stanley  
1976b. Late Quaternary Sedimentation and Stratigraphy in the Strait of Sicily. *Smithsonian Contributions to the Earth Sciences*, 16: 73 pages.



- Maldonado, A., and D. J. Stanley  
1976c. Menorca Fan and Nile Cone: Anomalous Submarine Fan Models? *Geological Society of America, Abstracts with Programs*, 1976:995.
- Mauffret, A.  
1976. *Etude géodynamique des Iles Baléares*. 137 pages. Thesis, University of Paris.  
1976. Le bloc continental Baléare (Espagne): Extension et évolution. *Marine Geology*, 12: 289-300.
- Menard, H. W.  
1955. Deep-sea Channels, Topography and Sedimentation. *American Association of Petroleum Geologists Bulletin*, 39:236-255.
- Menard, H. W., S. M. Smith, and R. M. Pratt  
1965. The Rhône Deep-Sea Fan. In W. F. Whittard and R. Bradshaw, editors, *Submarine Geology and Geophysics*, pages 217-285. London: Butterworths.
- Middleton, G. V., and M. A. Hampton  
1973. Mechanics of Flow and Deposition. In G. V. Middleton and A. H. Bouma, editors, *Turbidites and Deep Water Sedimentation*, pages 1-38. Anaheim: SEPM Pacific Section.
- Montadert, L., J. Sancho, J. P. Fail, J. Debyser, and E. Winnock  
1970. De l'âge tertiaire de la série salifère responsable des structures diapiriques en Méditerranée occidentale (nord-est des Baléares). *Comptes Rendus de l'Académie des Sciences de Paris*, 271-D:812-815.
- Nelson, H.  
1976. Late Pleistocene and Holocene Depositional Trends, Processes, and History of Astoria Deep-Sea Fan, Northeast Pacific. *Marine Geology*, 20:129-173.
- Normark, W. R.  
1970. Growth Patterns of Deep-sea Fans. *American Association of Petroleum Geologists Bulletin*, 54:2170-2195.
- Normark, W. R.  
1974. Submarine Canyons and Fan Valleys: Factors Affecting Growth Patterns of Deep-Sea Fans. In R. H. Dott, Jr., and R. H. Shaver, editors, *Modern and Ancient Geosynclinal Sedimentation. SEPM Special Publication*, 19:56-68. Tulsa.
- Normark, W. R., and D. J. W. Piper  
1972. Sediments and Growth Pattern of Navy Deep-Sea Fan, San Clemente Basin, California Borderland. *Journal of Geology*, 80:198-223.
- Obrador, A. B. Mercadal, and J. Rosell  
1971. Geology of Menora. In T. Freeman and R. Simancas, editors, *Guidebook, Tenth International Field Institute*, pages 139-148. Washington: American Geological Institute.
- Rupke, N. A., and D. J. Stanley  
1974. Distinctive Properties of Turbidites and Hemipelagic Mud Layers in the Algéro-Balearic Basin, Western Mediterranean Sea. *Smithsonian Contributions to the Earth Sciences*, 13: 40 pages.
- Ryan, W. B. F., and B. C. Heezen  
1965. Ionian Sea Submarine Canyons and the 1908 Messina Turbidity Current. *Geological Society of America Bulletin*, 76:915-932.
- Ryan, W.B.F., K. J. Hsü, M. B. Cita, P. Dumitrica, J. Lort, M. Maync, W. D. Nesteroff, G. Pautot, H. Stradner, and F. C. Wezel  
1973a. Balearic Rise-Site 124. In W. B. F. Ryan, K. J. Hsü, et al., editors, *Initial Reports of the Deep Sea Drilling Project*, 13(6):133-162. Washington, D.C.: U.S. Government Printing Office.
- Ryan, W.B.F., K. J. Hsü, et al., editors  
1973b. *Initial Reports of the Deep Sea Drilling Project*. Volume 13, 1447 pages. Washington, D.C.: U.S. Government Printing Office.
- Ryan, W.B.F., D. J. Stanley, J. B. Hersey, D. A. Fahlquist, and T. D. Allen  
1970. The Tectonics and Geology of the Mediterranean Sea. In A. E. Maxwell, editor, *The Sea*, pages 387-492. New York: Interscience Publishers.
- Shepard, F. P., R. F. Dill, and U. von Rad  
1969. Physiography and Sedimentary Processes of La Jolla Submarine Fan and Fan-valley. *American Association of Petroleum Geologists Bulletin*, 53:390-420.
- Shepard, F. P., and N. F. Marshall  
1973. Currents along Floors of Submarine Canyons. *American Association of Petroleum Geologists Bulletin*, 57:244-264.
- Stanley, D. J., H. Got, O. Leenhardt, and Y. Weiler  
1974a. Subsidence of the Western Mediterranean Basin in Plio-Quaternary Time: Further Evidence. *Geology*, 2:345-350.
- Stanley, D. J., F. W. McCoy, and L. Diester-Hass  
1974b. Balearic Abyssal Plain: An Example of Modern Basin Plain Deformation by Salt Tectonism. *Marine Geology*, 17:183-200.
- Stanley, D. J., H. Got, N. H. Kenyon, A. Monaco, and Y. Weiler  
1976. Catalanian, Eastern Betic, and Balearic Margins: Structural Types and Geologically Recent Foundering of the Western Mediterranean Basin. *Smithsonian Contributions to the Earth Sciences*, 20: 67 pages, Washington, D.C.
- Stanley, D. J., and A. Maldonado  
1977. Nile Cone: Late Quaternary Stratigraphy and Sediment Dispersal. *Nature*, 266:129-135.
- Stanley, D. J., A. Maldonado, and R. Stuckenrath  
1975. Strait of Sicily Depositional Rates and Patterns, and Possible Reversal of Currents in the Late Quaternary. *Paleogeography, Paleocology and Paleoclimatology*, 18:279-291.
- Stanley, D. J., D. H. Palmer, and R. F. Dill  
1978. Coarse Sediment Transport by Mass Flow and Turbidity Current Processes and Downslope Transformations in Annot Sandstone Canyon—Fan Valley Systems. In D. J. Stanley and G. Kelling, editors, *Sedimentation in Submarine Canyons, Fans and Trenches*, pages 85-115. Stroudsburg, Pennsylvania: Dowden, Hutchinson & Ross.
- Stauffer, P. H.  
1967. Grain Flow Deposits and Their Implications, Santa

Ynez Mountains, California. *Journal of Sedimentary Petrology*, 37:487-508.

U.S. Naval Oceanographic Office

1965. Oceanographic Atlas of the North Atlantic Ocean. Section V: Marine Geology, *U.S. NAVOCEANO Publication*, 700: 71 pages.

Van Straaten, L.M.J.U.

1972. Holocene Stages of Oxygen Depletion in Deep Waters of the Adriatic Sea. In D. J. Stanley, editor,

*The Mediterranean Sea: A Natural Sedimentation Laboratory*, pages 631-643. Stroudsburg, Pennsylvania: Dowden, Hutchinson & Ross.

Walker, R. G.

1975. Generalized Facies Models for Resedimented Conglomerates of Turbidite Association. *Geologic Society of America Bulletin*, 86:737-748.

Walker, R. G.

1976. Facies Models, 2: Turbidites and Associated Coarse Clastic Deposits. *Geoscience Canada*, 3:25-36.

## REQUIREMENTS FOR SMITHSONIAN SERIES PUBLICATION

**Manuscripts** intended for series publication receive substantive review within their originating Smithsonian museums or offices and are submitted to the Smithsonian Institution Press with approval of the appropriate museum authority on Form SI-36. Requests for special treatment—use of color, foldouts, casebound covers, etc.—require, on the same form, the added approval of designated committees or museum directors.

**Review** of manuscripts and art by the Press for requirements of series format and style, completeness and clarity of copy, and arrangement of all material, as outlined below, will govern, within the judgment of the Press, acceptance or rejection of the manuscripts and art.

**Copy** must be typewritten, double-spaced, on one side of standard white bond paper, with 1 $\frac{1}{4}$ " margins, submitted as ribbon copy (not carbon or xerox), in loose sheets (not stapled or bound), and accompanied by original art. Minimum acceptable length is 30 pages.

**Front matter** (preceding the text) should include: **title page** with only title and author and no other information, **abstract page** with author/title/series/etc., following the established format, **table of contents** with indents reflecting the heads and structure of the paper.

**First page of text** should carry the title and author at the top of the page and an unnumbered footnote at the bottom consisting of author's name and professional mailing address.

**Center heads** of whatever level should be typed with initial caps of major words, with extra space above and below the head, but with no other preparation (such as all caps or underline). Run-in paragraph heads should use period/dashes or colons as necessary.

**Tabulations** within text (lists of data, often in parallel columns) can be typed on the text page where they occur, but they should not contain rules or formal, numbered table heads.

**Formal tables** (numbered, with table heads, boxheads, stubs, rules) should be submitted as camera copy, but the author must contact the series section of the Press for editorial attention and preparation assistance before final typing of this matter.

**Taxonomic keys** in natural history papers should use the aligned-couplet form in the zoology and paleobiology series and the multi-level indent form in the botany series. If cross-referencing is required between key and text, do not include page references within the key, but number the keyed-out taxa with their corresponding heads in the text.

**Synonymy** in the zoology and paleobiology series must use the short form (taxon, author, year:page), with a full reference at the end of the paper under "Literature Cited." For the botany series, the long form (taxon, author, abbreviated journal or book title, volume, page, year, with no reference in the "Literature Cited") is optional.

**Footnotes**, when few in number, whether annotative or bibliographic, should be typed at the bottom of the text page on which the reference occurs. Extensive notes must appear at the end of the text in a notes section. If bibliographic footnotes are required, use the short form (author/brief title/page) with the full reference in the bibliography.

**Text-reference system** (author/year/page within the text, with the full reference in a "Literature Cited" at the end of the text) must be used in place of bibliographic footnotes in all scientific series and is strongly recommended in the history and technology series: "(Jones, 1910:122)" or ". . . Jones (1910:122)."

**Bibliography**, depending upon use, is termed "References," "Selected References," or "Literature Cited." Spell out book, journal, and article titles, using initial caps in all major words. For capitalization of titles in foreign languages, follow the national practice of each language. Underline (for italics) book and journal titles. Use the colon-parentheses system for volume/number/page citations: "10(2):5-9." For alinement and arrangement of elements, follow the format of the series for which the manuscript is intended.

**Legends** for illustrations must not be attached to the art nor included within the text but must be submitted at the end of the manuscript—with as many legends typed, double-spaced, to a page as convenient.

**Illustrations** must not be included within the manuscript but must be submitted separately as original art (not copies). All illustrations (photographs, line drawings, maps, etc.) can be intermixed throughout the printed text. They should be termed **Figures** and should be numbered consecutively. If several "figures" are treated as components of a single larger figure, they should be designated by lowercase italic letters (underlined in copy) on the illustration, in the legend, and in text references: "Figure 9 $\underline{b}$ ." If illustrations are intended to be printed separately on coated stock following the text, they should be termed **Plates** and any components should be lettered as in figures: "Plate 9 $\underline{b}$ ." Keys to any symbols within an illustration should appear on the art and not in the legend.

**A few points of style:** (1) Do not use periods after such abbreviations as "mm, ft, yds, USNM, NNE, AM, BC." (2) Use hyphens in spelled-out fractions: "two-thirds." (3) Spell out numbers "one" through "nine" in expository text, but use numerals in all other cases if possible. (4) Use the metric system of measurement, where possible, instead of the English system. (5) Use the decimal system, where possible, in place of fractions. (6) Use day/month/year sequence for dates: "9 April 1976." (7) For months in tabular listings or data sections, use three-letter abbreviations with no periods: "Jan, Mar, Jun," etc.

**Arrange and paginate sequentially EVERY sheet of manuscript**—including ALL front matter and ALL legends, etc., at the back of the text—in the following order: (1) title page, (2) abstract, (3) table of contents, (4) foreword and/or preface, (5) text, (6) appendixes, (7) notes, (8) glossary, (9) bibliography, (10) index, (11) legends.

